

Aus der Klinik für Psychiatrie und Psychotherapie
der Medizinischen Fakultät Charité – Universitätsmedizin Berlin

DISSERTATION

An investigation into the repetitive pathophysiology and the effect of a non-invasive targeted treatment strategy in an animal model overexpressing the dopamine transporter

zur Erlangung des akademischen Grades

Doctor of Philosophy (PhD)

vorgelegt der Medizinischen Fakultät
Charité – Universitätsmedizin Berlin

von

Henriette Edemann Callesen

aus Dänemark, Odense

Datum der Promotion: 13-12-2019

Table of content

Abbreviations	i
Abstract	1
Zusammenfassung	1
1.0 Introduction	2
1.1 Objectives	4
2.0 Methods	5
2.1 Animals	5
2.2 Experimental design	5
2.3 Behavioral assessment	6
2.4 Surgery	7
2.5 Brain stimulation	7
2.6 Post mortem neurobiology	8
2.7 Computational modeling of tDCS current	9
2.8 Data analysis	9
3.0 Results	9
3.1 <i>Study 1: The DAT-tg rat displays alterations distinct for repetitive disorders</i>	9
3.2 <i>Study 2: DAT-tg rats display cognitive deficits alongside dysfunctional neuronal integration</i>	10
3.3 <i>Study 3: tDCS improves symptoms and pathophysiology in the DAT-tg rats via the sensorimotor circuit</i>	11
4.0 Discussion	12
Limitations and future investigations	15
Bibliography	17
Affidavit	I
Selected publications	II
Curriculum vitae	III
List of publications	IV
Acknowledgements	V

Abbreviations

ANOVA	Analysis of variance
AP	Anterior-posterior
CPu	Caudate putamen
DA	Dopamine
DAT	Dopamine transporter
DAT-tg	Transgenic rat model overexpressing DAT
DBS	Deep brain stimulation
DRD1	Dopamine receptor 1
DRD2	Dopamine receptor 2
DV	Dorsal-ventral
FEM	Finite Element Method
GP	Globus pallidum
HPLC	High-performance liquid chromatography
MAO	Monoamine oxidase
M1	Primary motor cortex
ML	Medial- lateral
MWM	Morris water maze
mPFC	Medial prefrontal cortex
MRI	Magnetic resonance imaging
Nacc	Nucleus accumbens
NE	Northeast
NW	Northwest
OFC	Orbitofrontal cortex
Pv+	Parvalbumin

PND	Postnatal day
PFC	Prefrontal cortex
qPCR	Quantitative polymerase chain reaction
rmANOVA	Repeated measure analysis of variance
ROI	Region of interest
SE	Southeast
SW	Southwest
Thal	Thalamus
TS	Tourette Syndrome
tDCS	Transcranial direct current stimulation
WT	Wild type

Abstract

Introduction: Treatment of neuropsychiatric disorders may be optimized through targeted strategies that interact with neurobiological processes responsible for symptom generation. The overexpression of the dopamine transporter (DAT) has been linked to a wide range of neuropsychiatric afflictions with a specific involvement in repetitive disorders. However, the direct consequences of DAT overexpression remain unexplored. Transcranial direct current stimulation (tDCS) is a non-invasive technique suggested as a treatment for repetitive disorders. In-depth investigation into the role of DAT overexpression in repetitive pathophysiology and how tDCS potentially regulates these processes are clinically challenging, yet possible by employment of adequate animal models. **Objectives:** The aim of the present thesis was to investigate the direct consequences of DAT overexpression in relation to the pathophysiology of repetitive behavior and to test the potency of tDCS as a therapeutic approach for repetitive disorders. **Methods:** Initially, a transgenic rat overexpressing DAT (DAT-tg) was generated and its neurobiological and behavioral properties were assessed (*study 1+2*). Extensive deep brain stimulation (DBS) was applied to identify, which brain areas were involved in modulating repetitive behavior in the DAT-tg rat. Subsequently, DAT-tg rats received tDCS above the frontal cortex followed by behavioral and neurobiological assessment (*study 3*). **Results:** The DAT-tg rat displayed several neurobiological deficits within the corticostriatal circuit related to repetitive pathophysiology, which translated into repetitive behavior and treatment sensitivity as observed Tourette syndrome. Further, DAT-tg rats presented with profound cognitive deficits. The application of frontal anodal tDCS led to a decrease in repetitive symptoms in the DAT-tg rats, which was assigned to a specific modulation within the corticostriatal sensorimotor circuit. **Conclusion:** This thesis shows that DAT overexpression is implicated in the generation of among others repetitive pathophysiology, thus supporting the need for further investigations into its role in repetitive disorders. It further shows that the DAT-tg rat constitutes an ideal model for this endeavor, as it allows for a direct assessment of the neurobiological implications and how new interventions interact with these processes. This thesis further found, that following application of the appropriate stimulation parameters, tDCS reduces repetitive behavior by modulating the neuronal circuit considered responsible for symptom manifestation in the DAT-tg rats. This sets the stage for investigations into tDCS as targeted treatment for repetitive disorders.

Zusammenfassung

Einleitung: Die Behandlung neuropsychiatrischer Erkrankungen kann durch gezielte Therapiestrategien, die in die neurobiologischen Prozesse der Symptomentstehung eingreifen, optimiert werden. Die Überexpression des Dopamin-Transporters (DAT) wird mit einer Vielzahl neuropsychiatrischer Erkrankungen, die mit repetitiven Störungen einhergehen, in Verbindung gebracht. Dennoch sind die direkten Folgen der Überexpression des DAT bisher unerforscht. Die transkranielle Gleichstromstimulation (tDCS) ist eine nichtinvasive Technik, die zur Behandlung repetitiver Störungen vorgeschlagen wird. Die ausführliche Untersuchung der Rolle der DAT-Überexpression in der repetitiven Pathophysiologie sowie der potentiellen Regulation dieser Prozesse durch die tDCS ist klinisch herausfordernd, jedoch durch die Verwendung geeigneter Tiermodelle möglich. **Ziele:** Ziel der vorliegenden Studie war es, die direkten Konsequenzen einer DAT-Überexpression in Bezug auf die Pathophysiologie von repetitivem Verhalten zu untersuchen und die Wirksamkeit von tDCS als therapeutischen Ansatz für repetitive Störungen zu testen. **Methoden:** Zunächst wurde eine transgene Ratte mit überexprimiertem DAT (DAT-tg) generiert und ihre neurobiologischen und Verhaltensmerkmale untersucht (*Studie 1+2*). Um herauszufinden, welche Gehirnbereiche bei der Modulation des repetitiven Verhaltens in der DAT-tg-Ratte involviert sind, wurde eine umfassende Tiefenhirnstimulation (DBS) angewendet. Anschließend erhielten DAT-tg-Ratten tDCS über dem Frontalkortex und Auswirkungen auf Verhalten und Neurobiologie wurden geprüft (*Studie 3*). **Ergebnisse:** Die DAT-tg-Ratte wies in den kortikostriatalen Verbindungen mehrere neurobiologische Defizite auf, wie sie sich im repetitivem Verhalten und der Behandlungsempfindlichkeit bei Tourette-Syndrom beobachten lassen. Des Weiteren zeigten DAT-tg-Ratten schwerwiegende kognitive Defizite. Die Anwendung von einer frontalen anodalen tDCS führte zu einer Abnahme der repetitiven Symptomatik bei den DAT-tg-Ratten, die einer spezifischen Modulation innerhalb des kortikostriatalen-sensomotorischen Schaltkreises zugeordnet werden konnte. **Schlussfolgerung:** Diese Studie zeigt, dass die Überexpression des DAT unter anderem bei der Entstehung von repetitiver Pathophysiologie eine Rolle spielt. Dies unterstreicht die Notwendigkeit weiterer Untersuchungen zur Rolle der DAT Überexpression bei repetitiven Störungen. Es zeigt außerdem, dass die DAT-tg-Ratte ein ideales Modell dafür darstellt, als dass es die direkte Untersuchung neurobiologischer Implikationen und die Wirkung neuartiger Interventionen auf diese Prozesse ermöglicht. Diese Arbeit zeigt, dass tDCS nach Anwendung geeigneter Stimulationsparameter repetitives Verhalten durch Modulation des neuronalen Schaltkreises, welcher für die Symptommanifestation bei den DAT-tg-Ratten verantwortlich gemacht wird, reduziert. Damit sind die Voraussetzungen für tDCS als gezielte Behandlung von repetitiven Erkrankungen geschaffen.

1.0 Introduction

As for today, the etiology and understanding of the underlying pathophysiology of neuropsychiatric disorders is limited. This hinders the possibility of developing novel optimized treatment strategies. Conventional therapies, mostly in the form of psychopharmacological agents, are applied systematically and hence often yield insufficient symptom relief and possible side-effects (1,2). Thus, there is a need for a deeper knowledge of the underlying neuropathology, in order to promote the development of treatment strategies that more precisely interact and interfere with the pathological processes from which neuropsychiatric symptoms arise, i.e. targeted treatment strategies.

Based on its role in maintaining proper dopaminergic signaling, overexpression of the dopamine transporter (DAT) has been linked to a variety of neuropsychiatric disorders (3). In repetitive disorders, such as Tourette syndrome (TS), profound dopaminergic alterations exist, including imbalance in tonic/phasic dopamine (DA) firing properties and increased DA receptor availability, which collectively points to the presence of DAT overexpression (4–9). The pathophysiology of repetitive disorders has long been centered around an imbalance in the activity of the corticostriatal circuit. Here, manifestation of repetitive behavior is thought to rely on a combined action between dopaminergic hyperactivity and striatal disinhibition, that leads to thalamic overactivity and frontal cortical hyperexcitability, eventually resulting in the execution of involuntary movements (10–13). Apart from movement control, DA firing within the corticostriatal circuit also regulates cognitive and motivational functions, including learning and goal-directed behaviors (10,14). In correlation, cognitive deficits alongside other comorbidities have been found in patients with TS (15). As such, the palate of abnormal behaviors found in repetitive disorders, rely on several orchestrated events within specific neuronal systems, from which the DA system has a prominent regulatory role (9). Despite the implications of an overactive DAT in repetitive disorders, the direct consequences of DAT overexpression have not been fully assessed. Such investigations are clinically challenging, yet possible through employment of valid animal models. In neuropsychiatric research, mice models have traditionally provided a rational-driven approach based on genetic tools available in this species, whereas rat models are mostly constructed through behavioral and environmental manipulation, due to limited genetic possibilities along with their superior behavioral repertoire (16–18). Since the latter constitutes the core of neuropsychiatric disorders, there is a need for a rat

model that incorporates both essential features. Therefore, a transgenic rat overexpressing the DAT (DAT-tg) was constructed.

In repetitive disorders, application of deep brain stimulation (DBS) has been used as a focal treatment strategy, to directly modulate the aberrant activity of brain regions involved in repetitive pathophysiology (19–22). Currently, there is no conclusion, as to which DBS target is superior when it comes to reducing symptoms in repetitive disorders. This alongside the invasive nature of DBS limits a general application. Thus, there is the need for further research into the optimal brain target for repetitive disorders as well as investigations into more subtle treatment strategies, that still employs a spatial tactic. Transcranial direct current stimulation (tDCS) is a non-invasive, well-tolerated neuromodulating procedure, that by administration to the desired area of the skull, alters cortical excitability through delivery of a transcranial weak current. The effect involves a polarity-dependent shift in resting membrane potential, with anodal stimulation increasing and cathodal stimulation decreasing excitability, respectively (23–25). Based on the presence of cortical hyperexcitability, tDCS has been employed to alter cortical function and subsequent behavior in neuropsychiatric disorders, including TS (26–29). Establishing an appropriate protocol-design has however proven to be challenging, as the cumulative outcome of tDCS involves an interaction between the applied stimulation and the existing underlying neurobiology. Thus, when stimulating the pathological brain, the simplistic approach of excitability being singularly either decreased or increased, depending on tDCS polarity, falls short (30–32). This adds an additional layer of complexity when seeking the stimulation protocol necessary for therapeutic relief. As such, there are indications that tDCS may exert a positive therapeutic effect in repetitive disorders, however still needed is an in-depth investigation on how tDCS modulates the symptomatology and underlying repetitive pathophysiology (26). Such investigations are possible preclinically, as these settings allow for estimating the appropriate stimulation design and subsequent neurobiological responses within a controlled experimental environment.

1.1 Objectives

The objective of this thesis was to assess the neurobiological and behavioral consequences of DAT overexpression in relation to repetitive disorders, followed by an investigation of a non-invasive treatment approach sought to target the brain areas involved in symptom generation.

Initially, the neurobiological and behavioral alterations found in the DAT-tg rat were characterized (*study 1+2*). Subsequently, extensive DBS was applied in the DAT-tg rat to dissect the involvement of sub-circuits in the repetitive pathophysiology. This was followed by an assessment of the behavioral effects of tDCS alongside its impact on cortical and subcortical processes (*study 3*).

2.0 Methods

Key methods and study designs are outlined in this section. Further details are presented in the publications found in the appendix.

2.1 Animals

The hemizygous DAT-tg rat model was included in this thesis, alongside its respective controls (wildtype (WT)). Adult male rats were group-housed in a controlled vivarium with food and water ad libitum and single housed following surgeries. All studies were, after approval by the local ethic committees (Regierungsprasidium Dresden and Senate of Berlin), performed in accordance with the European Communities Council Directive of 22th September 2010 (2010/63/EU).

2.2 Experimental design

Study 1: Characterization of the DAT-tg model was carried forward through a battery of behavioral and neurobiological tests (postnatal day (PND) >90). Susceptibility towards repetitive behavior was investigated following amphetamine application (DAT-tg, n= 8; WT, n= 8). The pharmacoresponsiveness of this behavior was further tested through administration of clonidine (DAT-tg, n= 9; WT, n= 10) and fluoxetine (DAT-tg, n= 8; WT, n= 9). Neurobiological alterations were examined in regions within the corticostriatal circuit. These included alterations in parvalbumin (Pv+) cells (DAT-tg, n= 11; WT, n= 12), DA levels (DAT-tg, n= 10; WT, n= 7), DA receptor expression (DAT-tg, n= 7; WT, n= 8) and monoamine oxidase (MAO) activity (DAT-tg, n= 7; WT, n= 8).

Study 2: DAT-tg (n=16) and WT (n= 11) rats (PND >90) were injected with Bromodeoxyuridine (BrdU) (3x50 mg/kg, 6 hours interval between injections), to quantify neurogenesis. Rat were subsequently subjected to a battery of behavioral testing, including the Morris Water Maze (MWM) to examine learning and memory abilities. Animals only performed one test per day, with a 3-5 days recovery in between tests. Immunohistochemical analysis was performed post mortem.

Study 3: DAT-tg and WT rats (PND >90) intended for tDCS were divided into an overall control group (DAT-tg, n=8; WT n=8) and a tDCS group (DAT-tg, n=9; WT n=7). Rats in the tDCS group

received cathodal, anodal or sham stimulation. Controls rats received sham stimulation. Animals intended to receive DBS were divided into three groups and implanted with electrodes in the caudate putamen (CPu) and orbitofrontal cortex (OFC) (Group 1: DAT-tg, n=8, WT n=8); medial prefrontal cortex (mPFC) (Group 2: DAT-tg, n=8, WT n=8) and thalamus (Thal) and primary motor cortex (M1) (Group 3: DAT-tg, n=5, WT n=6). All three groups received either sham or DBS in a cross-over design. The repetitive behavioral paradigm established in study 1 was employed, with tDCS and DBS being applied in the beginning of this paradigm. Post mortem neurobiological assessment was conducted following finalization of the behavioral experiments.

2.3 Behavioral assessment

2.3.1 Repetitive behavior

Amphetamine-induced repetitive behavior (study 1): Rats were injected with three different dosages of amphetamine in a cross-over design (0.5mg/kg, 2.0mg/kg and 5.0mg/kg). Following injection, animals were placed in testing boxes (50x50x50cm) for 120min. Behavior was recorded and repetitive behavior was later analyzed offline using an adapted scoring protocol of Carter et al.(33) The results from this testing led to the construction of the repetitive behavioral paradigm.

Effect of pharmacotherapy on repetitive behavior (study 1): Rats were injected with amphetamine (2.0mg/kg) and placed in testing boxes for initial 50min. Subsequently, rats were injected with either clonidine (i.p 0.01 mg/kg), fluoxetine (i.p 20 mg/kg) or saline and placed back in the recording boxes for the remaining time (70min). Repetitive behavior was evaluated in the stereotypy phase.

Effect of brain stimulation on repetitive behavior (study 3): Rats were injected with amphetamine (2.0mg/kg) and immediately subjected to tDCS for 30min or DBS for 60min. Following the end of stimulation, jackets and cables were removed and animals freely moved around for the remaining time (tDCS 90min/ DBS 60min). Repetitive behavior was evaluated in the stereotypy phase.

2.3.2 Cognitive behavior

The Morris water maze (MWM) (study 2)

Rats were trained and tested in a water-filled pool, that included a submerged platform and distal visual cues. Rats underwent 4x 60 seconds acquisition trials per day for a total of 4 days, during which they had to find the platform. The pool was separated into four quadrants (southeast (SE); northeast (NE); southwest (SW); northwest (NW)). The platform was placed in NW quadrant

during all acquisition trials. Rats were released at different starting points over the 4 consecutive days. Latency to find the platform was recorded and thigmotaxis (swimming along the walls), non-spatial strategies (scanning the pool) and spatial strategies (swimming straight to the platform) were assessed. The platform was removed on day 5 and the probe trial test was performed. Time used in the former target quadrant was estimated.

2.4 Surgery

DAT-tg rats underwent surgery after reaching PND 90. Stereotactic surgery was performed under a general balanced anesthesia (s.c, medetomidine dihydrochloride (0.135mg/kg), midazolam (2mg/kg) and fentanyl (0.005mg/kg)). For tDCS application, an epicranial electrode (2.1mm in diameter) was placed onto the skull, over the left frontal cortex (AP +3.2; ML 1.5). For DBS application, monopolar electrodes were bilaterally implanted into the CPu (AP +1.5; ML +1.5; DV -4.0), OFC (AP +3.7; ML +2.4; DV -3.3), M1 (AP +1.5; ML +2.7; DV -1.5), mPFC (AP +3.5; ML +0.6; DV -3.4) and Thal (AP -4.1; ML +1.3; DV -6.4). Screws were drilled into the skull and the ground electrode from the monopolar electrodes were wrapped around the adjacent screw. Both monopolar and epicranial electrodes were fixed using dental cement. Coordinates were according to Paxinos rat brain atlas (34). Anesthesia was antagonized after completing surgery, using a blend of naloxone (s.c 0.12mg/kg), flumazenil (0.2mg/kg), antipamzol (0.75mg/kg). Analgesic (Meloxicam 0.2mg/kg, s.c) was applied for three days after surgery.

2.5 Brain stimulation

Transcranial direct current stimulation (study 3): For application of tDCS, saline (0.9%, contact area 3.5mm²) was filled into the epicranial electrode and the stimulating electrode inserted. A reference electrode (8cm²) was placed on the thorax and kept in place using a rat-jacket. Stimulation was applied via a computer-interfaced current generator, with the current strength ramped for 10sec. In the tDCS group, a single session of anodal or cathodal stimulation was applied at a current intensity of either 100 μ A, 200 μ A and 300 μ A for 30min in the beginning of the repetitive behavioral paradigm.

Deep brain stimulation (study 3): DBS was controlled by the same apparatus as used for tDCS application (see above). On the day prior to testing, stimulation was applied twice in the respective region for 60min (morning and afternoon). On testing day, stimulation was applied in the respective region for 60min in the beginning of the repetitive behavioral paradigm. DBS was applied with a

frequency of 130Hz, biphasic 100 μ s pulses, and current intensity of 150 μ A. For application of sham stimulation, animals were connected to the stimulating system without current flowing.

2.6 Post mortem neurobiology

High-performance liquid chromatography (HPLC) (study 1 and 3): Tissue samples were obtained via micropunches from 0.5-1.0mm thick slices from areas including the OFC, Nacc and CPu. Samples were homogenized via ultrasonification and the homogenate was centrifuged. From the supernatant, DA and its metabolite (DOPAC) were separated on a HPLC column (ProntoSil 120-3-C18-SH; Bischoff Analysentechnik und – geräte GmbH, Germany) and levels were detected electrochemically (Chromsystems Instruments & Chemicals GmbH, Germany). In addition, dopamine turnover (DOPAC/DA) was assessed.

Monoamine oxidase (MAO) activity assay (study 1): Micropunches from the CPu were homogenized via ultrasonification in a buffer from a fluorometric assay kit (biovision K795-100) and MAO activity was measured in accordance to manual.

Quantitative polymerase chain reaction (qPCR) (study 1 and 3): Areas investigated included the OFC, Nacc and CPu (study 1) and mPFC, MI, OFC and CPu (study 3). RNA concentration in the respective tissue samples were assessed using Nanodrop Spectrophotometer (peqlab) and cDNA was synthesized using RNA-to-cDNA Kit (Lifetechnologies). A TaqMan qPCR was performed with the following TaqMan gene expressions assays: DRD1 (Rn03062203_sl) and DRD2 (Rn01418275_ml) for study 1 and Pv+ (Rn 00574541_ml) and c-Fos (Mm00487425_ml) for study 3. CT values were normalized to GFAP (house-keeping gene). Fold change was estimated using the $\Delta\Delta$ CT method.

Immunohistochemistry (study 1 and 2): In study 1, free-floating sections were stained against c-Fos (1:100, Santa Cruz, sc-52) and Pv+ (1:500, Antikörper-online, ABIN1742405) and subsequently detected with secondary antibodies (1:1000, Vector Laboratories, BA1000). The number of positive nuclei was counted in amongst others the CPu, OFC and mPFC. In study 2, free-floating sections were stained against BrdU (1:500, AbD Serotec OBT0030), NeuN (1:500, Millipore, MAB377) and Ki-67+ (1:500, Novocasta laboratories, NCL-Ki67p), detected with secondary antibodies (1:500; Dianova) and visualized with 3,3'-diaminobenzidine. The double-labelled BrdU/NeuN samples were detected with fluorescence secondary antibodies (donkey anti-mouse Cy3, donkey anti-rat Alexa flour 488, and donkey anti-rabbit Alexa Flour 647, Jackson Immunoresearch) and

counterstained with 4', 6'-diamidino-2-phenylindole. Cells were sampled in the dentate gyrus of the hippocampus.

2.7 Computational modeling of tDCS current

The computational modeling was performed by the working group led by Professor Marom Bikson, (Department of Biomedical Engineering, City University of New York). A template rat head was constructed from a 7.0 tesla MRI and micro-CT scan (35). The tDCS electrode placement and stimulation approach as used in study 3 was modeled in Solidworks (Dassault Systems Corp. Waltham, MA) and for meshing imported to ScanIP. A Finite Element Method (FEM) model was constructed. This was done using electrostatic volume conductor physics, from which material conductivity included a combination of *in vitro* and *in vivo* measurements (36,37). Current boundaries were utilized to simulate direct current and predicted current density was created.

2.8 Data analysis

Basic differences between DAT-tg and WT rats were analyzed using a student's t-test. Behavioral and neurobiological results were analyzed using either one-way or two-way ANOVA. A one-way or two-way ANOVA with repeated measure (rmANOVA) was used to assess results taken repetitively from the same animal. Variables included animal groups (DAT-tg vs. WT) and treatments/trials. If applicable, further post-hoc t-tests were applied. A non-parametric Mann Whitney test was used to assess the effect of tDCS on Pv+ levels. A binomial mixed-effect model was used to assess the probability of applying different search strategies in the MWM, from which odds ratio was compared to chance in both DAT-tg and WT rats. A $p < 0.05$ was considered statistically significant.

3.0 Results

This section provides a summary of the results, with the figures referring to the respective publications. Further details are found in the publications listed in the appendix.

3.1 Study 1: The DAT-tg rat displays alterations distinct for repetitive disorders

The DAT-tg rats displayed significant increase in repetitive behavior (oral stereotypy) as compared to WT rats following administration of 2.0mg/kg amphetamine ($T = -3.545$, $p = 0.003$), that appeared 80-120min after injection (stereotypy phase). Same dosage led to hyperlocomotion in the WT rats ($T = 4.718$, $p = 0.000$). No effect was found for 0.5mg/kg amphetamine in either group,

whereas 5.0mg/kg led to repetitive behavior in both DAT-tg and WT rats (Fig. 8a). The subsequent effect of pharmacotherapy on this repetitive behavior was assessed. A two-way rmANOVA revealed that administration of clonidine led to a significant effect for animal groups ($F= 6.598$, $p= 0.019$) and interaction ($F= 6.887$, $p= 0.018$), with clonidine application significantly decreasing repetitive behavior in the DAT-tg rats ($p<0.05$). In contrast, fluoxetine administration led to a significant effect for treatment ($F = 15.127$, $p = 0.001$), as fluoxetine reduced locomotion in both animal groups (Fig. 8b).

The underlying neurobiological state was studied at different levels, including investigations into neurochemical and cellular alterations. A post mortem HPLC assessed DA contents in cortical and subcortical areas. As compared to the WT rats, the DAT-tg rats exhibited a decrease in DA levels in the OFC ($T = -7.504$, $p = 0.000$), Nacc ($T = -13.726$, $p = 0.000$) and CPu ($T = -14.611$, $p = 0.000$) as well as an increase in DA turnover (DOPAC/DA) in the same areas (OFC: $T = 13.467$, $p = 0.000$; Nacc: $T = 7.542$, $p = 0.000$; CPu $T = 19.314$, $p = 0.000$) (Fig. 3a,c). A qPCR of mRNA levels found, that in comparison to the WT rats, the DAT-tg rats displayed an increase in DRD1 mRNA levels in the OFC ($T = -3.534$, $p= 0.000$), Nacc ($T= - 2.136$, $p= 0.029$) and CPu ($T= -6.217$, $p= 0.036$) (Fig. 2b) and an increase in DRD2 mRNA levels in OFC ($T= -2.610$, $p= 0.022$), Nacc ($T= -1.917$, $p= 0.029$) and CPu ($T= -3.252$, $p= 0.006$) (Fig. 2c). A MAO activity assay was employed to test for compensatory mechanisms. As compared to WT rats, DAT-tg rats displayed a significant increase in MAO activity. ($T = -2.470$, $p = 0.028$) (Fig. 3d). Immunostaining was conducted to investigate for cellular changes. In the DAT-tg rats, results showed a significant reduction of P_v⁺ cells in the CPu ($T = 3.228$, $p = 0.004$) and a significant increase of c-fos expressing cells in the OFC ($T = -2.884$, $p = 0.011$) in comparison to WT rats (Fig. 5b-c).

3.2 Study 2 DAT-tg rats display cognitive deficits alongside dysfunctional neuronal integration

In the MWM, a rmANOVA test revealed that DAT-tg rats exhibited a significantly lower success rate in finding the hidden platform as compared to WT rats (trial $F(6.8,171)= 3.516$, $p= 0.002$, animal groups: $F(1,25)= 181.2$, $p<0.001$, interaction $F(6.8,171)= 3.941$, $p=0.001$), with none of the DAT-tg finding the platform above chance (fig. 2d). Furthermore, DAT-tg rats engaged in different search strategies as compared to WT rats. DAT-tg rats displayed a lower chance of employing a spatial dependent strategy (Estimate= -0.81, SE= 0.22, $z= -3.71$, OR= 0.44, $p<0.001$). In addition, the chance of DAT-tg rats engaging in thigmotaxic behavior was three-fold higher than in the WT rats (Estimate= 1.07, SE= 0.23, $z= 4.54$, OR=2.9, $p<0.001$) (fig. 2e). During probe trial

performance, the platform was removed. Here, a student's t-test showed, that WT rats spend the majority of time on the target quadrant, indicating successful spatial learning (NW/NE $t(10)= 3.451$, $p=0.007$; NW/SE $t(10)= 2.303$, $p=0.047$; all other $p>0.05$). The DAT-tg rats showed no specific preference to any of the quadrants (all $p>0.05$) (fig. 2f).

Searching for a neurobiological correlate of this behavior, adult hippocampal neurogenesis was assessed. Here, a student t-test showed no difference in the number of Ki-67+ cells ($t(14)= 1$, $p=0.332$) nor in the overall number of BrdU labelled cells ($t(18)= -0.891$, $p=0.385$) between DAT-tg and WT rats. As compared to WT rats, the co-labelling (BrdU+/NeuN+) revealed a reduction in the population of BrdU+ in the DAT-tg rats ($t(18)= 2.140$, $p=0.046$) (fig. 4).

3.3 Study 3 tDCS improves symptoms and pathophysiology in the DAT-tg rats via the sensorimotor circuit

The effect of tDCS on repetitive behavior was assessed. Here, a one-way rmANOVA showed an effect for treatment ($F(5,33) = 2.727$, $p=0.036$) as anodal tDCS (200 μ A) significantly reduced repetitive behavior in the DAT-tg rats as compared to sham stimulation ($p=0.012$) (Fig. 1a). Furthermore, a one-way rmANOVA showed a significant effect for treatment in the WT rats ($F(5,28)= 3.388$, $p=0.016$), with anodal tDCS (200 μ A) significantly increasing head movements as compared to sham stimulation ($p=0.015$) (Fig. 1b). No effect was seen for cathodal tDCS at any intensities tested in either DAT-tg or WT rats. Computational modelling revealed a peak of average current density and power dissipation 1.5mm anterior to bregma following anodal tDCS, which correlates with the coordinate of the M1 (Fig 2a,b). Extensive DBS was further employed to pin down, which specific cortical subregion and related circuit were involved in the repetitive behavior observed in the DAT-tg rats. In the DAT-tg rats, one-way rmANOVA showed an effect for treatment ($F(10,51) = 4.112$, $p<0.001$), with DBS reducing oral stereotypy when applied to the CPu ($p=0.001$) and the M1 ($p=0.019$) as compared to sham. DBS applied to the mPFC, OFC or thal yielded no effect (Fig. 1c).

Looking for the neurobiological effects of anodal tDCS (200 μ A), a two-way ANOVA found a significant effect across groups for all the investigated areas (OFC ($F(1,22) = 5.270$, $p=0.032$); Nacc ($F(1,23)=29.285$ $p<0.001$); CPu ($F(1,23)= 247.623$, $p<0.001$)), with the DAT-tg rats displaying a general decrease in DA levels compared to WT rats (fig. 4a-c). In regards to DA turnover, a significant effect was found for animal groups (OFC: $F(1,22)= 37.471$, $p<0.001$; Nacc: $F(1,22)=45.293$, $p <0.001$); CPu: $F(1,23)=43.789$, $p<0.001$), with DAT-tg rats showing higher DA

turnover in comparison to WT rats across all areas (fig. 4d-f). A qPCR analysis was conducted to assess the immediate effects of anodal tDCS (200 μ A) on Pv+ and c-fos mRNA. DAT-tg rats showed significant lower levels of Pv+ mRNA after tDCS, in comparison to sham stimulation (Mann-Whitney $U=1.500$, $p=0.005$). There was no difference observed in WT rats. (Fig. 6). Following investigation into cortical activity patterns, a one-way ANOVA revealed a significant effect in the OFC ($F(1,10)=5.129$, $p=0.043$) and mPFC, ($F(1,13)= 7.732$, $p=0.016$), with anodal tDCS significantly increasing c-fos mRNA levels in these areas in the DAT-tg rats. Stimulation had no effect on c-fos expression levels in the WT rats. (Fig. 3).

4.0 Discussion

The present thesis aimed at investigating the consequences of DAT overexpression, followed by the assessment of tDCS as a potential non-invasive treatment strategy for repetitive disorders. Overexpression of DAT lead to neurobiological alterations, beyond the expected implications on the dopaminergic system, which translated into several behavioral deficits related to repetitive disorders. Application of anodal tDCS promoted symptom relief in the DAT-tg rat, which involved modulation of pathological findings related to symptom manifestation.

DAT overexpression leads to deficits found in repetitive disorders

Characterization of the DAT-tg rat revealed several behavioral and neurobiological deficits observed in repetitive disorders, such as TS. Involuntary movements have shown to increase following stress exposure and amphetamine application (38,39). This heightened susceptibility was also found in the DAT-tg rats, that displayed significant increase in repetitive behavior (oral stereotypy) following a low dose of amphetamine, ineffective in the WT rats. Induction of repetitive behavior evolved over time, with a maximum expression seen 80-120 min after injection (stereotypy phase). To inspect the pharmaco-responsiveness profile of the DAT-tg rats, clonidine and fluoxetine were tested. Clonidine is employed to reduce tics, whereas fluoxetine improves repetitive symptoms seen in obsessive compulsive disorder (OCD) (40,41). The pharmacotherapeutic assessment of the amphetamine-induced behavior, found clonidine to reduce repetitive behavior in the DAT-tg rats, whereas fluoxetine led to an unspecific reduction in locomotion in both groups. Dysfunction in the DA system and corticostriatal circuit has long been considered the driving force of repetitive pathophysiology (9–13,42). Accordingly, DAT-tg rats displayed increased DRD1 and DRD2 mRNA levels, increase in DA turnover and decrease in DA content in

the OFC, Nacc and CPu, that was paralleled with heightened MAO enzymatic activity – a finding also observed in TS (43). The imbalance in the corticostriatal circuit seen in repetitive disorders, is linked to striatal disinhibition due to specific disruption of Pv⁺ expressing interneurons (11,44–46). In correlation, DAT-tg rats displayed a significant reduction of Pv⁺ cells solely in the CPu, alongside heightened cortical activity measured by an increase in c-fos expression in the OFC. This collectively points towards the existence of corticostriatal dysbalance in the DAT-tg rats.

Following cognitive assessment, DAT-tg rats displayed a compromised ability to execute cognitive tasks. DA dysfunction within the nigrostriatal system as well as dorsal striatal lesions have both shown to result in inadequate spatial learning and memory abilities, which in mice and rats amongst others translates into increased thigmotaxis (47,48). Indeed, DAT-tg displayed continuous thigmotaxis when placed in the MWM, as well as the inability to employ spatial search strategies. To sustain spatial learning, there is the need for neurogenesis and cellular rearrangement within the hippocampus, in which DA signaling plays an important role (49,50). Neurobiological assessment showed no apparent difference in neuronal proliferation between the control and DAT-tg groups, yet the DAT-tg rats displayed a reduction in neuronal integration (BrdU⁺/NeuN⁺), indicating an insufficient incorporation of newly formed neurons into the hippocampal circuit. Whether the lack of neuronal integration is linked to the learning disabilities observed in the DAT-tg rats needs further assessment. Cognitive deficits such as inadequate spatial recognition memory and learning abilities are also observed in patients with TS, which is subsequently related to abnormal activity especially within the limbic corticostriatal circuit (15,51–53). As such, to fully comprehend the extent of the repetitive disease profile, there is the need for further investigations into its neuropsychological aspects. Here, the DAT-tg rat may be of help to disentangle the relationship between dopamine-induced corticostriatal dysfunction and subsequent cognitive impairments.

Taken together, apart from the expected dopaminergic alterations, direct overexpression of the DAT led to the formation of additional pathological events within key brain regions relevant to repetitive disorders. These abnormalities collectively resulted in an overall aberrant neuronal circuit, that translated into repetitive movements responsive towards TS-drug treatment, and to cognitive impairments also observed in the repetitive disease profile. As such, DAT overexpression seems to be implicated in the generation of repetitive behavior and its underlying pathophysiology, raising the need for further investigations into its role in repetitive disorders. Here the DAT-tg rat constitutes an ideal model for such investigations, also enabling the assessment of new therapeutic interventions targeted to affect the aberrant processes related to symptom generation.

Anodal tDCS improves behavioral and neurobiological deficits in the DAT-tg rat

DBS is an invasive treatment approach, that through direct stimulation modulates both the targeted structure and its associative circuitry (54). Apart from its therapeutic effect, DBS may also in preclinical settings, be employed to investigate the involvement of specific brain regions within a given disorder. The corticostriatal circuit is comprised of topographical organized sub-circuits individually linked to different aspects of the repetitive disorder profile. Undesirable movements are related to the sensorimotor sub-circuit, whereas cognitive deficits and comorbidity are linked to the limbic - and associative sub-circuits, respectively (55,56). Application of DBS to various brain areas in the DAT-tg rats showed that repetitive behavior observed in the DAT-tg model, was solely reduced when structures of the sensorimotor circuit were stimulated (M1 and CPu). Stimulating areas of the limbic/associative circuit (mPFC and OFC) had no effect. This indicates that generation of repetitive behavior in the DAT-tg rats mainly resides within the sensorimotor corticostriatal circuit.

Given the existence of cortical hyperexcitability, tDCS has been suggested as a non-invasive approach to tackle this particular pathological process involved in abnormal movements (26). However, despite some positive results, the most appropriate stimulation parameters and brain targets still need to be determined (57). When investigating the impact of frontal tDCS in the DAT-tg rats, the effect was polarity specific and followed a non-linear dose-dependency, as solely anodal tDCS at 200 μ A reduced repetitive behavior. On the contrary, same type of stimulation led to an increase in repetitive behavior in the WT rats (head movements). These findings counteract the classic approach of a dichotomous tDCS effect that solely involves a polarity-dependent shift in cortical excitability. Due to the presence of cortical hyperexcitability in the DAT-tg rats, cathodal stimulation would theoretically be ideal for symptomatic relief whereas anodal stimulation potentially could worsen symptoms. However, the positive effect of anodal stimulation in the DAT-tg rats as well as its opposing behavioral effects found in the WT rats, revealed that interacting parameters eventually determines the cumulative output of tDCS. Especially dopaminergic alterations have shown to interact with polarity effects of tDCS, with increased DA levels reversing anodal stimulation to resemble cathodal stimulation (58–62). As shown in study 1, DAT-tg rats display immense dopaminergic alterations as opposed to WT rats. This may be accountable for the opposing behavioral outcome between the two groups and underlines the notion of tDCS effects being state-dependent. In conjunction, anodal tDCS did not affect DA levels or turnover, indicating that the provided therapeutic effect goes beyond DA regulation.

The magnitude and location of current density following tDCS application has shown to vary across the cortex despite a uniform application (63). A computer model was constructed to assess the current flow pattern mediated by anodal tDCS (200 μ A) across the cortex. Here, results showed a prominent peak of current density and power dissipation above the coordinates correlating with the primary motor cortex (M1). Supporting our DBS findings, this indicates that improved movement control following anodal tDCS involves the sensorimotor circuit. In correlation, tic generation is linked to increased motor cortex excitability, which improves following M1 modulation (64–69). As assessed by c-fos mRNA levels, the application of frontal anodal tDCS increased the activity of the OFC and mPFC in the DAT-tg rats. No change was seen in the WT rats. Increased activity between frontal and sensorimotor area has been found in TS patients, who gain the ability to voluntarily suppress tics (70). The heightened activity in the DAT-tg rats after anodal tDCS, leaves thought for investigating the ability of tDCS to modify cortico-cortical interactions and subsequent behavior.

Further investigation into the subcortical effects, revealed a general decrease in striatal Pv+ mRNA levels following anodal tDCS in the DAT-tg rats. Decrease in PV+ mRNA levels have shown to enhance inhibition, whereas inhibition is reduced following loss of PV+ interneurons (71). The reduction of PV+ mRNA levels indicate that modulation of striatal activity is implicated in the effect of anodal tDCS in the DAT-tg rat. This shows that the therapeutic effect of tDCS goes beyond the direct modulation of cortical activity, and also includes regulation of subcortical activity properties. Indeed, circuit-wide modulation of anodal and not cathodal stimulation has been observed clinically (72). Interestingly, there was no behavioral effect of cathodal stimulation in DAT-tg rats, which may indicate that circuit-wide modulation is essential when seeking symptom relief. In correlation, a recent published clinical study found that cathodal tDCS is ineffective in patients with TS (73).

Taken together, this shows that when the appropriate protocol design is applied, anodal tDCS can mediate symptom relief in the DAT-tg rats through a modulation of both cortical and subcortical events residing within the sensorimotor circuit. This potentially sets the stage for using tDCS as a targeted treatment for repetitive disorders.

Limitations and future investigations

Animal models in general do not comprise the entire pathological spectrum of a human disorder. This thesis was based on an animal model with a distinct genetic abnormality considered involved

in neuropsychiatric disorders, including repetitive disorders. The generation of the DAT-tg model is driven by the NSE promoter, resulting in a ubiquitous DAT overexpression. Thus, the DAT-tg rat mainly constitutes an experimental framework, from which the consequences of DAT overexpression can be assessed. Employing other animal models in parallel to the DAT-tg rat, that are generated based on other etiologies, would essentially allow for a more complex insight into the repetitive pathophysiology and subsequent treatment effects of tDCS.

Behavioral data in preclinical settings are averaged across groups to become evident, which renders the possibility of taking endophenotypes into account. Patients with repetitive disorders such as TS consist of a heterogeneous patient group, including treatment responders and treatment resistant patients (74). Thus, individual assessment in accordance to endophenotype is needed. Indeed, tDCS effects have shown to produce both within-participant and intra-patient variability, which has been linked to the inconsistent results often seen across tDCS studies (75). As a positive consequence of this observation, further studies into endophenotypes and intra-patient variabilities may allow for a future personalized application of tDCS fitted to the individual needs of the patient.

Bibliography

1. Parker GB, Graham RK. Determinants of treatment-resistant depression: the salience of benzodiazepines. *The Journal of nervous and mental disease*. 2015 Sep 1;203(9):659-63.
2. Baldessarini RJ. The Impact of Psychopharmacology on Contemporary Psychiatry. *Can J Psychiatry CanJPsychiatry*. 2014;5959(88):401–5.
3. McHugh PC, Buckley DA. The structure and function of the dopamine transporter and its role in CNS diseases. In *Vitamins & Hormones* 2015 Jan 1 (Vol. 98, pp. 339-369). Academic Press.
4. Serra-Mestres J, Ring HA, Costa DC, Gacinovic S, Walker Z, Lees AJ, Robertson MM, Trimble MR. Dopamine transporter binding in Gilles de la Tourette syndrome: a [¹²³I] FP-CIT/SPECT study. *Acta Psychiatrica Scandinavica*. 2004 Feb;109(2):140-6.
5. Paschou P. The genetic basis of Gilles de la Tourette Syndrome. *Neuroscience & Biobehavioral Reviews*. 2013 Jul 1;37(6):1026-39
6. Singer HS, Szymanski S, Giuliano J, Yokoi F, Dogan AS, Brasic JR, Zhou Y, Grace AA, Wong DF. Elevated intrasynaptic dopamine release in Tourette's syndrome measured by PET. *American Journal of Psychiatry*. 2002 Aug 1;159(8):1329-36.
7. Ernst M, Zametkin AJ, Jons PH, Matochik JA, Pascualvaca D, Cohen RM. High presynaptic dopaminergic activity in children with Tourette's disorder. *Journal of the American Academy of Child & Adolescent Psychiatry*. 1999 Jan 1;38(1):86-94.
8. Cheon KA, Ryu YH, Namkoong K, Kim CH, Kim JJ, Lee JD. Dopamine transporter density of the basal ganglia assessed with [¹²³I] IPT SPECT in drug-naive children with Tourette's disorder. *Psychiatry Research: Neuroimaging*. 2004 Jan 15;130(1):85-95
9. Buse J, Schoenefeld K, Münchau A, Roessner V. Neuromodulation in Tourette syndrome: dopamine and beyond. *Neuroscience & Biobehavioral Reviews*. 2013 Jul 1;37(6):1069-84.
10. Mink JW. Basal ganglia dysfunction in Tourette's syndrome: a new hypothesis. *Pediatric neurology*. 2001 Sep 1;25(3):190-8
11. Singer HS, Minzer K. Neurobiology of Tourette's syndrome: concepts of neuroanatomic localization and neurochemical abnormalities. *Brain and Development*. 2003 Jan 1;25:S70-84.
12. Leckman JF, Vaccarino FM, Kalanithi PS, Rothenberger A. Annotation: Tourette syndrome: a relentless drumbeat—driven by misguided brain oscillations. *Journal of Child Psychology and Psychiatry*. 2006 Jun;47(6):537-50.
13. Leckman JF, Bloch MH, Smith ME, Larabi D, Hampson M. Neurobiological substrates of Tourette's disorder. *Journal of child and adolescent psychopharmacology*. 2010 Aug 1;20(4):237-47.
14. Haber SN. Corticostriatal circuitry. *Dialogues Clin Neurosci*. 2016;18(1):7–21.
15. Morand-Beaulieu S, Leclerc JB, Valois P, Lavoie ME, O'Connor KP, Gauthier B. A review of the neuropsychological dimensions of Tourette syndrome. *Brain sciences*. 2017 Aug 18;7(8):106.
16. Szechtman H, Ahmari SE, Beninger RJ, Eilam D, Harvey BH, Edemann-Callesen H, Winter C. Obsessive-compulsive disorder: Insights from animal models. *Neuroscience & Biobehavioral Reviews*. 2017 May 1;76:254-79.
17. Bortolato M, Pittenger C. Modeling tics in rodents: Conceptual challenges and paths forward. *Journal of neuroscience methods*. 2017 Dec 1;292:12-9.
18. Matthysse S. Animal models in psychiatric research. In *Progress in brain research* 1986 Jan 1 (Vol. 65, pp. 259-270). Elsevier.
19. Andrade P, Visser-Vandewalle V. DBS in Tourette syndrome: where are we standing now?. *Journal of Neural Transmission*. 2016 Jul 1;123(7):791-6.
20. Frait A, Pal G. Deep brain stimulation in Tourette's syndrome. *Frontiers in neurology*. 2015 Aug 4;6:170.
21. Bour LJ, Ackermans L, Foncke EM, Cath D, Van Der Linden C, Vandewalle VV, Tijssen MA. Tic related local field potentials in the thalamus and the effect of deep brain stimulation in Tourette syndrome: report of three cases. *Clinical Neurophysiology*. 2015 Aug 1;126(8):1578-88.
22. Priori A, Giannicola G, Rosa M, Marceglia S, Servello D, Sassi M, Porta M. Deep brain electrophysiological recordings provide clues to the pathophysiology of Tourette syndrome.

- Neuroscience & Biobehavioral Reviews. 2013 Jul 1;37(6):1063-8.
23. Nitsche MA, Paulus W. Sustained excitability elevations induced by transcranial DC motor cortex stimulation in humans. *Neurology*. 2001 Nov 27;57(10):1899-901.
 24. Nitsche MA, Cohen LG, Wassermann EM, Priori A, Lang N, Antal A, Paulus W, Hummel F, Boggio PS, Fregni F, Pascual-Leone A. Transcranial direct current stimulation: state of the art 2008. *Brain stimulation*. 2008 Jul 1;1(3):206-23
 25. Nitsche MA, Schauenburg A, Lang N, Liebetanz D, Exner C, Paulus W, Tergau F. Facilitation of implicit motor learning by weak transcranial direct current stimulation of the primary motor cortex in the human. *Journal of cognitive neuroscience*. 2003 May 15;15(4):619-26
 26. Mrakic-Spota S, Marceglia S, Mameli F, Dilena R, Tadini L, Priori A. Transcranial direct current stimulation in two patients with Tourette syndrome. *Movement disorders: official journal of the Movement Disorder Society*. 2008 Nov 15;23(15):2259-61
 27. Mondino M, Bennabi D, Poulet E, Galvao F, Brunelin J, Haffen E. Can transcranial direct current stimulation (tDCS) alleviate symptoms and improve cognition in psychiatric disorders?. *The World Journal of Biological Psychiatry*. 2014 May 1;15(4):261-75.
 28. Carvalho S, Gonçalves ÓF, Soares JM, Sampaio A, Macedo F, Fregni F, Leite J. Sustained effects of a neural-based intervention in a refractory case of Tourette syndrome. *Brain Stimulation: Basic, Translational, and Clinical Research in Neuromodulation*. 2015 May 1;8(3):657-9.
 29. Eapen V, Baker R, Walter A, Raghupathy V, Wehrman JJ, Sowman PF. The Role of Transcranial Direct Current Stimulation (tDCS) in Tourette Syndrome: A Review and Preliminary Findings. *Brain sciences*. 2017 Dec 8;7(12):161
 30. Ridding MC, Ziemann U. Determinants of the induction of cortical plasticity by non-invasive brain stimulation in healthy subjects. *The Journal of physiology*. 2010 Jul 1;588(13):2291-304.
 31. Stagg CJ, Nitsche MA. Physiological basis of transcranial direct current stimulation. *The Neuroscientist*. 2011 Feb;17(1):37-53
 32. Jackson MP, Rahman A, Lafon B, Kronberg G, Ling D, Parra LC, Bikson M. Animal models of transcranial direct current stimulation: methods and mechanisms. *Clinical Neurophysiology*. 2016 Nov 1;127(11):3425-54
 33. Carter CJ, Pycock CJ. The effects of 5, 7-dihydroxytryptamine lesions of extrapyramidal and mesolimbic sites on spontaneous motor behaviour, and amphetamine-induced stereotypy. *Naunyn-Schmiedeberg's Archives of Pharmacology*. 1979 Jul 1;308(1):51-4
 34. Paxinos G, Watson C. *The Rat Brain in Stereotaxic Coordinates*. Acad Press San Diego. 1997;3rd.
 35. Song W, Truong DQ, Bikson M, Martin JH. Transspinal direct current stimulation immediately modifies motor cortex sensorimotor maps. *Journal of neurophysiology*. 2015 Feb 11;113(7):2801-11
 36. Datta A, Bansal V, Diaz J, Patel J, Reato D, Bikson M. Gyri-precise head model of transcranial direct current stimulation: improved spatial focality using a ring electrode versus conventional rectangular pad. *Brain stimulation*. 2009 Oct 1;2(4):201-7
 37. Minhas P, Bansal V, Patel J, Ho JS, Diaz J, Datta A, Bikson M. Electrodes for high-definition transcutaneous DC stimulation for applications in drug delivery and electrotherapy, including tDCS. *Journal of neuroscience methods*. 2010 Jul 15;190(2):188-97
 38. Denys D, de Vries F, Cath D, Figeet M, Vulink N, Veltman DJ, van der Doef TF, Boellaard R, Westenberg H, van Balkom A, Lammertsma AA. Dopaminergic activity in Tourette syndrome and obsessive-compulsive disorder. *European neuropsychopharmacology*. 2013 Nov 1;23(11):1423-31
 39. Leckman JF. Tourette's syndrome. *The Lancet*. 2002 Nov 16;360(9345):1577-86.
 40. McNaught KS, Mink JW. Advances in understanding and treatment of Tourette syndrome. *Nature Reviews Neurology*. 2011 Dec;7(12):667.
 41. Montgomery SA, McIntyre A, Osterheider M, Sarteschi P, Zitterl W, Zohar J, Birkett M, Wood AJ, Lilly European OCD Study Group. A double-blind, placebo-controlled study of fluoxetine in patients with DSM-III-R obsessive-compulsive disorder. *European Neuropsychopharmacology*. 1993 Jun 1;3(2):143-52.
 42. Haber SN. Corticostriatal circuitry. *Dialogues Clin Neurosci*. 2016;18(1):7-21.
 43. Shapiro AK, Baron M, Shapiro E, Levitt M. Enzyme activity in Tourette's syndrome. *Archives of neurology*. 1984 Mar 1;41(3):282-5

44. Kalanithi PS, Zheng W, Kataoka Y, DiFiglia M, Grantz H, Saper CB, Schwartz ML, Leckman JF, Vaccarino FM. Altered parvalbumin-positive neuron distribution in basal ganglia of individuals with Tourette syndrome. *Proceedings of the National Academy of Sciences*. 2005 Sep 13;102(37):13307-12
45. Kataoka Y, Kalanithi PS, Grantz H, Schwartz ML, Saper C, Leckman JF, Vaccarino FM. Decreased number of parvalbumin and cholinergic interneurons in the striatum of individuals with Tourette syndrome. *Journal of Comparative Neurology*. 2010 Feb 1;518(3):277-91
46. Koós T, Tepper JM. Inhibitory control of neostriatal projection neurons by GABAergic interneurons. *Nature neuroscience*. 1999 May;2(5):467
47. Mura A, Feldon J. Spatial learning in rats is impaired after degeneration of the nigrostriatal dopaminergic system. *Movement disorders: official journal of the Movement Disorder Society*. 2003 Aug;18(8):860-71.
48. Pooters T, Gantois I, Vermaercke B, D'hooge R. Inability to acquire spatial information and deploy spatial search strategies in mice with lesions in dorsomedial striatum. *Behavioural brain research*. 2016 Feb 1;298:134-41
49. McNamara CG, Tejero-Cantero Á, Trouche S, Campo-Urriza N, Dupret D. Dopaminergic neurons promote hippocampal reactivation and spatial memory persistence. *Nature neuroscience*. 2014 Dec;17(12):1658
50. Gasbarri A, Sulli A, Innocenzi R, Pacitti C, Brioni JD. Spatial memory impairment induced by lesion of the mesohippocampal dopaminergic system in the rat. *Neuroscience*. 1996 Oct 1;74(4):1037-44.
51. Rasmussen C, Soleimani M, Carroll A, Hodlevskyy O. Neuropsychological functioning in children with Tourette syndrome (TS). *Journal of the Canadian Academy of Child and Adolescent Psychiatry*. 2009 Nov;18(4):307
52. Watkins LH, Sahakian BJ, Robertson MM, Veale DM, Rogers RD, Pickard KM, Aitken MR, Robbins TW. Executive function in Tourette's syndrome and obsessive-compulsive disorder. *Psychological medicine*. 2005 Apr;35(4):571-82.
53. Jeter CB, Patel SS, Morris JS, Chuang AZ, Butler IJ, Sereno AB. Oculomotor executive function abnormalities with increased tic severity in Tourette syndrome. *Journal of Child Psychology and Psychiatry*. 2015 Feb;56(2):193-202
54. Tye SJ, Frye MA, Lee KH. Disrupting disordered neurocircuitry: treating refractory psychiatric illness with neuromodulation. In *Mayo Clinic Proceedings* 2009 Jun 1 (Vol. 84, No. 6, pp. 522-532). Elsevier.
55. Tremblay L, Worbe Y, Thobois S, Sgambato-Faure V, Féger J. Selective dysfunction of basal ganglia subterritories: from movement to behavioral disorders. *Movement Disorders*. 2015 Aug;30(9):1155-70.
56. Groenewegen HJ, van den Heuvel OA, Cath DC, Voorn P, Veltman DJ. Does an imbalance between the dorsal and ventral striatopallidal systems play a role in Tourette's syndrome? A neuronal circuit approach. *Brain and Development*. 2003 Jan 1;25:S3-14
57. Pedroarena-Leal N, Ruge D. Toward a Symptom-Guided Neurostimulation for Gilles de la Tourette Syndrome. *Frontiers in psychiatry*. 2017 Feb 27;8:29
58. Baeken C, Brunelin J, Duprat R, Vanderhasselt MA. The application of tDCS in psychiatric disorders: a brain imaging view. *Socioaffective neuroscience & psychology*. 2016 Jan 1;6(1):29588
59. Nitsche MA, Lampe C, Antal A, Liebetanz D, Lang N, Tergau F, Paulus W. Dopaminergic modulation of long-lasting direct current-induced cortical excitability changes in the human motor cortex. *European Journal of Neuroscience*. 2006 Mar;23(6):1651-7
60. Kuo MF, Paulus W, Nitsche MA. Boosting focally-induced brain plasticity by dopamine. *Cerebral Cortex*. 2007 Jun 24;18(3):648-51.
61. Monte-Silva K, Liebetanz D, Grundey J, Paulus W, Nitsche MA. Dosage-dependent non-linear effect of l-dopa on human motor cortex plasticity. *The Journal of physiology*. 2010 Sep 15;588(18):3415-24
62. Hasan A, Nitsche MA, Rein B, Schneider-Axmann T, Guse B, Gruber O, Falkai P, Wobrock T. Dysfunctional long-term potentiation-like plasticity in schizophrenia revealed by transcranial direct current stimulation. *Behavioural brain research*. 2011 Oct 10;224(1):15-22
63. Jackson MP, Rahman A, Lafon B, Kronberg G, Ling D, Parra LC, Bikson M. Animal models of

- transcranial direct current stimulation: methods and mechanisms. *Clinical Neurophysiology*. 2016 Nov 1;127(11):3425-54
64. Ziemann U, Paulus W, Rothenberger A. Decreased motor inhibition in Tourette's disorder: evidence from transcranial magnetic stimulation. *The American journal of psychiatry*. 1997 Sep 1;154(9):1277
 65. Stern E, Silbersweig DA, Chee KY, Holmes A, Robertson MM, Trimble M, Frith CD, Frackowiak RS, Dolan RJ. A functional neuroanatomy of tics in Tourette syndrome. *Archives of general psychiatry*. 2000 Aug 1;57(8):741-8
 66. Berardelli A, Currà A, Fabbrini G, Gilio F, Manfredi M. Pathophysiology of tics and Tourette syndrome. *Journal of neurology*. 2003 Jul 1;250(7):781-7.
 67. Mantovani, A., Lisanby, S.H., Pieraccini, F., Ulivelli, M., Castrogiovanni, P. and Rossi, S., 2006. Repetitive transcranial magnetic stimulation (rTMS) in the treatment of obsessive-compulsive disorder (OCD) and Tourette's syndrome (TS). *International Journal of Neuropsychopharmacology*, 9(1), pp.95-100.
 68. Serrien DJ, Orth M, Evans AH, Lees AJ, Brown P. Motor inhibition in patients with Gilles de la Tourette syndrome: functional activation patterns as revealed by EEG coherence. *Brain*. 2004 Oct 20;128(1):116-25.
 69. Orth M, Münchau A, Rothwell JC. Corticospinal system excitability at rest is associated with tic severity in Tourette syndrome. *Biological psychiatry*. 2008 Aug 1;64(3):248-51.
 70. Jackson SR, Parkinson A, Jung J, Ryan SE, Morgan PS, Hollis C, Jackson GM. Compensatory neural reorganization in Tourette syndrome. *Current Biology*. 2011 Apr 12;21(7):580-5.
 71. Schwaller B. The use of transgenic mouse models to reveal the functions of Ca²⁺ buffer proteins in excitable cells. *Biochimica et Biophysica Acta (BBA)-General Subjects*. 2012 Aug 1;1820(8):1294-303
 72. Polanía R, Paulus W, Nitsche MA. Modulating cortico-striatal and thalamo-cortical functional connectivity with transcranial direct current stimulation. *Human brain mapping*. 2012 Oct;33(10):2499-508
 73. Behler N, Leitner B, Mezger E, Weidinger E, Musil RL, Blum B, Kirsch B, Wulf L, Löhns L, Winter C, Padberg F. Cathodal tDCS over motor cortex does not improve Tourette Syndrome: Lessons learned from a case series. *Frontiers in behavioral neuroscience*. 2018;12:194
 74. McNaught KS, Mink JW. Advances in understanding and treatment of Tourette syndrome. *Nature Reviews Neurology*. 2011 Dec;7(12):667
 75. Filmer HL, Dux PE, Mattingley JB. Applications of transcranial direct current stimulation for understanding brain function. *Trends in neurosciences*. 2014 Dec 1;37(12):742-53.

Affidavit

I, Henriette Edemann Callesen certify under penalty of perjury by my own signature that I have submitted the thesis on the topic “**An investigation into the repetitive pathophysiology and the effect of a non-invasive targeted treatment strategy in an animal model overexpressing the dopamine transporter**”. I wrote this thesis independently and without assistance from third parties, I used no other aids than the listed sources and resources.

All points based literally or in spirit on publications or presentations of other authors are, as such, in proper citations (see "uniform requirements for manuscripts (URM)" the ICMJE www.icmje.org) indicated. The sections on methodology (in particular practical work, laboratory requirements, statistical processing) and results (in particular images, graphics and tables) correspond to the URM (s.o) and are answered by me. My contributions in the selected publications for this dissertation correspond to those that are specified in the following joint declaration with the responsible person and supervisor. All publications resulting from this thesis and which I am author of correspond to the URM (see above) and I am solely responsible.

The importance of this affidavit and the criminal consequences of a false affidavit (section 156,161 of the Criminal Code) are known to me and I understand the rights and responsibilities stated therein.

_____ Date

Signature

Declaration of any eventual publications

Henriette Edemann Callesen had the following share in the following publications:

Publication 1: Hadar, R., **Edemann-Callesen, H.**, Reinel, C., Wieske, F., Voget, M., Popova, E., Sohr, R., Avchalumov, Y., Priller, J., Van Riesen, C. and Puls, I. Rats overexpressing the dopamine transporter display behavioral and neurobiological abnormalities with relevance to repetitive disorders. Scientific reports, 6. (2016). Impact Factor: **4.1**

Contribution in detail:

- Established the repetitive behavioural testing paradigm.
- Conducted the following experiments: the startle stress response, pre-pulse inhibition, elevated plus maze, forced swim test and sucrose consumption test, amphetamine-induced stereotypy, clonidine/fluoxetine treatment and MRI analysis. This led to the data found in figure 6a, figure 7c-g and figure 8a-b.
- Contributed to the data interpretation and statistical analyses of the results found in figure 6a, figure 7c-g and figure 8a-b,
- Contributed to the writing, submission and revision of the manuscript.

Publication 2: Bernhardt N, Lieser MK, Hlusicka EB, Habelt B, Wieske F, **Edemann-Callesen H**, Garthe A, Winter C. Learning deficits in rats overexpressing the dopamine transporter. Scientific reports. 2018 Sep 21;8(1):14173. Impact Factor: **4.1**

Contribution in detail:

- Contributed to the overall interpretation of results
- Contributed to the writing of the manuscript
- Contributed to the revision and final approval of the manuscript.

Publication 3: **Edemann-Callesen, H.**, Habelt, B, Wieske, F, Jackson, M, Khadka, N, Mattei, D, Bernhardt, N, Heinz, A, Liebetanz, D, Bikson, M, Padberg, F, Hadar, R, Nitsche, M.A, Winter, C. Non-invasive modulation reduces repetitive behavior in a rat model through the sensorimotor cortico-striatal circuit. Translational Psychiatry. (2017) Impact Factor: **5.6**

Contribution in detail:

- Established the tDCS testing paradigm
- Conducted the tDCS and DBS surgeries
- Conducted the behavioural testing and tDCS/DBS application, that led to the data found in figure 1
- Contributed to the data interpretation and statistical analysis of the results found in figure 1, figure 3, figure 4, table 1, figure 5, figure S2, figure S3, table S3 and figure S4
- Wrote the manuscript
- Submitted and revised the manuscript


Signature, date and stamp of the supervising University teacher

_____ Date

Signature of the doctoral candidate

_____ Date

SCIENTIFIC REPORTS



OPEN

Rats overexpressing the dopamine transporter display behavioral and neurobiological abnormalities with relevance to repetitive disorders

Ravit Hadar¹, Henriette Edemann-Callesen^{1,2}, Claudia Reinel¹, Franziska Wieske¹, Mareike Voget^{1,2}, Elena Popova³, Reinhard Sohr¹, Yosef Avchalumov¹, Josef Priller⁴, Christoph van Riesen⁵, Imke Puls⁶, Michael Bader^{3,7,8,9} & Christine Winter¹

Received: 08 April 2016
Accepted: 18 November 2016
Published: 15 December 2016

The dopamine transporter (DAT) plays a pivotal role in maintaining optimal dopamine signaling. DAT-overactivity has been linked to various neuropsychiatric disorders yet so far the direct pathological consequences of it has not been fully assessed. We here generated a transgenic rat model that via pronuclear microinjection overexpresses the DAT gene. Our results demonstrate that DAT-overexpression induces multiple neurobiological effects that exceeded the expected alterations in the corticostriatal dopamine system. Furthermore, transgenic rats specifically exhibited behavioral and pharmacotherapeutic profiles phenotypic of repetitive disorders. Together our findings suggest that the DAT rat model will constitute a valuable tool for further investigations into the pathological influence of DAT overexpression on neural systems relevant to neuropsychiatric disorders.

In the realm of neuroscience, preclinical studies promote our understanding of normal and pathological brain function as well as the development of new treatment strategies and are thus invaluable. This leads to ongoing innovation and generation of new model rodents. The development of new models is either done by the selection of existing phenomena or the rationale driven manipulation of a specific mechanism. The latter may comprise environmental, pharmacological or genetic manipulations. Genetic models start with addressing the etiology of the modeled disorder¹ however they may only be considered complete upon meeting further construct, face and predictive validity criteria. In neuro-psychiatry etiology is mostly obscure, forcing scientists into testing the assumed etiology by comprehensively evaluating the consequences of the manipulation on aspects of brain and behavior known to be aberrant in the modeled disorder. Preclinical studies succumb to a classical differentiation between mice and rats, such that it is mostly mice, which provide rationale-driven genetic models whereas rats are devoted to behavioral and environmental manipulations, due to their superior social and behavioral repertoire. Clearly, the latter is the essence of psychiatric disorders, hence genetic rat models would ideally incorporate both aspects.

Interdisciplinary evidence suggests a pivotal role of the dopamine system and the corticostriatal circuitry² in the pathology underlying repetitive disorders. Reduced tonic extracellular³, increased presynaptic⁴, and pharmacologically released intrasynaptic dopamine contents⁵ as well as increased dopamine receptor availability⁶, suggests an overactive dopamine transporter (DAT)^{7,8} in repetitive disorders, including Tourette syndrome (TS). Still, investigations into the direct consequences of DAT overexpression is underrepresented in preclinical studies with only very few models that allow insights into its relation to such neuropsychiatric disorders.

¹Department of Psychiatry and Psychotherapy, University Hospital Carl Gustav Carus, Technische Universität, Dresden, Germany. ²International Graduate Program Medical Neurosciences, Charité Universitätsmedizin Berlin, Germany. ³Max-Delbrück-Center for Molecular Medicine, Berlin, Germany. ⁴Department of Neuropsychiatry and Laboratory of Molecular Psychiatry, Charité Universitätsmedizin Berlin, Cluster of Excellence NeuroCure, BIH and DZNE, Berlin, Germany. ⁵Department of Neurology, Charité Universitätsmedizin Berlin, Germany. ⁶Klinik für Psychiatrie und Psychotherapie, Charité Universität, Berlin, Germany. ⁷Department of Endocrinology, Charité Universitätsmedizin Berlin, Germany. ⁸Institute for Biology, University of Lübeck, Lübeck, Germany. ⁹Department of Physiology and Biophysics, Federal University of Minas Gerais, Belo Horizonte, Brazil. Correspondence and requests for materials should be addressed to C.W. (email: christine.winter@uniklinikum-dresden.de)

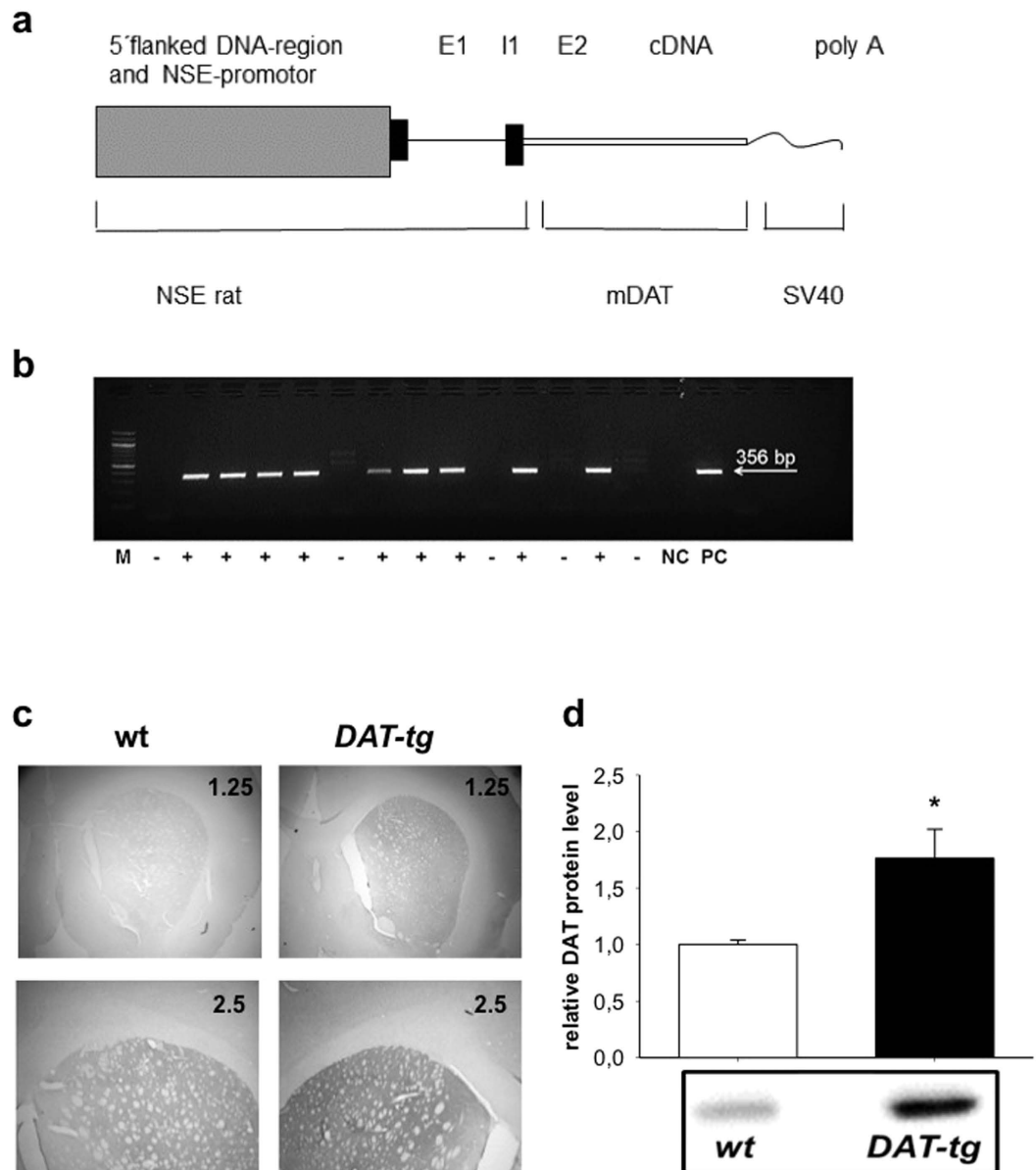


Figure 1. Generation of *DAT-tg* rats. (a) Schematic representation of the 4-kb DNA fragment used for the generation of the *DAT* transgenic rats. E1/2 = exon 1/2, and I1 = intron 1 of NSE, m*DAT* = murine *DAT* sequence, SV40 = Simian virus 40. (b) Representative *DAT* PCR products from *wt* (-) and *DAT-tg* (+) rats. M = marker, NC = negative control, PC = positive control, transgenic band = 356 bp. One founder line was used for the study. Here one litter from this generation is shown. (c) Representative coronal sections of immunohistochemical stain of *DAT* expression for *wt* (left) and *DAT-tg* (right). (d) *DAT* Western blot analysis of striatal tissue from *wt* (n = 5) and *DAT-tg* rats (n = 10).

On this basis we created a transgenic rat model that via pronuclear microinjection overexpresses the *DAT* gene (Fig. 1). Neurobiological and behavioral studies were conducted on adult male hemizygous *DAT*-transgenic rats (*DAT-tg*) ubiquitously overexpressing *DAT* in the corticostriatal and associated networks.

Results

***DAT* and *DRD1/2* receptor expression.** Western blot and qPCR were performed in order to assess the protein and mRNA expression levels of the dopamine transporter (*DAT*). qPCR was conducted to assess mRNA expression levels of the dopamine receptor 1 (*DRD1*), and dopamine receptor 2 (*DRD2*). Western blots showed that in comparison to *wt* rats, *DAT-tg* rats exhibited increased striatal protein-levels of the *DAT* transporter (striatum: $T = -2.171$, $p = 0.05$) (Fig. 1d). qPCR showed that in comparison to *wt* rats *DAT-tg* rats exhibited significantly increased *DAT* mRNA levels in the following areas: medial prefrontal cortex (mPFC ($T = -2.588$, $p = 0.023$)), orbitofrontal cortex (OFC ($T = 9.161$, $p = 0.000$)), nucleus accumbens (Nacc ($T = -2.755$, $p = 0.016$)), caudate putamen (CPu ($T = -8.337$, $p = 0.000$)), globus pallidus (GP ($T = -4.579$, $p = 0.000$)),

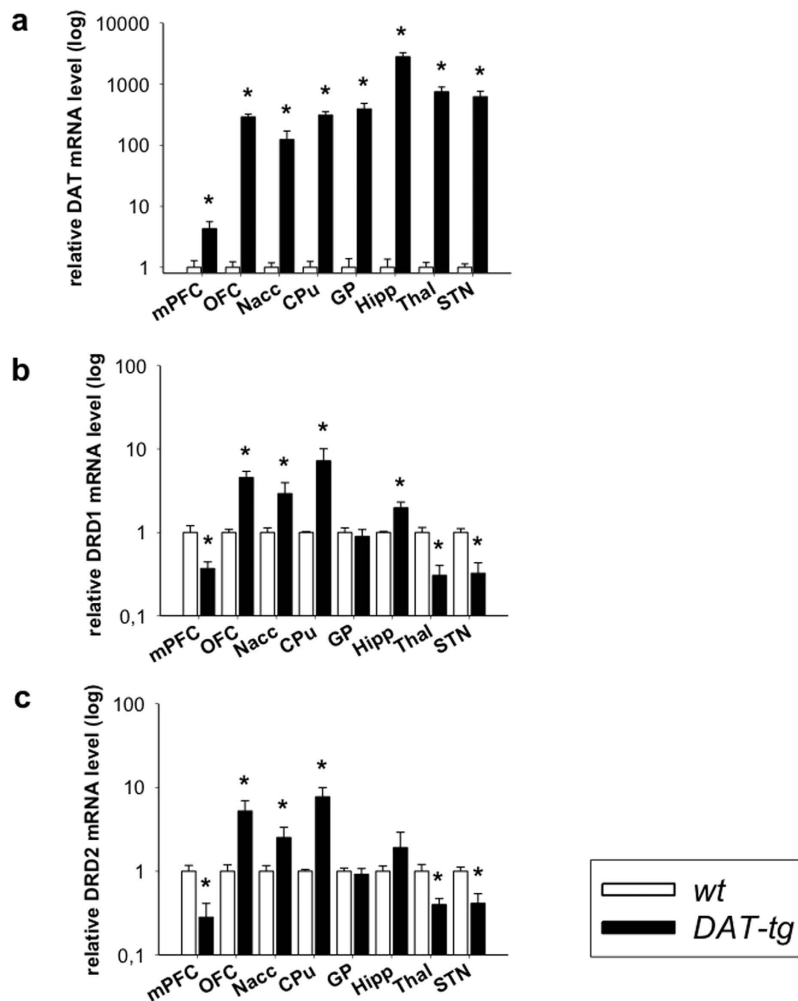


Figure 2. DAT and DRD1/2 receptor expression. (a) DAT qPCR analysis of corticostriatal and associated network regions in *wt* ($n = 8$) and *DAT-tg* rats ($n = 7$). (b) Dopamine receptor 1 (DRD1) and (c) Dopamine receptor 2 (DRD2) qPCR analysis of corticostriatal and associated network regions in *wt* ($n = 8$) and *DAT-tg* rats ($n = 7$). mPFC: medial prefrontal cortex, OFC: orbitofrontal cortex, Nacc: nucleus accumbens, CPu: caudate putamen, GP: globus pallidus, Hipp: hippocampus, Thal: dorsomedial thalamus, STN: subthalamic nucleus. All data are means \pm s.e.m. Asterisk (*) indicates significant difference to *wt* rats with $p < 0.05$.

hippocampus (Hipp ($T = 6.463$, $p = 0.001$)), thalamus (Thal ($T = -5.410$, $p = 0.000$)), and subthalamic nucleus (STN ($T = -4.589$, $p = 0.000$)) (Fig. 2a). Further, *DAT-tg* rats exhibited increased DRD1 mRNA levels in the OFC ($T = -3.534$, $p = 0.000$), Nacc ($T = -2.136$, $p = 0.029$), CPu ($T = -6.217$, $p = 0.036$) and Hipp ($T = -3.089$, $p = 0.009$) and decreased DRD1 mRNA levels in the mPFC ($T = 2.756$, $p = 0.016$), Thal ($T = 3.812$, $p = 0.002$) and STN ($T = 4.332$, $p = 0.000$) (Fig. 2b). In a similar fashion, DRD2 receptors were upregulated in the OFC ($T = -2.610$, $p = 0.022$), Nacc ($T = -1.917$, $p = 0.029$) and CPu ($T = -3.252$, $p = 0.006$) whereas levels were downregulated in the mPFC ($T = 3.246$, $p = 0.006$), Thal ($T = 2.646$, $p = 0.02$) and STN ($T = 3.414$, $p = 0.005$) (Fig. 2c).

Neurotransmitter contents and compensatory mechanisms. Post mortem HPLC was conducted to assess neurochemical contents of different neurotransmitter system. *DAT-tg* rats exhibited a decrease in tissue dopamine contents in the OFC ($T = -7.504$, $p = 0.000$), Nacc ($T = -13.726$, $p = 0.000$) and CPu ($T = -14.611$, $p = 0.000$), whereas an increase in dopamine was seen in the Hipp ($T = 2.617$, $p = 0.020$) and STN ($T = 2.414$, $p = 0.029$). With regards to metabolites and turnover, *DAT-tg* rats exhibited increased DOPAC contents and dopamine turnover (DOPAC/dopamine) in the mPFC (DOPAC: $T = 4.255$, $p = 0.000$; turnover: $T = 2.916$, $p = 0.011$), OFC ($T = 3.225$, $p = 0.006$; turnover: $T = 13.467$, $p = 0.000$), Nacc ($T = 4.391$, $p = 0.000$; turnover: $T = 7.542$, $p = 0.000$), CPu ($T = 9.134$, $p = 0.000$; turnover: $T = 19.314$, $p = 0.000$), GP ($T = 6.177$, $p = 0.000$; turnover: $T = 7.417$, $p = 0.000$), Hipp ($T = 5.884$, $p = 0.000$; turnover: $T = 1.35$, $p = 0.022$), Thal ($T = 4.009$, $p = 0.001$; turnover: $T = 1.505$, $p = 0.001$) and STN ($T = 4.503$, $p = 0.000$; turnover: $T = 2.962$, $p = 0.010$) (Fig. 3a–c). For glutamate, *DAT-tg* rats exhibited increased contents in the CPu ($T = 2.701$, $p = 0.016$), GP ($T = 4.934$, $p = 0.000$) and STN ($T = 4.113$, $p = 0.000$) whereas a decrement was found in the thalamus ($T = -4.574$, $p = 0.000$). With respect to GABA, *DAT-tg* rats exhibited decreased contents in the Nacc ($T = -2.665$, $p = 0.018$) and GP

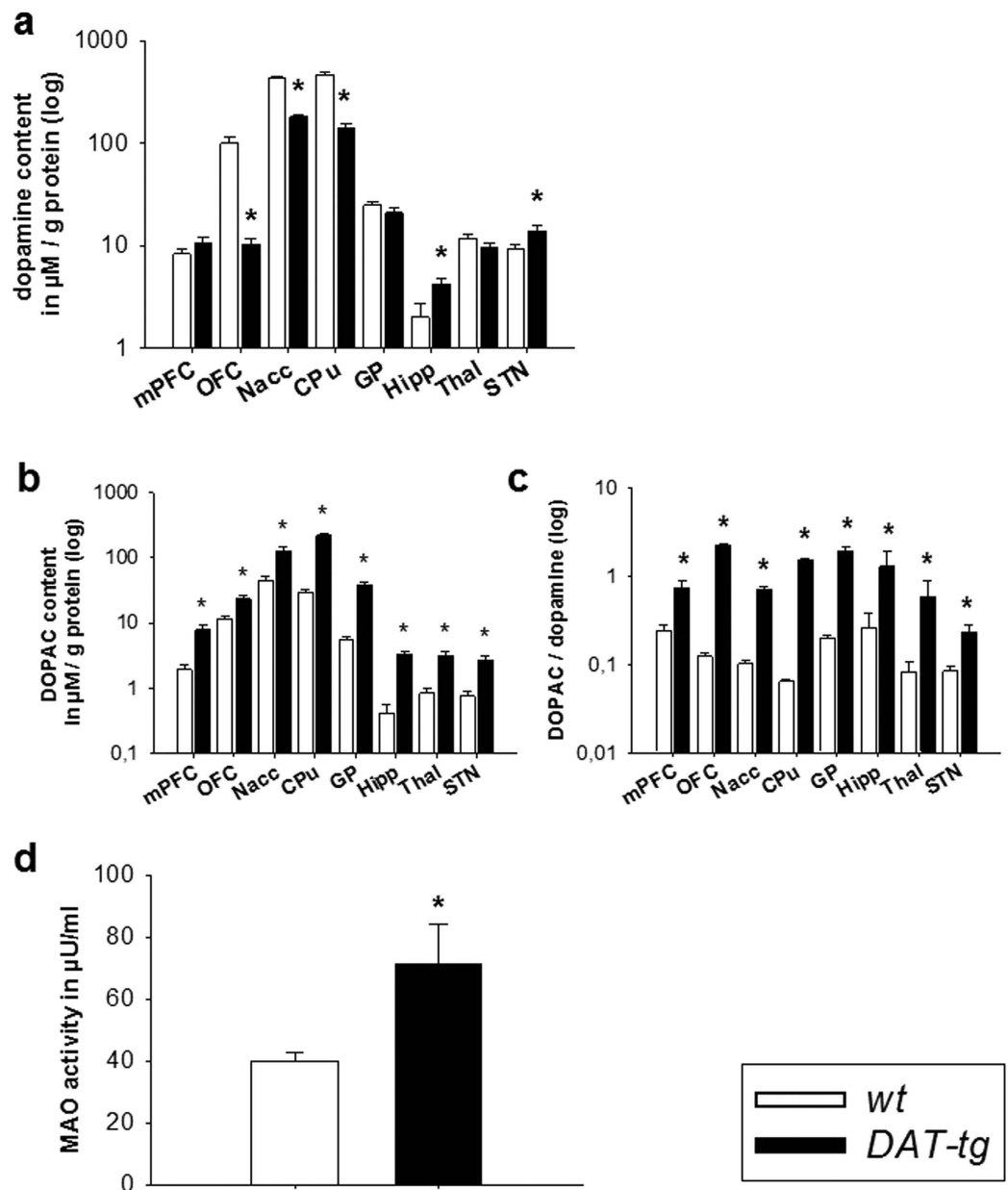


Figure 3. Neurotransmitter contents and compensatory mechanisms. Post mortem tissue (a) dopamine and (b) DOPAC contents as well as (c) dopamine turnover in corticostriatal and associated network regions in *wt* ($n = 7$) and *DAT-tg* rats ($n = 10$). mPFC: medial prefrontal cortex, OFC: orbitofrontal cortex, Nacc: nucleus accumbens, CPu: caudate putamen, GP: globus pallidus, Hipp: hippocampus, Thal: dorsomedial thalamus, STN: subthalamic nucleus. (d) Monoamine oxidase (MAO) activity of striatal tissues in *wt* ($n = 8$) and *DAT-tg* rats ($n = 7$). All data are means \pm s.e.m. Asterisk (*) indicates significant difference to *wt* rats with $p < 0.05$.

($T = -2.231$, $p = 0.041$) and increased contents in the mPFC ($T = 2.962$, $p = 0.009$), OFC ($T = 3.161$, $p = 0.006$) and CPu ($T = 3.449$, $p = 0.004$) (Fig. 4).

To investigate for possible compensatory mechanisms, monoamine oxidase (MAO) activity was assessed in striatal tissues. *DAT-tg* rats here exhibited a significant increase in total MAO activity as opposed to the *wt* rats ($T = -2.470$, $p = 0.028$) (Fig. 3d).

Oscillatory activity. Oscillatory activity within the vmPFC, Nacc and STN was investigated via *in vivo* electrophysiological recording. The assessed frequency bands included: theta (4–8 Hz), alpha (8–12 Hz), beta (12–30 Hz), and gamma (30–100 Hz). Results show that in comparison to *wt* rats *DAT-tg* rats exhibited increased alpha, beta and gamma activity within the STN (alpha: $T = -8.667$, $p = 0.000$; beta: $T = -8.972$, $p = 0.000$; gamma: $T = -2.781$, $p = 0.006$) as well as increased beta and gamma activity within the mPFC (beta: $T = -6.701$, $p = 0.000$; gamma: $T = -3.389$, $p = 0.000$) and Nacc (beta: $T = -3.723$, $p = 0.000$; gamma: $T = -2.594$, $p = 0.01$) (Fig. 5a).

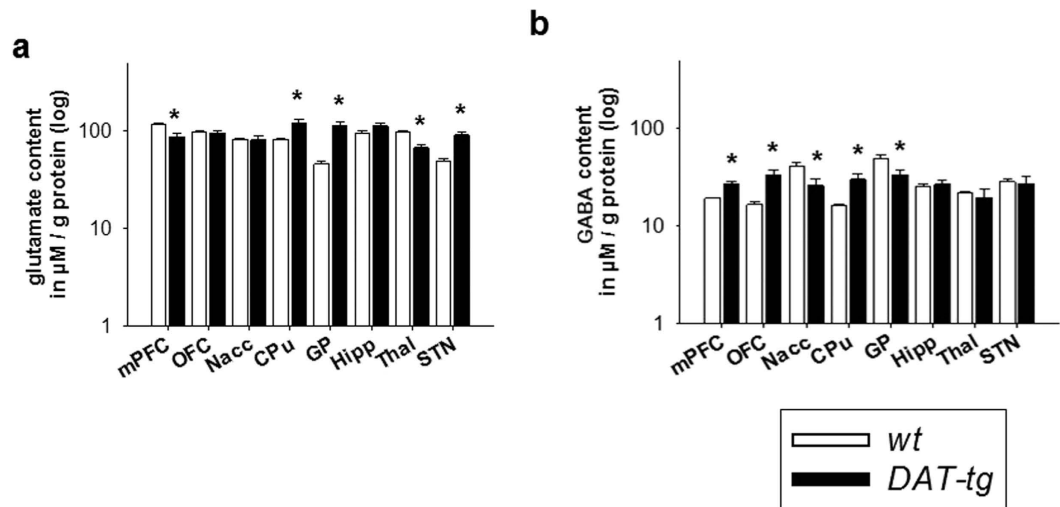


Figure 4. Glutamate and GABA contents. Neurochemical contents were examined in *wt* ($n = 7$) and *DAT-tg* rats ($n = 10$). Glutamate and GABA were measured in the medial prefrontal cortex (mPFC), orbitofrontal cortex (OFC), nucleus accumbens (Nacc), caudate putamen (CPu), globus pallidus (GP), hippocampus (Hipp), dorsomedial thalamus (Thal), and subthalamic nucleus (STN). All data are means \pm s.e.m. Asterisk (*) indicates significant difference to *wt* rats with $p < 0.05$.

Immunostaining. Immunostaining of parvalbumin expressing (PV)+ interneurons, c-Fos expressing nuclei and Ki67 expressing cells was conducted to investigate for possible cellular changes reflecting altered network activity. Results show that *DAT-tg* rats exhibited a significant reduction of PV+ cells specifically in the CPu as opposed to *wt* rats ($T = 3.228$, $p = 0.004$) (Fig. 5b). Further, *DAT-tg* rats exhibited a significant increase in cFos expressing cells specifically in the OFC as compared to *wt* rats ($T = -2.884$, $p = 0.011$) (Fig. 5c). No significant difference was found for Ki67 expression between *DAT-tg* and *wt* rats (Fig. 5d).

Structural analysis of brain volumes. The whole brain volume and the volumes of the mPFC, Hipp, and CPu were assessed using structural MRI. *DAT-tg* rats exhibited a significant increase in Hipp volumes as compared to the *wt* rats ($T = -3.326$, $p = 0.01$) alongside unaltered whole brain volumes (Fig. 6a). NeuN immunostaining further revealed no difference between *DAT-tg* and *wt* rats (Fig. 6b).

General behavioral assessment. *Wt* and *DAT-tg* rats were weighed across lifespan and body weights of *DAT-tg* rats were analyzed relative to body weight of age-matched *wt* rats. T-Test revealed *DAT-tg* rats to have significantly decreased body weights in comparison to *wt* rats across lifespan ($T = 6.801$, $P = 0.000$) (Fig. 7a). Figure 7b locomotion was analyzed as the total distance travelled on an open field over 30 min. T-Test revealed *DAT-tg* rats to travel significantly less than *wt* rats ($T = 5.745$, $P = 0.001$) (Fig. 7b). Figure 7a to study repetitive behavior upon stress-exposure, rats were exposed to unpredictable acoustic stimuli. T-test revealed *DAT-tg* rats to show a tendency towards more grooming ($T = -2.070$, $P = 0.063$) when compared to *wt* rats, but no significant increment in the number of whole body shakes ($T = -1.527$, $P = 0.156$) (Fig. 7c).

In the prepulse inhibition (PPI) paradigm, *DAT-tg* rats showed normal sensorimotor gating when compared to *wt* rats such that they expressed an unaltered suppression of the acoustic startle reflex (ASR) following acoustic stimuli of 69 db, 73 db, and 81 db. However *DAT-tg* rats did show increased overall ASR reflecting hyper-arousal ($T = -2.449$, $P = 0.024$) (Fig. 7d). In the elevated-plus-maze and the forced swim test, no difference were found between *DAT-tg* rats and *wt* rats (Fig. 7e,f). In the sucrose consumption test *DAT-tg* rats showed when compared to *wt* rats a tendency to increased anhedonia as expressed in a reduced consumption of sweetened condense milk ($T = 1.659$, $P = 0.071$) (Fig. 7g).

Repetitive behavior analysis. Repetitive behavior was assessed following the application of amphetamine (0.5 mg/kg, 2.0 mg/kg, and 5.0 mg/kg body weight (BW)) and saline over three consecutive days. To diminish the possibility of amphetamine-sensitization, dosages were applied in a randomized fashion. The assessed behavior included: no locomotion, locomotion, excessive rearing and sniffing as well as oral stereotypy and head movements. Administration of 0.5 mg/kg amphetamine was ineffective in both strains and administration of 5.0 mg/kg amphetamine induced repetitive behavior in both, *wt* and *DAT-tg* rats. Upon administration of 2.0 mg/kg amphetamine, *DAT-tg* rats exhibited a significant increase in repetitive oral movements ($T = -3.545$, $p = 0.003$), which effectively emerged 80–120 min after injection, whereas *wt* rats exhibited hyper-locomotion throughout the observation period ($T = 4.718$, $P = 0.000$) (Fig. 8a).

The effect of clonidine (0.01 mg/kg BW) and fluoxetine (20 mg/kg BW) versus saline on amphetamine (2 mg/kg BW) -induced behavior was assessed with respect to general movement and oral stereotypy. Same animals were exposed to drug administrations over a period of three consecutive days, with dosages applied in a randomized fashion. For the effect of clonidine on oral stereotypy, ANOVA revealed a significant effect for the factor

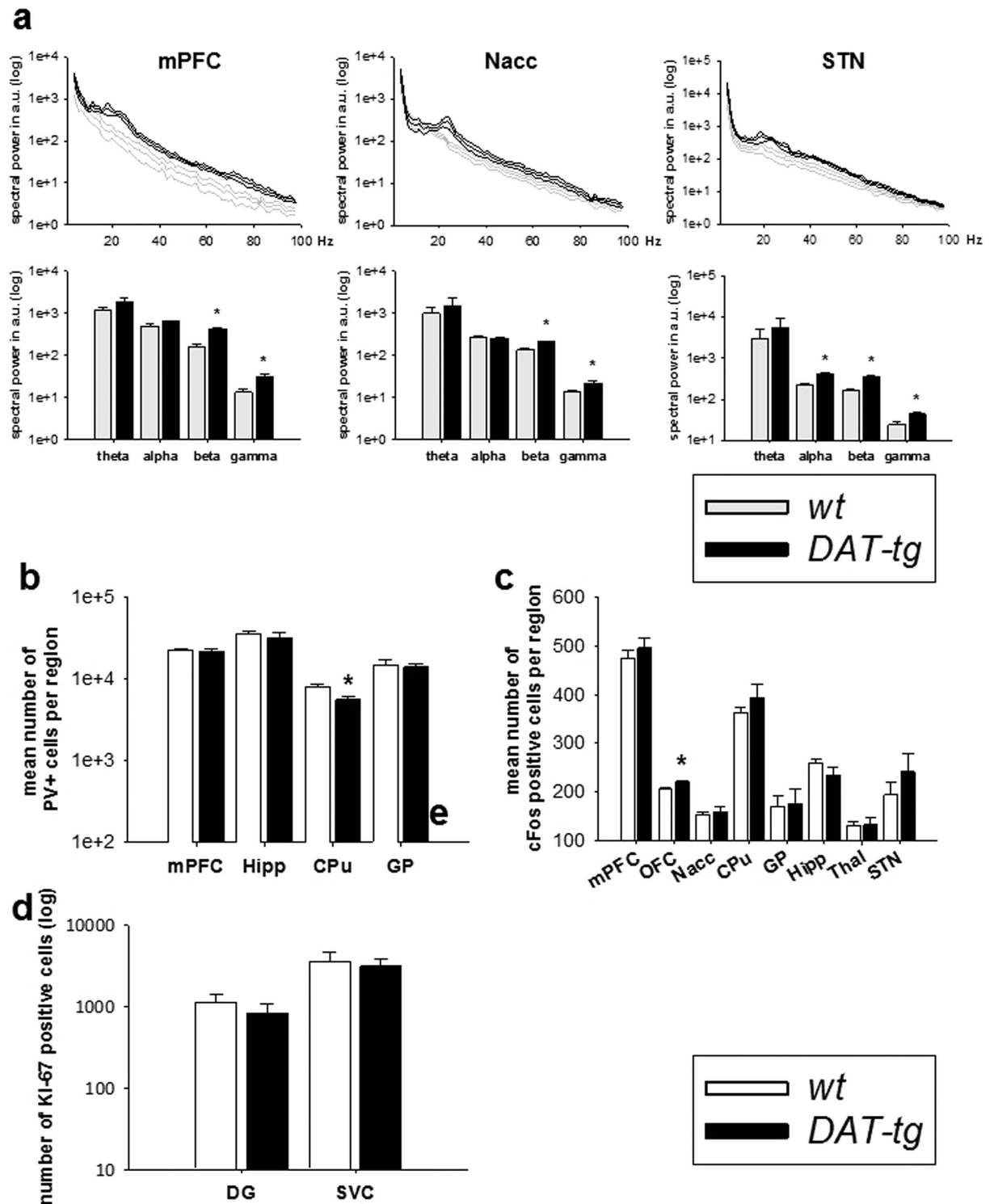


Figure 5. Oscillatory activity and immunostaining. (a) Oscillatory activity of the vmPFC, Nacc and STN in *wt* ($n = 5$) and *DAT-tg* rats ($n = 7$). Upper panel shows entire frequency range, lower panel shows mean values for the frequency bands: theta (4–8 Hz), alpha (8–12 Hz), beta (12–30 Hz), and gamma (30–100 Hz). (b) Immunohistochemical cell counts of parvalbumin expressing (PV+) cells of the medial prefrontal cortex (mPFC), hippocampus (Hipp), caudate putamen (CPu) and globus pallidus (GP) in *wt* ($n = 12$) and *DAT-tg* rats ($n = 11$). (c) c-Fos expressing cells on representative slices of the mPFC, orbitofrontal cortex (OFC), nucleus accumbens (Nacc), CPu, GP, Hipp, thalamus (Thal) and subthalamic nucleus (STN) in *wt* ($n = 8$) and *DAT-tg* rats ($n = 8$). (d) Immunohistochemical cell counts of Ki67 expressing cells in the neurogenic zones of the hippocampus (dentate gyrus, DG) and the subventricular zone (SVZ) in *wt* ($n = 9$) and *DAT-tg* rats ($n = 9$).

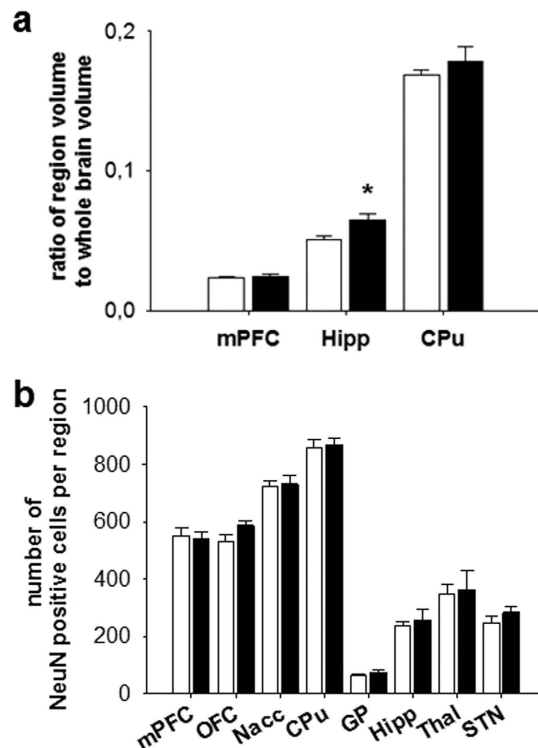


Figure 6. Structural analysis. (a) Volumes of the medial prefrontal cortex (mPFC), hippocampus (Hipp) and caudate putamen (CPu) relative to whole brain volumes as derived from MRI scans in *wt* ($n = 6$) and *DAT-tg* rats ($n = 4$). (b) NeuN expressing cells on representative slices of the mPFC, orbitofrontal cortex (OFC), nucleus accumbens (Nacc), CPu, globus pallidus (GP), Hipp, thalamus (Thal) and subthalamic nucleus (STN) in *wt* ($n = 7$) and *DAT-tg* rats ($n = 5$). All data are means \pm s.e.m. Asterisk (*) indicates significant difference to *wt* rats ($p < 0.05$).

phenotype ($F = 6.598$, $p = 0.019$) and a significant interaction ($F = 6.887$, $p = 0.018$). Subsequent post hoc analysis revealed that untreated *DAT-tg* rats exhibited significantly more repetitive behavior than untreated *wt* rats ($p < 0.05$) and that clonidine significantly reduced repetitive behavior in *DAT-tg* rats ($p < 0.05$). With regards to the effects of clonidine on locomotion, no significant effect was found. The effect of fluoxetine on oral stereotypy showed a significant effect for the factors phenotype ($F = 27.061$, $p = 0.000$) and treatment ($F = 10.382$, $p = 0.006$) with *DAT-tg* rats displaying significantly more repetitive behavior than *wt* rats and fluoxetine reducing it in both, *wt* and *DAT-tg* rats. With regards to the effect of fluoxetine on locomotion, a significant effect of treatment was found ($F = 15.127$, $p = 0.001$) (Fig. 8b) such that fluoxetine reduced locomotion in both, *wt* and *DAT-tg* rats.

The effect of quinpirole (0.5 mg/kg BW) and saline on compulsive checking and grooming was assessed using the following groups: *wt* + saline, *wt* + quinpirole, *DAT-tg* + saline, *DAT-tg* + quinpirole. For compulsive checking, a significant effect was found for phenotype ($F = 11.464$, $p = 0.003$) as well as a significant interaction across the factors phenotype and treatment. ($F = 5.283$, $p = 0.032$). Subsequent post hoc analysis revealed that quinpirole treated *wt* rats exhibited significantly more compulsive checking behavior as compared to untreated *wt* ($p < 0.05$) and quinpirole treated *DAT-tg* rats ($p < 0.05$). For grooming, a significant effect was found for both factors (phenotype: $F = 22.960$, $p = 0.001$; treatment: $F = 17.091$, $p = 0.003$) as well as a significant interaction ($F = 21.278$, $p = 0.002$) (Fig. 8b). Figure 8c following up on these effects, post hoc analysis revealed that in *DAT-tg* but not *wt* ($p < 0.05$) quinpirole significantly increased grooming when compared to saline conditions ($p < 0.05$).

Discussion

Our results show that overexpression of the DAT induces multiple neurobiological and behavioral deficits that have also been observed in repetitive disorders.

Involuntary repetitive movements have shown to worsen under stress and upon amphetamine challenge. Such accentuated susceptibility to amphetamine has been reported for TS and differentiates this condition from obsessive-compulsive disorders (OCD), a further disorder belonging to the repetitive spectrum⁹. In terms of pharmacotherapy, the alpha-adrenergic and imidazoline receptor agonist α -clonidine serves as first line treatment due to its efficacy and tolerability^{10,11}.

In rats, a typical expression of repetitive movements is grooming¹². We here report, that *DAT-tg* rats showed increased grooming upon stress exposure. Upon d-amphetamine administration, both *wt* and *DAT-tg* rats developed repetitive behavior¹³. However, *DAT-tg* rats developed repetitive behavior already at amphetamine dosages ineffective in *wt* rats suggesting a susceptibility to amphetamine. This low-dose amphetamine induced repetitive behavior manifested over time with maximal expression 80–120 min after drug administration. It

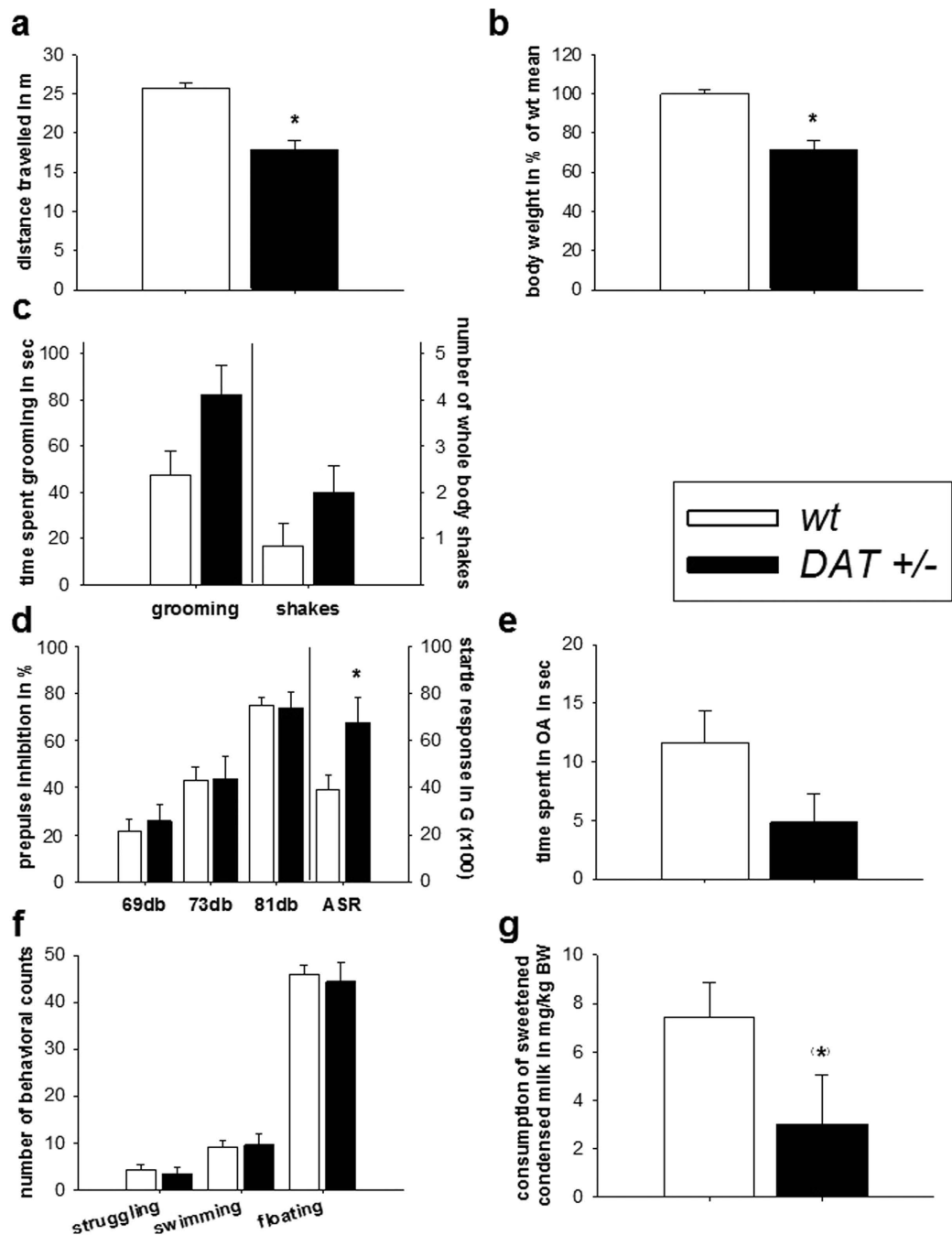


Figure 7. General behavioral assessment. General assessment of hemizygote *DAT* transgenic (*DAT-tg*) rats in comparison to *wt* rats. (a) *wt* and *DAT-tg* rats were weighed across lifespan. Body weight of *DAT-tg* rats was analyzed relative to body weight of age-matched *wt* rats. (b) Locomotion was analyzed as the total distance travelled on an open field over 30 min in each *n* = 10 *wt* and *DAT-tg* rats. (c) To study repetitive behavior upon stress-exposure, each *n* = 7 *wt* and *DAT-tg* rats were placed within the chambers used for prepulse inhibition (PPI) test and exposed to unpredictable acoustic stimuli. (d) Sensorimotor gating and arousal was analyzed in the PPI paradigm in *wt* (*n* = 14) and *DAT-tg* rats (*n* = 7). (e) Anxious behavior was measured in the elevated-plus-maze in *wt* (*n* = 15) and *DAT-tg* rats (*n* = 6). (f) In the forced swim test, the amount of time spent on struggling, swimming and floating was analyzed in *wt* (*n* = 14) and *DAT-tg* rats (*n* = 7). (g) In the sucrose consumption test the amount of sweetened condense milk consumed relative to body weight (BW) was measured in *wt* rats (*n* = 16) and *DAT-tg* rats (*n* = 7). All data are given as mean \pm s.e.m. Asterisks (*) indicates significant difference between groups with $p < 0.05$.

consisted of fragmented grooming patterns of face and paws that rarely continued into a full-body grooming syntax, and was associated with a typical motor confinement. Interestingly, this particular behavior was also

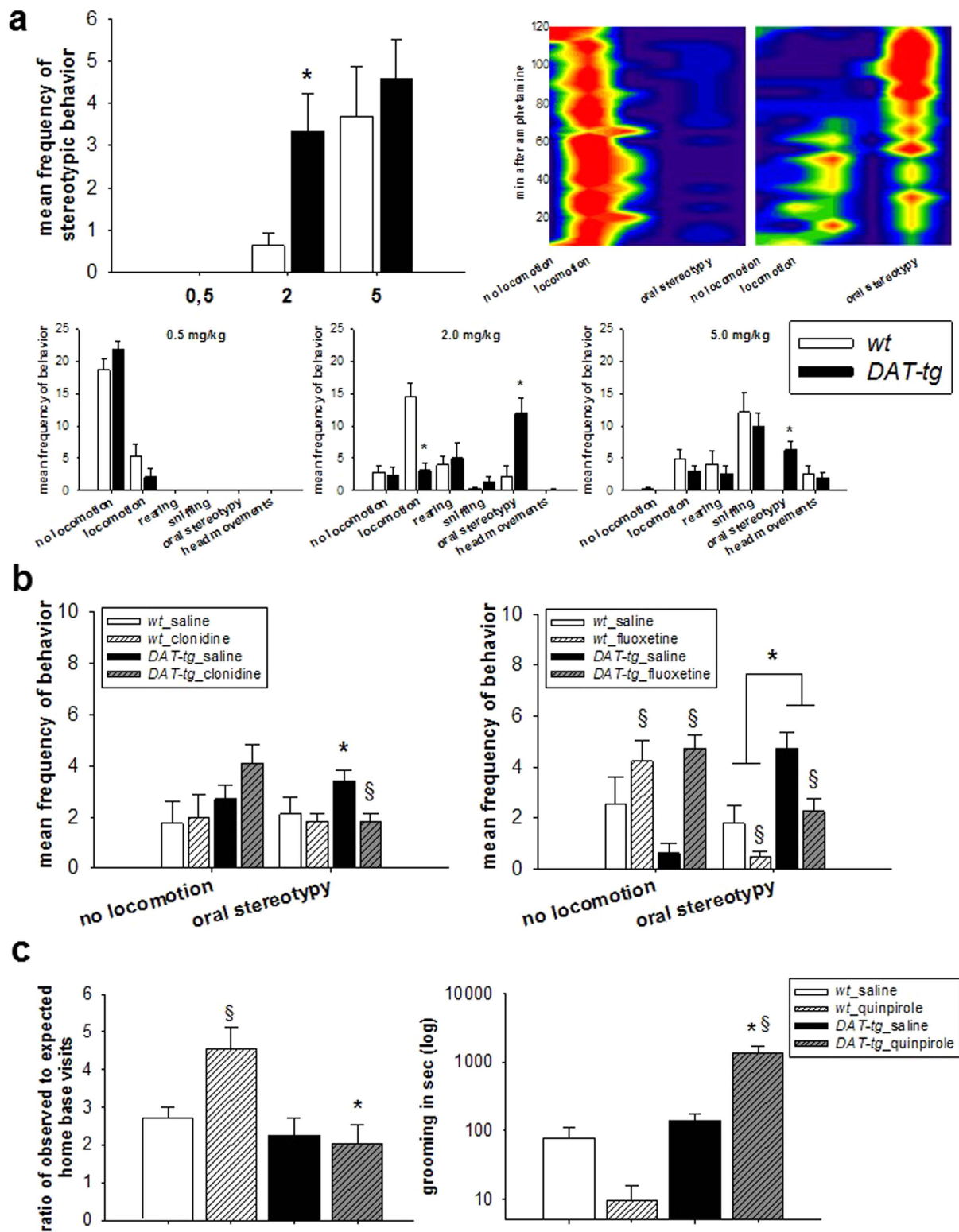


Figure 8. Repetitive behavior analysis. (a) Upper panel left: Repetitive behavior induced by d-amphetamine (0.5, 2.0 and 5.0 mg per kg body weight (BW)). Upper panel right: In *DAT-tg* rats, repetitive behavior evolves 80–120 min after d-amphetamine (2 mg/kg BW). The *wt* rats display hyperlocomotion throughout the period (120 min). Hot colors (red) indicate presence and cold colors (blue) absence of behavior. Lower panel: dose-dependent effects of d-amphetamine. (b) Clonidine effects (left) and fluoxetine (right) on locomotion and oral stereotypy following d-amphetamine (2 mg/kg BW) in *wt* (clonidine: $n = 10$; fluoxetine: $n = 9$) and *DAT-tg* rats (clonidine: $n = 9$; fluoxetine: $n = 8$). (c) Effects of quinpirole (QNP) on compulsive checking (left) and grooming behavior (right) in *wt* ($n = 10$) and *DAT-tg* rats ($n = 10$). All data are means \pm s.e.m. Asterisk (*) indicates significant difference to *wt* rats, paragraph (§) indicates treatment effect ($p < 0.05$).

the dominant behavior observed upon chronic intermittent application of the DRD2/DRD3 agonist quinpirole, which in *wt* rats induced compulsive checking behavior as previously reported^{14–16}. Despite increased arousal and a tendency to anhedonia *DAT-tg* rats displayed intact sensorimotor gating, and scored normal in anxiety- and depression-associated paradigms. All together this suggests that behavioral abnormalities in *DAT-tg* rats are largely restricted to repetitive behavior symptomatology.

Testing pharmacotherapy, we found that clonidine specifically reduced repetitive behavior in *DAT-tg* rats whereas the serotonin reuptake inhibitor (SSRI) fluoxetine did not selectively affect repetitive behavior in *DAT-tg* rats. As expected, fluoxetine decreased locomotion in both phenotypes¹⁷. Clonidine is known to alleviate tics in TS whereas SSRI agents have been shown to ameliorate repetitive symptoms in OCD but not in TS.

The potential utility of *DAT-tg* rats in the context of repetitive disorder research is further supported by the neurobiological investigations of this study. TS has previously been associated with increased and decreased dopamine receptor availability^{6,9,18,19} and dopamine contents^{5,18,20–22}. We found that ubiquitously induced DAT overexpression induced a region specific pattern of up- and downregulation. *DAT-tg* rats showed relative overexpression of DRD1 + DRD2 in the OFC, CPu and Nacc. This was further paralleled by increased striatal MAO enzymatic activity, previously linked to TS²³. Increased MAO activity leads to increased dopamine turnover, resulting in decreased dopamine levels. In contrast, DRD1 + DRD2 expressions were downregulated in the mPFC, Thal and STN and dopamine contents were reduced in the Thal and STN, which suggests a reciprocal regulation of dopamine receptor expression and tissue dopamine contents²⁴.

In TS patients, an altered balance between GABAergic cells and glutamatergic projections is associated with abnormal corticostriatal circuit activity². This imbalance is thought to result from reduced numbers of GABAergic parvalbumin expressing (PV+) interneurons. In accordance with that *DAT-tg* displayed region-specific increments and decrements in GABAergic and glutamatergic contents in the corticostriatal circuit. Further, we found a reduction of PV+ interneurons in *DAT-tg* rats as compared to *wt* rats. In line with clinical data^{25,26}, this reduction was restricted to the CPu. Striatal PV+ interneurons coordinate striatal activity by increasing medium spiny neurons' (MSN) firing threshold in response to cortical inputs^{25,27}. Loss of PV+ interneurons found in TS patients is suggested to lead to MSN hyperactivity^{25,26}. Both MSN and PV+ cells express dopamine receptors and depending on the membrane-potential are susceptible to dopaminergic activation^{27,28}. The excessive depolarized state of MSNs facilitates the effect of dopamine on MSNs, which further reinforces their hyperactivity. As such, abnormalities in the striatal PV+ interneuron and dopamine systems may together induce an excessive activation of the cortico-striato-thalamic circuit leading to repetitive behavior^{28,29}.

Further linkages of *DAT-tg* to repetitive disorders were gained by studies into neuronal cellular and population activity. *DAT-tg* rats exhibited upregulation of c-Fos in the OFC. Increased OFC activity is observed in patients with repetitive disorders^{29,30}. *DAT-tg* rats further displayed increased beta and gamma oscillations in the mPFC, Nacc and STN and increased alpha oscillation in the STN. Beta activity in the STN is associated with movement abnormalities and inversely regulated by mesostriatal dopamine³¹. Alpha and gamma activity has been associated with spontaneous tic exertion and TS³². In general, alterations in LFP oscillatory activity are proposed as biomarkers of dopamine dysfunction³¹ and neuro-psychiatric disorders³³.

Ectopic DAT overexpression has previously been linked to neurotoxic events including oxidative stress and neuronal loss^{34–36}. To explore whether DAT overexpression induced neuropathological changes in the *DAT-tg* rat, we measured the volume of the mPFC, the striatum and the hippocampus as these areas in the *DAT-tg* rat displayed both ectopic DAT expression and dopaminergic input but showed differential effects of DAT-overexpression on DA contents. MRI data displayed no atrophy in either the mPFC or the CPu but increased Hipp volumes in *DAT-tg* as compared to control rats. Increased Hipp volumes have been suggested to constitute a compensatory response in TS³⁷. Further immunostaining of the neuron-specific marker (NeuN) revealed no difference between the phenotypes, which stresses the notion that ubiquitous overexpression of DAT does not induce neurotoxicity in the *DAT-tg* rat.

Our findings support the hypothesis that the DAT may constitute one important key component in repetitive pathophysiology and that DAT overexpression might be of relevance for further comprehension of neurobiological mechanisms underlying neuropsychiatric disorders.

Experimental Procedures

Rats. Rats were housed in a temperature- and humidity-controlled vivarium with a 12-h light dark cycle (lights on 06:00 a.m.) with food and water available ad libitum. The study was carried out in accordance with the European Communities Council Directive of 22th September 2010 (2010/63/EU) and after approval by the local ethic committees (Senate of Berlin and Regierungspräsident Dresden). All efforts were made to reduce animal suffering and number of animals used.

Preparation of the construct. The pcDNA3-murine dopamine transporter³⁸ (mDAT) cDNA-vector was kindly provided by Heinz Bönisch (Institute of Pharmacology and Toxicology, University of Bonn, Germany) (Fig. 1a). It contains the full coding region of the mDAT cDNA and has been cloned by PCR with a sense primer derived from the partial mDAT gene sequence and an antisense primer deduced from the rat DAT cDNA. In this construct the CMV promoter was replaced by the rat NSE promoter isolated from the pNSE-Ex4 vector comprising 2.6 kb of 5'-untranslated sequence plus exon 1, intron 1, and 6 bp of exon 2 but not the ATG start codon of NSE. Sequencing was performed by the University of Calgary DNA Sequencing Laboratory to confirm the sequence of the construct. The construct consisting of NSE promoter, mDAT coding sequence, and bovine growth hormone polyadenylation sequence was excised from the pcDNA3 vector with NruI/NaeI, purified by agarose gel electrophoresis and gel extraction using the QIAquick gel extraction kit and used for microinjection. The NSE promoter was chosen for the expression of DAT to avoid probable unpredictable effects due to increment in monoamine in dopaminergic nerve endings.

Generation of transgenic rats was conducted as reported previously³⁹. Briefly, immature female Sprague-Dawley (SD) Hanover rats (28 to 35-day-old from Janvier Labs, France) were induced to superovulate by intraperitoneal (i.p.) injection of PMSG (15 IU, Intervet) and hCG (30 IU Sigma). Thereafter, rats were mated with fertile males and 24 h later sacrificed to collect fertilized eggs. The DNA construct was microinjected into the pronucleus of zygotes^{40,41}. Eggs were cultured for two hours and the surviving DNA-injected zygotes were transferred into the oviducts of pseudopregnant SD recipients at the day the vaginal plug was detected. Integration of the transgene was determined by transgene-specific PCRs with genomic DNA isolated from tail biopsies of the offspring after weaning (Fig. 1b). Neurobiological and behavioral studies were conducted on adult male hemizygous *DAT*-transgenic rats (*DAT-tg*) ubiquitously overexpressing *DAT* in the corticostriatal and the associated networks. Wildtype (*wt*) rats served as controls. Immunohistochemical staining of *DAT* expression was carried out for *wt* and *DAT-tg* rats (Fig. 1c).

Tissue processing. For Western blotting (WB), quantitative real time PCR (qPCR), and post mortem HPLC, and MAO activity assay, rats were decapitated and micropunches were taken bilaterally from 0.5–1 mm thick brain slices from the medial prefrontal cortex (mPFC), orbitofrontal cortex (OFC), thalamus (Thal), hippocampus (Hipp), nucleus accumbens (Nacc), caudate putamen (CPu), globus pallidus (GP) and subthalamic nucleus (STN) as described previously⁴². The total RNA and protein was extracted using the NucleoSpin RNA/Protein-Kit (Machery-Nagel, Düren, Germany). For immunostaining, rats were transcardially perfused, brains postfixed in 4% paraformaldehyde and cryosectioned in 40- μ m serial coronal frozen sections.

Western blotting. Protein concentrations were determined using a Nanodrop Spectrophotometer (peqlab) (UV 280 nm). Samples (pooled Nacc and CPu specimen only) were loaded alongside Precision Plus Protein Kaleidoscope Standards (Bio-Rad), subjected to discontinuous electrophoresis on 10% SDS-polyacrylamide gels and then transferred onto PVDF membranes (Roht) by electroblotting. Membranes were first incubated in SuperBlock T20 (TBS) Blocking Buffer (Lifetechnologies) at room temperature for 1 hour, and then incubated at 4 °C overnight with the primary antibodies: anti-DAT (1:200 dilution, Santa Cruz, sc-14002). A β -actin antibody (1:800 dilution, Cell Signaling, 4967S) was used for internal control. Membranes were washed and incubated with horseradish peroxidase-conjugated secondary antibodies (1:5000 dilution, Amersham, ECL Rabbit IgG, HRP-linked whole antibody: GE Healthcare Life Science NA934) at room temperature for one hour. For repeated analysis, membranes were stripped with Restore™ Plus Western Blot Stripping Buffer (ThermoFisher). Detection of immunoreactive bands was conducted using the Western lighting plus enhanced chemiluminescence (ECL) reagent (PerkinElmer) on a cooled charge-coupled device camera (FLI Proline PL09000, PA, USA). Images were processed using the Image J software.

qPCR. RNA concentrations were determined using a Nanodrop Spectrophotometer (peqlab). cDNA was synthesized using the High Capacity RNA-to-cDNA Kit (Lifetechnologies). TaqMan qPCR was performed with StepOne Real-Time PCR System (Lifetechnologies) using TaqMan fast advanced master mix (Lifetechnologies). The following TaqMan Gene Expression assays (Lifetechnologies) were used: *DAT* (Rn00562224_m1), *DRD1* (Rn 03062203_s1), and *DRD2* (Rn01418275_m1). CT values were normalized to the house keeping gene *GFAP* (Rn00566603_m1, Lifetechnologies), fold change was calculated using the $\Delta\Delta$ CT method.

Monoamine oxidase activity assay. For assessing monoamine oxidase (MAO) activity, CPu punches were homogenized by ultrasonication in 70 μ l assay buffer of a fluorometric assay kit (biovision K795–100). MAO activity was assessed according to the user manual.

Post mortem HPLC. Post mortem HPLC was conducted as described previously⁴². Dopamine and its metabolite DOPAC were separated on a column (ProntoSil 120-3-C18-SH; Bischoff Analysentechnik und -geräte GmbH, Germany) and electrochemically detected (Chromsystems Instruments & Chemicals GmbH, Germany). Glutamate and GABA were precolumn-derivatized with *o*-phthalaldehyde-2-mercaptoethanol, separated on a column (ProntoSil C18 ace-EPS) and detected by their fluorescence at 450 nm after excitation at 330 nm.

Immunostaining. Free-floating sections were stained with antibodies against Ki67 (1:500, Novocastra, NCL-Ki67p), NeuN (1:5000, Millipore MAB377), *DAT* (1:50, Millipore AP1569P), Parvalbumin (PV+, 1:500, Antikörper-online, ABIN1742405), *c-Fos* (1:100, Santa Cruz, sc-52) and detected with goat-anti-rabbit biotinylated secondary antibodies (1:1000, Vector Laboratories, BA1000). For PV+ immunostaining, one-in-twelve series from the rostral-caudal extent of the mPFC, Hipp, CPu and GP and for Ki67 immunostaining one-in-twelve series from the Hipp and the subventricular zone (SVC) were analyzed. For *c-Fos* and NeuN immunostaining, the number of positive nuclei that fell within a 0.5 \times 0.5 mm area (x 2,5 objective) in the mPFC, OFC, Thal, Hipp, Nacc, CPu, GP and STN was counted from one-in-twelve series sections from the rostral-caudal extent of the respective regions⁴³. A representative picture of the *DAT* transporter was obtained.

MRI. MRI was performed using a 7 Tesla rodent scanner (Pharmascan 70/16, Bruker BioSpin, Ettlingen, Germany) and a ¹H-RF quadratur-volume resonator with an inner diameter of 20 mm on *ex vivo* brains. Data acquisition and image processing were carried out with the Bruker software Paravision 5. All brains had been perfused and snap frozen in methylbutan. 24 hours prior to the scan, all brains were placed in phosphate-buffered saline (PBS) and stored at 4 °C, to allow for the defrosting of the brains. On the day of MRI acquisition, rat brains were placed in a 15 ml Falcon tube containing PBS—with the anterior-posterior axis of the brain co lining with the long axis of the tube. For imaging the whole brain a T2-weighted 2D turbo spin-echo sequence was used (imaging parameters TR/TE = 5980.3/36 ms, rare factor 8, 4 averages, 50 axial slices with a slice thickness of 0.5 mm, field

of view of (FOV) 20.59×20.59 mm, matrix size 256×256). Brain structure volume was estimated as the mean magnitude of regions of interest (ROI) using ImageJ software.

Electrophysiology. Local field potentials (LFPs) were recorded under urethane anesthesia (1.2 g/kg i.p., Sigma Aldrich, Germany) as described previously⁴⁴. Monopolar recording electrodes (polyimide insulated stainless steel, 0.125 mm, Plastics One, USA) were implanted ipsilaterally into the left mPFC, Nacc shell, and STN at the following coordinates with respect to bregma: mPFC: AP = 3.5, ML = 0.6, DV = -3.4, Nacc: AP = 1.2, ML = 1.8, DV = -8.1, STN: AP = -3.6, ML = 2.5, DV = -7.6⁴⁵. Recordings were referenced against 1.2 mm steel screws affixed to the skull in close proximity to each recording electrode. Signals were bandpass filtered (0.05 Hz–300 Hz), amplified, sampled at 1 kHz and digitized using a programmable neuronal data acquisition system (Omniplex, Plexon, Texas, USA). Recordings were conducted over a period of five hours. Offline data from the mPFC were inspected visually to identify and analyze epochs (40–50 s) of robust activated synchronization states (AS) reflecting signals of awake behaving rats⁴⁶. The same time segments identified to show robust AS in the mPFC were also used for analysis of LFPs from the Nacc shell. Power spectral densities of the LFP data segments were calculated by employing the Fast Fourier Transform function (Spike 2 Version 6 data analysis software; Hanning Window (1024 ms), 0.9766 Hz resolution). Frequency spectrum was divided into four EEG bands: theta (4–8 Hz), alpha (8–12 Hz), beta (12–30 Hz), gamma (30–100 Hz). Power spectra were normalized to total power between 103–147 Hz and 153–197 Hz. Power was averaged across the specific frequency bands and further expressed in arbitrary units (a. u.). Correct electrode tip placements were histologically verified.

Behavioral analysis and drug treatment. *Amphetamine-Induced stereotypy.* Testing took place in individual testing boxes ($50 \times 50 \times 50$) composed of 4 identical Plexiglas walls. Boxes were visually isolated from each other by an opaque screen. Experiments were performed over three consecutive days, during which animals were subjected to the three different dosages of d-amphetamine (i.p. 0.5 mg/kg, 2.0 mg/kg or 5.0 mg/kg, dissolved in 0.9% saline at a volume of 1.0 ml/kg, Sigma Aldrich, Germany) in a cross over design. On testing days and prior to injection animals were habituated to the testing boxes for 20 min. Following injection, animals were immediately placed back into the testing boxes and behavior was recorded for 120 min. For analysis, the 120 min test was divided into 5-min segments and the most prominent behavior was scored for each segment. Behavioral scoring was based on an adapted version of the scoring protocol employed by Carter *et al.*⁴⁷ dividing behavioral expression into (i) limited exploratory activity with discontinuous sniffing/grooming/rearing (no locomotion), (ii) constant exploratory activity with discontinuous sniffing/grooming/rearing (locomotion), (iii) continuous rearing (rearing), (iv) continuous sniffing (sniffing), (v) continuous biting, gnawing or licking (oral stereotypy), (vi) continuous head swaying/head bobbing (head movements).

Amphetamine and clonidine/fluoxetine treatment. Testing took place in testing boxes as described above. Experiments were performed over two testing days 72 h apart, during which animals were randomly assigned to treatment (clonidine/fluoxetine) or control (saline) conditions in a cross over design. On both testing days, all animals were initially habituated to testing boxes for 20 min after which they were injected with amphetamine (2.0 mg/kg, dissolved in 0.9% saline at a volume of 1.0 ml/kg, Sigma Aldrich, Germany), placed back into the testing boxes and video recorded. 50 min after amphetamine injection, animals were injected with clonidine (i.p. 0.01 mg/kg, dissolved in 0.9% saline at a volume of 10 ml/kg, Sigma-Aldrich, Germany), fluoxetine (20 mg/kg, dissolved in 0.9% saline at a volume of 1.0 ml/kg, Hexal, Germany) or saline after which they were placed back into the testing boxes. Behavior was analyzed for the period of most prominent expression of oral stereotypy in drug-free conditions, i.e. 80–120 min post amphetamine application. For analysis, the 40 min test period was divided into 5-min segments and the most prominent behavior was scored for each segment as described above.

Quinpirole induced repetitive behavior. Rats treated chronically with the dopamine D2/D3 receptor agonist quinpirole (QNP) develop compulsive-like behaviors that resemble compulsive checking behavior of OCD patients¹⁵. Rats were injected subcutaneously twice weekly for a total of 10 injections with either saline or QNP hydrochloride (0.5 mg/kg body weight, 0.5 mg/ml 0.9% NaCl, Sigma[®] Aldrich, Germany). Fifteen minutes after each injection, animals were placed in an open field that consisted of a glass table (140×140 and 20 cm high) subdivided into 25 rectangles (locales) and equipped with 4 plexiglas boxes at fixed locations. The 10th session, when QNP treated rats are known to display compulsive checking behavior was videotaped and analyzed using tracking software (VideoMot 2 system, TSE, Bad Homburg, Germany). The following measures were assessed: (i) total distance traveled, (ii) total time of activity/inactivity, (iii) frequency of stops at each open field locale, (iv) mean duration of return time to a given locale, (v) mean stop duration at a given locale, (vi) total duration of stops at a given locale. The locale with the highest total duration of stops was individually defined as the home base and compulsive checking behavior was analyzed with reference to the HB. Compulsive checking is present if the rat meets the following three criteria: it returns to HB excessively often, excessively rapidly, and visits less places before returning to the HB. As repeated administration of QNP increases locomotion and since checking behavior requires locomotion, arithmetic was applied allowing the assessment of checking behavior relatively independent from locomotion. Specifically, for each rat individually, the expected rate of return to a locale was calculated by dividing the total number of visits in a session by the number of locales visited. Next, the ratio of observed to expected HB visits was calculated by dividing the number of visits to the HB with the expected rate of return to a locale. Additionally, the total time spent on grooming/oral stereotypy on the 10th test day was calculated.

Startle stress response. Animals were exposed to unpredictable acoustic stimulus to investigate the effect of stressor-exposure on repetitive behaviour. Animals were placed in the chambers used for prepulse inhibition (PPI) test. The plastic enclosure used to restrain the rats during PPI testing was removed. The door was left open and a piece of clear Plexiglas was placed in front of the opening of the chamber to prevent the rats from escaping. Rats were acclimated to the box for 10 min, then a PPI protocol was initiated and run for 10 min, thereafter rats were left undisturbed for further 10 min¹². The process was recorded and scored on playbacks. The total time spent on grooming as well as the number of whole body shakes during the 20 min after PPI protocol initiation was analyzed.

Prepulse inhibition of an acoustic startle response. Acoustic startle response (ASR) and PPI of the ASR was assessed using a standard startle chamber (SR-lab, San Diego Instruments). An adapted version of the general SR-LAB startle response user manual was applied. Animals were exposed to a 5 min acclimatization phase of white noise at 65 dB, followed by 5 initial startle stimuli (120 dB, each presented for 40 ms). The test session was pseudorandomized and composed of 40 startle stimuli presented either alone (120 dB for 40 msc), or proceeded by a pre-pulse of either 69, 73 or 81 dB for 20 ms, 100 ms before the startle. Each pulse or pre-pulse trial was separated by inter-trial intervals of a randomized duration ranging from 15–30 seconds, during which white background noise was presented (65 dB), leading to a total testing time of approximately 40 min. The animals' startle reaction to the stimuli alone and to the pre-pulse trials was measured for 100 ms following the stimulus and amplitude as well as percentage decrease in startle response with pre-pulses (pre-pulse inhibition) was estimated⁴¹.

Elevated plus maze. Animals were placed in the center of an elevated plus maze (EPM, 42 × 42 cm, arm width: 23 cm), composed of two closed and two open arms. The animals were allowed to freely explore the maze for 5 min, while behavior was recorded via a web camera. The total time spent on open arms (OA, with both front- and hind paws placed on the arm) was determined⁴⁸.

Forced swim test. Animals were conditioned to water-filled glass cylinders (depth of 30 cm, 25 °C) for 15 min 24 h prior to testing. The cylinders were visually isolated from each other by an opaque screen. On testing day, animals were placed in the cylinders for 5 min and behavior was recorded via a web camera. For behavioral analyses, the 5 min test was divided into 5-second segments and the most predominant behavior was determined per segment (struggling, swimming and floating behaviour)⁴⁸.

Sucrose consumption test. 48 h prior to testing, animals were habituated to the individual testing cages and bottles (containing water). 24 h thereafter, animals were habituated to the sweetend condensed milk (Nestlé, Milchkädchen gezuckerte Kondensmilch, (1:3)) for 30 min in their home cage and subsequently food restricted until time of testing (15 g per animal). On the day of testing, animals were placed in the individual cages with free access to the sweetend condensed milk for 15 min. Bottles were weighed before and after testing. The amount of sweetend condensed milk consumed normalized to individual body weight was calculated⁴⁸.

Blinding. Throughout the experiments best possible blinding was conducted. For video tracking during behavioral testing, animals were number-coded such that the experimenter was blinded to phenotype and treatment condition during later video analysis. The same system was applied to neurobiological analysis.

Statistical analysis. Data are shown as means ± s.e.m. We used Student's t test to calculate significant differences between wt and DAT-tg rats. We used two-way ANOVA with the factors phenotype (*wt*, *DAT+/-*) and treatment (saline, QNP) for behavioral analysis of QNP induced repetitive behavior, and two-way ANOVA with repeated measure with the factors phenotype (*wt*, *DAT-tg*) and treatment (saline, clonidine/fluoxetine) for drug experiments followed by Holm-Sidak post hoc test if applicable. Significance was set at $P < 0.05$.

References

- Matthysse, S. Animal models in psychiatric research. *Prog Brain Res* **65**, 259–70 (1986).
- Leckman, J. F., Bloch, M. H., Smith, M. E., Larabi, D. & Hampson, M. Neurobiological substrates of Tourette's disorder. *J Child Adolesc Psychopharmacol* **20**, 237–247 (2010).
- Singer, H. S. & Walkup, J. T. Tourette Syndrome and Other Tic Disorders Diagnosis, Pathophysiology, and Treatment. *Medicine* **70**, 15–32 (1991).
- Ernst, M. *et al.* High presynaptic dopaminergic activity in children with Tourette's disorder. *J. Am. Acad. Child Adolesc. Psychiatry* **38**, 86–94 (1999).
- Singer, H. S. *et al.* Elevated intrasynaptic dopamine release in Tourette's syndrome measured by PET. *Am J Psych.* **159**, 1329–36 (2002).
- Cheon, K. A. *et al.* Dopamine transporter density of the basal ganglia assessed with [123 I] IPT SPECT in drug-naive children with Tourette's disorder. *Psychiatry Res Neuroimaging* **130**, 85–95 (2004).
- Serra-Mestres, J. *et al.* Dopamine transporter binding in Gilles de la Tourette syndrome: a [123I] FP-CIT/SPECT study. *Acta Psychiatrica Scand* **109**, 140–6 (2004).
- Paschou, P. The genetic basis of Gilles de la Tourette Syndrome. *Neurosci Biobehav Rev* **37**, 1026–1039 (2013).
- Denys, D. *et al.* Dopaminergic activity in Tourette syndrome and obsessive-compulsive disorder. *Eur Neuropsychopharmacol* **23**, 1423–1431 (2013).
- Kossoff, E. H. & Singer, H. S. Tourette syndrome: clinical characteristics and current management strategies. *Paediatr Drugs* **3**, 355–63. (2001).
- McNaught, K. S. P. & Mink, J. W. Advances in understanding and treatment of Tourette syndrome. *Nat Rev Neurol* **7**, 667–676 (2011).
- Xu, M. *et al.* Targeted ablation of cholinergic interneurons in the dorsolateral striatum produces behavioral manifestations of Tourette syndrome. *PNAS* **112**, 893–898 (2015).

13. Antoniou, K., Kafetzopoulos, E., Papadopoulou-Daifoti, Z., Hyphantis, T. & Marselos, M. D-amphetamine, cocaine and caffeine: a comparative study of acute effects on locomotor activity and behavioural patterns in rats. *Neurosci Biobehav Rev* **23**, 189–196 (1998).
14. Winter, C. *et al.* High frequency stimulation and temporary inactivation of the subthalamic nucleus reduce quinpirole- induced compulsive checking behavior in rats. *Exp Neurol* **210**, 217–28 (2008).
15. Mundt, A. *et al.* High-frequency stimulation of the nucleus accumbens core and shell reduces quinpirole-induced compulsive checking in rats. *Eur J Neurosci* **29**, 2401–2412 (2009).
16. Djodari-Irani, A. *et al.* Activity modulation of the globus pallidus and the nucleus entopeduncularis affects compulsive checking in rats. *Behav Brain Res* **219**, 149–58 (2011).
17. Pic-Taylor, A. *et al.* Behavioural and neurotoxic effects of ayahuasca infusion (Banisteriopsis caapi and Psychotria viridis) in female Wistar rats. *Behav Processes* **118**, 102–110(2015).
18. Wong, D. F. *et al.* Mechanisms of dopaminergic and serotonergic neurotransmission in Tourette syndrome: clues from an *in vivo* neurochemistry study with PET. *Neuropsychopharmacology* **33**, 1239–51 (2008).
19. Gilbert, D. L., Christian, B. T., Gelfand, M. J., Shi, B., Mantil, J. & Sallee, F. R. Altered mesolimbocortical and thalamic dopamine in Tourette syndrome. *Neurology* **67**, 1695–1697 (2006).
20. Singer, H. S., Butler, I. J., Tune, L. E., Seifert, W. E. Jr. & Coyle, J. T. Dopaminergic dysfunction in Tourette syndrome. *Ann Neurol* **12**, 361–6 (1982).
21. Butler, I. J., Koslow, S. H., Seifert, W. E. Jr, Caprioli, R. M. & Singer, H. S. Biogenic amine metabolism in Tourette syndrome. *Ann Neurol* **6**, 37–9 (1979).
22. Cohen, D. J., Shaywitz, B. A., Caparulo, B., Young, J. G. & Bowers, M. B. Jr. Chronic, multiple tics of Gilles de la Tourette's disease. CSF acid monoamine metabolites after probenecid administration. *Arch Gen Psychiatry* **35**, 245–50 (1978).
23. Shapiro, A. K., Baron, M., Shapiro, E. & Levitt, M. Enzyme activity in Tourette's syndrome. *Arch Neurol* **41**, 282–285 (1984).
24. Segawa, M. Neurophysiology of Tourette's syndrome: pathophysiological considerations. *Brain Dev* **25**, S62–S69 (2003).
25. Kalanithi, P. S. *et al.* Altered parvalbumin-positive neuron distribution in basal ganglia of individuals with Tourette syndrome. *PNAS* **102**, 13307–13312 (2005).
26. Kataoka, Y. *et al.* Decreased number of parvalbumin and cholinergic interneurons in the striatum of individuals with Tourette syndrome. *J Comp Neurol* **518**, 277–291 (2010).
27. Koós, T. & Tepper, J. M. Inhibitory control of neostriatal projection neurons by GABAergic interneurons. *Nat Neurosci* **2**, 467–472 (1999).
28. Singer, H. S. & Minzer, K. Neurobiology of Tourette's syndrome: concepts of neuroanatomic localization and neurochemical abnormalities. *Brain Dev* **25**, S70–S84 (2003).
29. Mink, J. W. Basal ganglia dysfunction in Tourette's syndrome: a new hypothesis. *Pediatr Neurol* **25**, 190–198. (2001).
30. Menzies, L. *et al.* Integrating evidence from neuroimaging and neuropsychological studies of obsessive-compulsive disorder: the orbitofronto-striatal model revisited. *Neurosci Biobehav Rev* **32**, 525–549 (2008).
31. Mallet, N. *et al.* Disrupted dopamine transmission and the emergence of exaggerated beta oscillations in subthalamic nucleus and cerebral cortex. *J Neurosci* **28**, 4795–4806 (2008).
32. Hong, H. J. *et al.* Increased frontomotor oscillations during tic suppression in children with Tourette syndrome. *J Child Neurol* **28**, 615–624 (2013).
33. Neumann, W. J. *et al.* Different patterns of local field potentials from limbic DBS targets in patients with major depressive and obsessive compulsive disorder. *Mol Psych* **19**, 1186–92 (2014).
34. Masoud, S. T. *et al.* "Increased expression of the dopamine transporter leads to loss of dopamine neurons, oxidative stress and l-DOPA reversible motor deficits". *Neurobiol Dis* **74**, 66–75 (2015).
35. Fazeli, G. *et al.* "The role of Dopamine Transporter in Dopamine-Induced DNA Damage". *Brain Pathol* **21**(3), 237–248 (2011).
36. Chen, L. *et al.* "Unregulated cytosolic dopamine causes neurodegeneration associated with oxidative stress in mice". *J Neurosci* **28**(2), 425–433 (2008).
37. Peterson, B. S. *et al.* Morphologic features of the amygdala and hippocampus in children and adults with Tourette syndrome. *Arch Gen Psychiatry* **64**, 1281–1291 (2007).
38. Brüss, M., Wieland, A. & Bönsch, H. Molecular cloning and functional expression of the mouse dopamine transporter. *J Neural Transm* **106**, 657–662 (1999).
39. Popova, E., Bader, M. & Krivokharchenko, A. Strain differences in superovulatory response, embryo development and efficiency of transgenic rat production. *Transgenic Res* **14**, 729–738 (2005).
40. Forss-Petter, S. *et al.* Transgenic mice expressing β -galactosidase in mature neurons under neuron-specific enolase promoter control. *Neuron* **5**, 187–197 (1990).
41. Mucke, L. *et al.* Synaptotrophic effects of human amyloid β protein precursors in the cortex of transgenic mice. *Brain Res* **666**, 151–167 (1994).
42. Hadar, R. *et al.* Using a maternal immune stimulation model of schizophrenia to study behavioral and neurobiological alterations over the developmental course. *Schiz Res* **166**, 238–247 (2015).
43. Carson, D. S. *et al.* Systemically administered oxytocin decreases methamphetamine activation of the subthalamic nucleus and accumbens core and stimulates oxytocinergic neurons in the hypothalamus. *Addict Biol* **15**, 448–463 (2010).
44. Voget, M. *et al.* Altered local field potential activity and serotonergic neurotransmission are further characteristics of the Flinders sensitive line rat model of depression. *Behav Brain Res* **291**, 299–305(2015).
45. Paxinos, G. & Watson, C., *A stereotaxic atlas of the rat brain*. New York: Academic (1998).
46. Magill, P. J. *et al.* Changes in functional connectivity within the rat striatopallidal axis during global brain activation *in vivo*. *J Neurosci* **26**, 6318–6329 (2006).
47. Carter, C. J. & Pycoc, C. J. The effects of 5, 7-dihydroxytryptamine lesions of extrapyramidal and mesolimbic sites on spontaneous motor behaviour, and amphetamine-induced stereotypy. *Naunyn-Schmiedeberg's Arch Pharmacol* **308**, 51–54 (1979).
48. Edemann-Calleen, H. *et al.* Medial Forebrain Bundle Deep Brain Stimulation has Symptom-specific Anti-depressant Effects in Rats and as Opposed to Ventromedial Prefrontal Cortex Stimulation Interacts With the Reward System. *Brain Stim* **8**, 714–23 (2015).

Acknowledgements

We thank Renate Winter, Christiane Kölske, Jennifer Altschüler, Sarina Sabrina Richter and Christian Böttcher for excellent technical support, Dirk Megow and Susanne Müller for profound support on Western blotting and MRI studies. The study was funded by Else Kröner-Fresenius Foundation (Grant 2008_A132) and the Federal Ministry of Education and Research, Germany (Grant 01EW1409 (EraNet Neuron framework) and Grant 01EE1403A (GCBS)). RH, FW, MV, and JP partly were or are financed by the German Research Foundation (Grant PAK 591: WI 2140/2-1, Grant KFO247: WI 2140/1-1/2 and Grant FOR1336-2: C4).

Author Contributions

R.H. contributed to experimental design, data analysis and interpretation and wrote the ms. H.E.-C. conducted behavioral and MRI experiments, contributed to behavioral data analysis and writing the ms. C.R. conducted molecular biological and contributed to biochemical investigations. F.W. conducted immunohistochemical and biochemical and contributed to molecular biological investigations. M.V. conducted electrophysiological experiments, contributed to immunohistochemical investigations and writing the ms. E.P. generated transgenic rats. R.S. supervised biochemical investigations. Y.A. contributed to electrophysiological investigation and data analysis. J.P. supervised Western blotting and C.v.R. electrophysiological experiments. I.P. generated the construct. M.B. supervised generation of construct and transgenic rats. C.W. conceived the study, designed experiments, conducted data analysis and interpretation and wrote the ms.

Additional Information

Competing financial interests: The authors declare no competing financial interests.

How to cite this article: Hadar, R. *et al.* Rats overexpressing the dopamine transporter display behavioral and neurobiological abnormalities with relevance to repetitive disorders. *Sci. Rep.* **6**, 39145; doi: 10.1038/srep39145 (2016).


Publisher's note: Springer Nature remains neutral with regard to jurisdictional claims in published maps and institutional affiliations.



This work is licensed under a Creative Commons Attribution 4.0 International License. The images or other third party material in this article are included in the article's Creative Commons license, unless indicated otherwise in the credit line; if the material is not included under the Creative Commons license, users will need to obtain permission from the license holder to reproduce the material. To view a copy of this license, visit <http://creativecommons.org/licenses/by/4.0/>

© The Author(s) 2016

SCIENTIFIC REPORTS



OPEN

Learning deficits in rats overexpressing the dopamine transporter

Nadine Bernhardt¹, Maike Kristin Lieser¹, Elizabeth-Barroeta Hlusicka^{1,2}, Bettina Habelt^{1,2}, Franziska Wieske^{1,2}, Henriette Edemann-Callesen^{1,2,3}, Alexander Garthe⁴ & Christine Winter^{1,2}

With its capacity to modulate motor control and motivational as well as cognitive functions dopamine is implicated in numerous neuropsychiatric diseases. The present study investigated whether an imbalance in dopamine homeostasis as evident in the dopamine overexpressing rat model (DAT-tg), results in learning and memory deficits associated with changes in adult hippocampal neurogenesis. Adult DAT-tg and control rats were subjected to the Morris water maze, the radial arm maze and a discrimination reversal paradigm and newly generated neurons in hippocampal circuitry were investigated post mortem. DAT-tg rats were found to exhibit a striking inability to acquire information and deploy spatial search strategies. At the same time, reduced integration of adult-born neurons in hippocampal circuitry was observed, which together with changes in striatal dopamine signalling might explain behavioural deficits.

Midbrain neurons located in the substantia nigra pars compacta (SNc) and ventral tegmental area (VTA)¹ provide a 'tonic' baseline level and 'phasic' large changes of dopamine (DA) concentrations to downstream cortical and subcortical structures^{2,3}. DA is released after reinforcing stimuli and novel experiences⁴ and is fundamental for cognition-related brain functions through its modulation of motivation, memory, motor output, and neuroendocrine integration.

Within the striatum, DA firing encodes errors in reward prediction, providing a learning signal to guide future behavior⁵. Striatal DA contributes to formation and expression of associations^{6,7}, action selection and modulation of motivation^{8,9} together supporting learning and goal-directed behaviour.

In the hippocampus DA release occurs following novelty exposure¹⁰ and affects plasticity, synaptic transmission and the network activity within hippocampal circuitry^{11–14}. Primarily through D1-class receptor activation, hippocampal DA release facilitates long-term potentiation^{15,16} thereby stabilizing new place maps necessary for spatial learning¹⁷.

Hippocampal and striatal memory systems have long been thought to operate independently. Recently, however they have been shown to act in synergism¹⁸. Animal studies demonstrate that hippocampal oscillatory activity increases during place learning and that hippocampal-striatal coherence appears after training, a mechanism considered necessary in switching from place learning to the usage of a proper response strategy¹⁹.

Further, DA is an important component of neurogenic niche signals and influences several aspects of neurogenesis including proliferation, migration and differentiation²⁰ associated to hippocampal learning²¹. DA not only modulates ontogenetic neurogenesis²², in the adult brain DA fibres directly target subventricular zone (SVZ) and subgranular zone (SGZ) neuronal precursors^{23,24} expressing DA receptors^{24–26}. In this line ablation of midbrain DA neurons in rodents, results in reduced adult neurogenesis both in striatum and hippocampus^{24,27}.

The dopamine transporter (DAT) constitutes one regulatory mechanism of extracellular DA and altered DAT functioning has been linked to several neuropsychiatric diseases with dysregulation of DA neuronal function²⁸. Rats overexpressing the DAT (DAT-tg) display profound alterations within the DA system, i.e. increased striatal and hippocampal D1/D2 receptor expression as well as decreased striatal DA and two-fold increased hippocampal DA content²⁹. In addition, DAT-tg rats exhibit increased hippocampal volumes suggesting also functional

¹Department of Psychiatry and Psychotherapy, University Hospital Carl Gustav Carus, Technische Universität Dresden, Dresden, Germany. ²Department of Psychiatry and Psychotherapy, Charité Universitätsmedizin Berlin, Berlin, Germany. ³International Graduate Program Medical Neurosciences, Charité Universitätsmedizin Berlin, Berlin, Germany. ⁴German Center for Neurodegenerative Diseases (DZNE) Dresden, Dresden, Germany. Correspondence and requests for materials should be addressed to C.W. (email: christine.winter@charite.de)

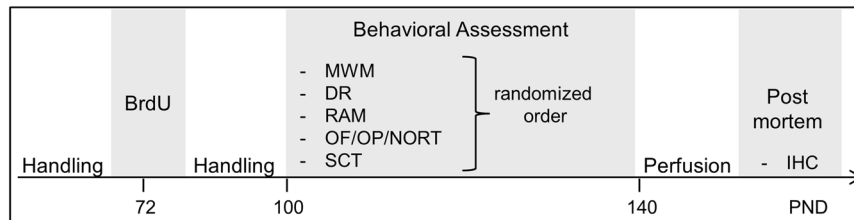


Figure 1. Experimental design. Labelling of newly generated cells for analysis of hippocampal neurogenesis was achieved by injecting proliferation marker BrdU into rats, three times with a six hours interval at a dose of 50 mg/kg. Following BrdU injections, animals performed a series of tasks investigating aspects of learning and memory and sensorimotor function. Behavioural experiments were performed in 3 batches of animals (A: wt n = 4, het n = 8; B: wt n = 2, het n = 4; C: wt n = 5, het n = 4). Test order Batch A: RAM, DR, SCT, OF/OP/NOR, MWM; Batch B: RAM, OF/OP/NOR, MWM, SCT, DR; Batch C: MWM, RAM, OF/OP/NOR, SCT, DR. BrdU = 5-Bromo-2'-Deoxyuridine, MWM = Morris water maze, DR = Discrimination Learning, RAM = Radial arm maze, OF = open -field, OP = open platform, NOR = novel object recognition, SCT = sucrose consumption test, PND = postnatal day, IHC = immunohistochemistry.

consequences within hippocampal circuitry. So far, neurobiological alterations were shown to translate into repetitive behaviour. We here studied whether these profound alterations in striatal and hippocampal DA homeostasis also affect hippocampal adult neurogenesis translating into learning and memory deficits.

Results

Experiments were conducted on male hemizygous dopamine transporter overexpressing rats (DAT-tg) and their respective control littermates (wildtypes, wt) as outlined in Fig. 1.

Morris water maze (MWM). *Acquisition training.* Control animals successfully learned to find the hidden platform during the acquisition period. In comparison DAT-tg animals showed a significantly lower rate of successful navigation to the platform (trial: $F(6.8, 171) = 3.516, p = 0.002$; genotype: $F(1, 25) = 181.2, p < 0.001$; trial \times genotype interaction: $F(6.8, 171) = 3.941, p = 0.001$; repeated measures ANOVA) and none of the DAT-tg animals has been found to reach the platform above chance level (Fig. 2d). In accordance path length was significantly increased in DAT-tg animals compared to wt with significant differences on all days of the acquisition phase (day: $F(2.4, 59.8) = 47.61, p < 0.001$; genotype: $F(1, 25) = 78.673, p < 0.001$; day \times genotype interaction: $F(2.4, 59.8) = 3.655, p = 0.025$; repeated measures ANOVA; Fig. 2b). Both, a significant trial \times genotype interaction for successful navigation to the platform and a significant day \times genotype interaction for path length, reflect a substantial learning defect i.e. shallow learning curve in DAT-tg rats. Latency to find the platform could not be analysed due to the few numbers of successful trials exhibit by DAT-tg animals. However DAT-tg animals performed equally in regard to swim speed (day: $F(3, 75) = 17.612, p < 0.001$; genotype: $F(1, 25) = 0.571, p > 0.05$; day \times genotype, $F(3, 75) = 1.797, p > 0.05$; repeated measures ANOVA; Fig. 2c).

Spatial search strategies. At each trial in the course of learning in the water maze, animals have a specific probability to choose an effective, more hippocampus-dependent spatial search strategy that depends on the already learned spatial knowledge over a less hippocampus dependent nonspatial strategy³⁰. To assess such qualitative aspects of learning during acquisition training, swimming paths were categorized into different behavioural strategies, representing progression from thigmotaxis to direct swimming (namely: thigmotaxis, random search, scanning, chaining, directed search, focal search and direct swimming³¹). As illustrated through visual inspection of probability plots (Fig. 2e) control animals were found to proceed reliably from initial thigmotactic behaviour towards using allocentric strategies, where distal cues provide geometric reference to the animal's location while DAT-tg rats failed to do so. Using a repeated measures logistic regression model, we statistically assessed changes in the chance (odds) for using either a more hippocampus-dependent or less hippocampus-dependent strategy comparing DAT-tg to wt rats. We found a statistically significant effect on strategy choice for the use of more hippocampus versus less hippocampus dependent strategies on genotype ($Estimate_{genotype} = -0.81, SE = 0.22, z = -3.71, p < 0.001$). The estimated odds-ratio (OR) was $OR = 0.44 (p < 0.001)$. Thus, DAT overexpression in DAT-tg rats significantly reduced the chance of an animal to use a spatial, more hippocampus-dependent strategy. We then specifically tested the use of thigmotaxis versus all other more complex strategies and found a statistically significant effect ($Estimate_{genotype} = 1.07, SE = 0.23, z = 4.54, OR = 2.9, p < 0.001$). Thus, in DAT-tg rats the chance to use thigmotaxis as a strategy is almost 3fold higher compared to wt.

Probe trial performance. On the fifth day when the platform had been removed wt rats spent most of the time in the previous goal quadrant indicative of successful spatial learning (NW/NE $t(10) = 3.452, p = 0.007$; NW/SE $t(10) = 2.303, p = 0.047$; all other $p > 0.05$; Student's t-test, Fig. 2f). In contrast, DAT-tg rats did not exhibit significant preferences for any of the pool quadrants (all $p > 0.05$; Student's t-test, Fig. 2f) and showed significantly fewer crossings over the former platform position compared to controls ($U(27) = -4.559, p < 0.001$; Fig. 2g). Again DAT-tg animals differed by significantly exhibiting thigmotactic swimming while controls exploited egocentric and allocentric search strategies ($U(27) = -4.941, p < 0.001$; Fig. 2e).

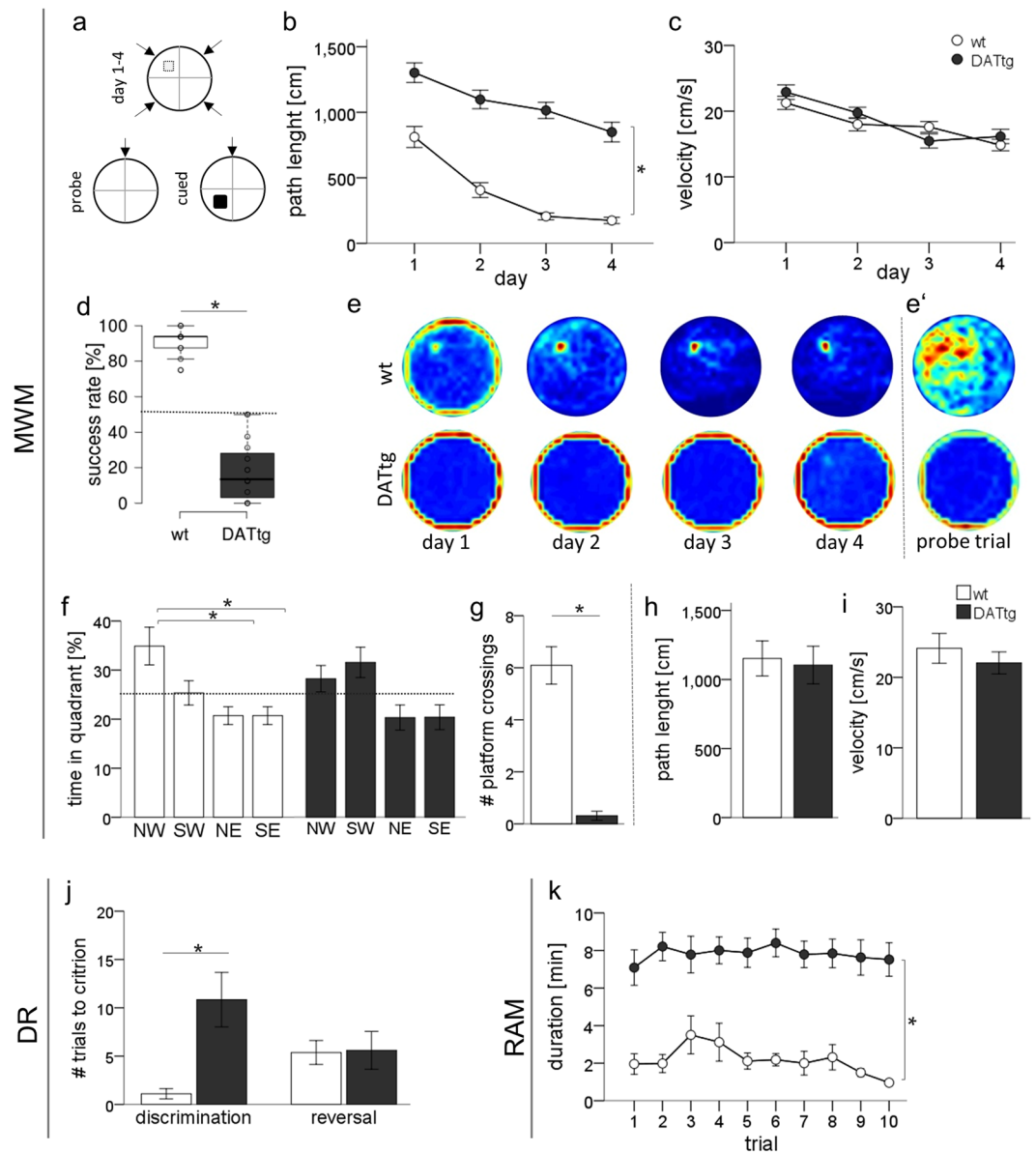


Figure 2. Behavioural assessment of learning and memory. **(d)** Schematics of MWM set up. In the Acquisition phase (day1–4) DAT-tg rats do not learn to locate the hidden platform **(a)**, thereby showing longer path length compared to controls **(b)** but intact motor function (velocity **(c)**). **(e)** The probabilistic occupancy plots represent sum data over trials and rats within respective groups and illustrate the rapid development of a place-specific preference for the platform position for control animals but not DAT-tg animals. **(e–g)** In accordance to the impairment in learning during acquisition DAT-tg animals do not prefer the former goal quadrant after platform removal as found for controls. **(e)** During probe trial DAT-tg rats continuously show thigmotactic swimming around the wall of the pool. DAT-tg: $n = 16$; wt: $n = 11$ **(h,i)** Performance during cued platform trials indicates intact sensorimotor function when platform is visible. DAT-tg: $n = 10$; wt: $n = 8$ **(j)** During the discrimination learning paradigm DAT-tg rats exhibit impairments in initial acquisition. DAT-tg: $n = 9$; wt: $n = 11$ **(k)** During RAM DAT-tg rats exhibit significantly longer trial durations due to lack in exploratory behaviour. DAT-tg: $n = 16$; wt: $n = 11$ Dashed line **(a,f)** indicates chance level. Error bars indicate the standard error of the mean, significance level $p < 0.05$.

Cued platform trial. Performance in cued trial was not significant different in DAT-tg compared to wt rats. Independent of the genotype not all animals were found to successfully approach the platform within 60 s ($\chi^2(1) = 1.8, p = 0.178$). Further similar path length ($t(16) = 0.250, p = 0.806$; Fig. 2h,) and velocity ($t(16) = 0.806, p = 0.435$; Fig. 2i) support the notion that sensorimotor function cannot account for the spatial learning and retention deficits observed in the DAT-tg animals.

Discrimination reversal (DR). The DR paradigm initially requires learning to discriminate the favourable T-Maze arm providing the escape platform. 43.8% of DAT-tg rats dropped out at this stage ($n = 3$ drowning/not

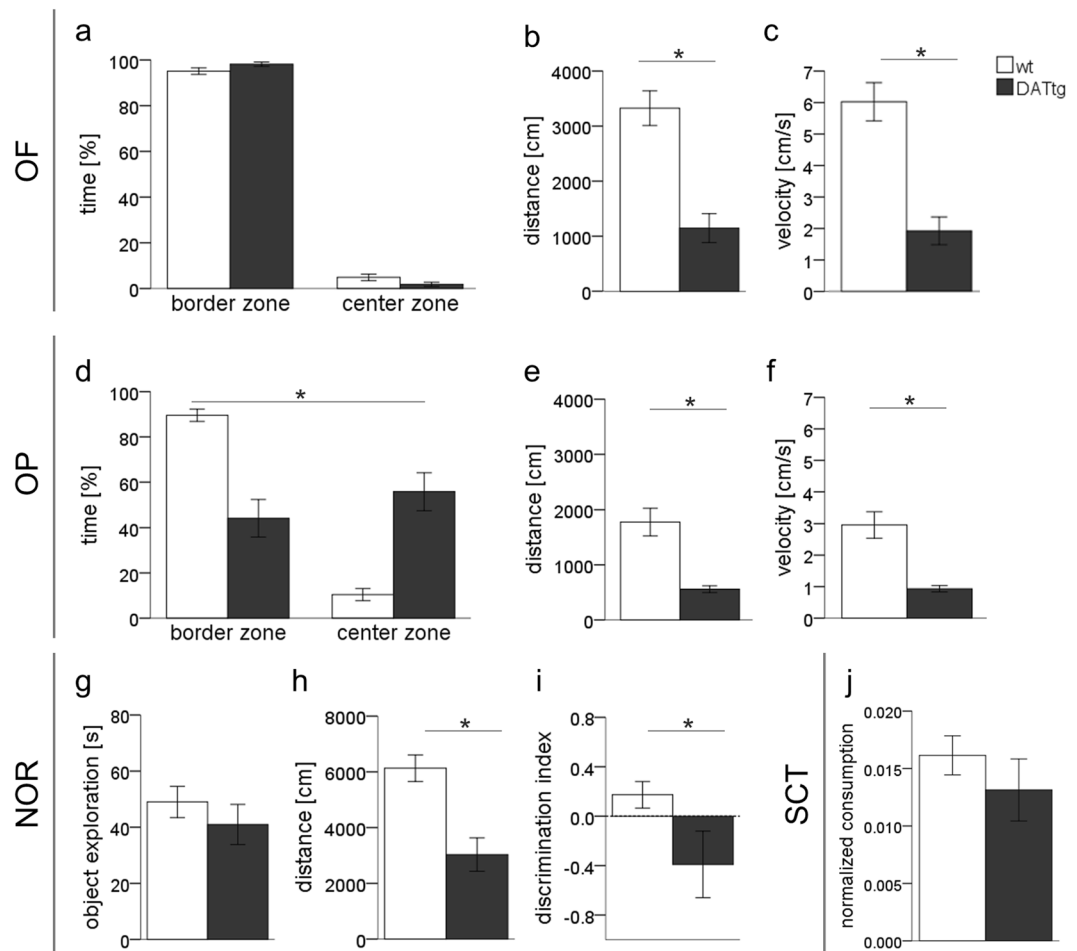


Figure 3. Exploratory behaviour and general locomotor activity. Results from the (a–c) Open-field (OF) (d–f) Open-platform (OP) (g–i) novel object recognition (NOR) and (j) Sucrose consumption test (SCT) are presented. (i) Discrimination index can vary between +1 and –1, where a positive score indicates more time spent with the novel object for controls, and a negative score for DAT-tg rats indicates more time spent with the familiar object. The dashed line indicates a null preference of novel-object investigation. (a–f,j) DAT-tg: n = 16; wt: n = 11 (g–i) DAT-tg: n = 7; wt: n = 11 Error bars indicate the standard error of the mean, significance level $p < 0.05$.

swimming, n = 4 did not reach criterion) while all control rats reached criterion of 5 consecutive correct choices within 25 trials. ANOVA for animals completing the task showed a significant difference between genotypes; that is DAT-tg animals needed significantly more trials for discrimination learning than wt rats ($U(20) = -2.381$, $p = 0.022$; Fig. 2j). Performance during the reversal stage, which reflects the ability to change behaviour in the face of altering contingencies did not significantly differ between genotypes ($U(20) = -0.956$, $p = 0.356$; Fig. 2j).

Radial maze. DAT-tg exhibited lower explorative behaviour already during habituation trials, i.e. they did not explore all arms and therefore did not consume all baits. During test trials DAT-tg animals continually showed a significantly lower rate of successful completion of the task over all trials i.e. location and consumption of all baits within 10 min ($U(27) = -3.461$, $p < 0.001$). This was caused by a reduced exploration behaviour i.e. staying in one arm over the whole trial duration. In accordance trial duration was significantly increased in DAT-tg compared to wt rats, with no improvement over task progression (day x genotype: $F(4, 92) = 1.22$, $p = 0.278$; genotype: $F(1, 23) = 46.799$, $p < 0.001$; day: $F(4, 92) = 1.232$, $p = 0.308$; repeated measures ANOVA; (Fig. 2k). The observed highly reduced engagement of DAT-tg animals in task activity impeded further analysis of working memory and reference memory errors.

Exploratory behaviour. Analysis of general locomotor activity in the open field (OF) revealed a significant difference in genotypes for distance travelled ($t(25) = 5.302$, $p < 0.001$; Fig. 3b) and velocity ($t(25) = 5.611$, $p < 0.001$; Fig. 3c). As expected rats, independent of their genotype did spend a significantly greater amount of time in the wall zone of the arena. The time spent in centre zone did not differ between genotypes ($t(25) = 1.860$, $p = 0.075$; Fig. 3a). Analogous in the open platform (OP) test locomotor activity was reduced in DAT-tg rats; distance travelled ($t(25) = 0.415$, $p = 0.001$; Fig. 3e), velocity ($t(25) = 5.534$, $p = 0.001$; Fig. 3f). Further a significant difference was found for the time spent in border and centre zone, respective ($t(25) = 4.399$, $p < 0.001$; Fig. 3d).

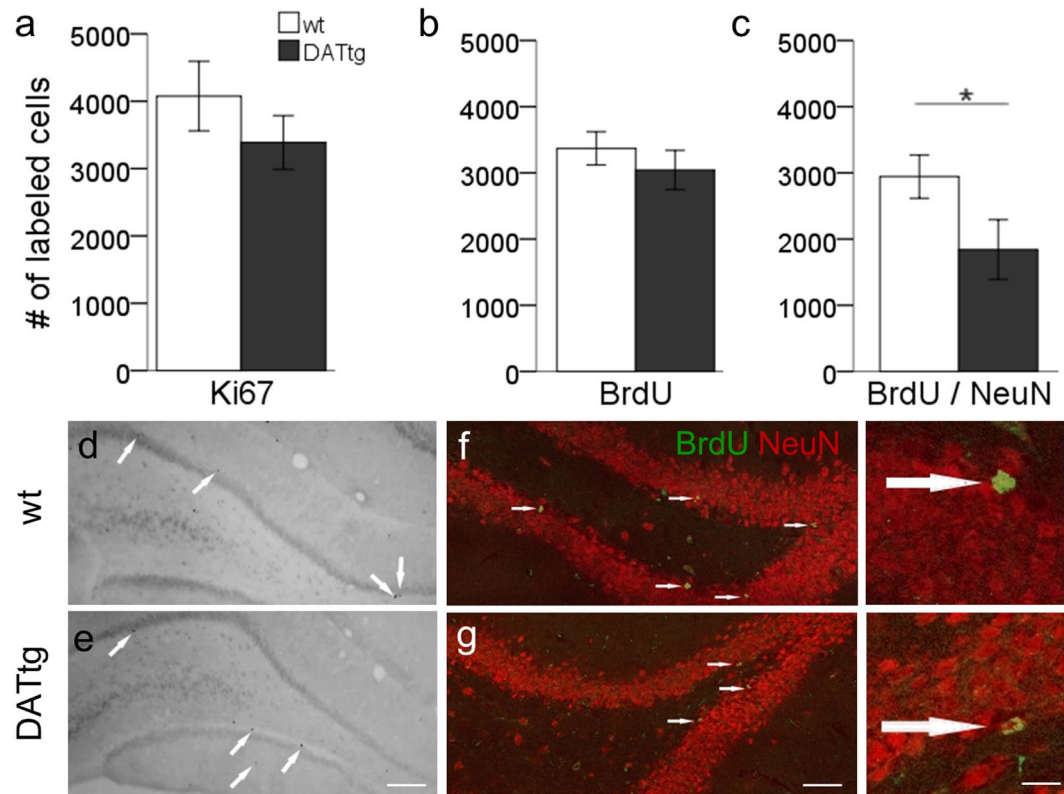


Figure 4. Histochemical analysis of hippocampal neurogenesis. Ten weeks after injection and behavioural assessment proliferation (Ki67) survival of newly generated cells (BrdU) and proportion of generated neurons (BrdU/NeuN) was quantified. The number of (a) Ki67-positive cells for DAT-tg; $n = 9$; wt: $n = 7$ and (b) BrdU-positive cells. DAT-tg; $n = 13$; wt: $n = 7$ did not differ between genotypes. However in DAT-tg rats lower numbers of BrdU/NeuN double-labelled cells could be detected. DAT-tg; $n = 13$; wt: $n = 7$. Error bars indicate the standard error of the mean, significance level $p < 0.05$. (d–g) Representative images for Ki67 DAB staining (d,e) and BrdU/NeuN immunofluorescent staining (f,g) are shown. Ki67 bright field, NeuN, red; BrdU, green; Scale bar: (d,e) 150 μm, (f,g) 100 μm, (insets) 15 μm.

During the familiarization phase of the novel object recognition (NOR) test individual DAT-tg animals were found to explore only one of the two objects while over the group this preference was not biased for object or object location. Accordingly overall distance travelled ($t(17) = 2.832$, $p = 0.011$; Fig. 3h) was significantly reduced in DAT-tg compared to wt rats however the total time spend with object exploration was not different ($t(17) = 0.583$, $p = 0.568$; Fig. 3g). During test-phase one-sample Wilcoxon rank test revealed that the average discrimination index (DI) was not significantly above or below chance level for neither wt nor DAT-tg rats ($p > 0.05$). However DAT-tg compared to control exhibit a reduced novel-object preference ($t(17) = 2.192$, $p = 0.045$; Fig. 3i).

No difference between genotypes was found in sucrose consumption ($t(25) = 0.865$, $p = 0.396$; Fig. 3j).

Hippocampal neurogenesis. Quantitative analysis of active proliferating progenitors in the SGZ of the dentate gyrus (DG) following our extensive behavioural experimental program was done using Ki-67, an endogenous marker for proliferating cells. There was no difference in the number of Ki-67+ cells between DAT-tg and wt rats ($t(14) = 1$, $p = 0.332$; students-t test; Fig. 4a). Similarly no significant difference was found in the number of bromodeoxyuridine (BrdU) labelled cells 10 weeks post injection ($t(18) = -0.891$, $p = 0.385$; students-t test; Fig. 4b). However co-labelling analysis with the mature neuronal marker NeuN (BrdU+/NeuN+) showed a significant reduction in the neuronal BrdU+ population in DAT-tg compared to wt rats ($t(18) = 2.140$, $p = 0.046$; students-t test; Fig. 4b), indicative of reduced incorporation of newly generated neurons into hippocampal circuitry in DAT-tg rats.

Discussion

DAT-tg rats displayed immense deficits in acquiring information as well as a reduced integration of newly generated neurons into hippocampal circuitry. Balanced DA levels are crucial for cognitive performance and both too little and too much DA impairs performance e.g. for reward-based learning³².

Previously, dopamine deficient mice have been shown to not engage in behaviours in which food is used as reinforcement³³. Likewise, DAT-tg rats were unable to perform in the radial arm maze. DAT provides a rapid and efficient mechanism for reuptake of synaptic DA. DAT-overactivity consequently causes exceptionally fast DA reuptake and therefore rapid clearing of DA from synapses, modelling synaptic DA deficiency. Changes in DA levels have repeatedly been reported to immediately affect willingness to engage in work, supporting the

idea that fast DA fluctuations influence motivational aspects of decision-making³⁴. Correspondingly, as seen in the OF as well as the NORT, novelty was not sufficient to provide motivation to move in the DAT-tg rats. While sucrose consumption data indicates a similar hedonic impact, altered DA and its motivational function i.e. the willingness to engage in work to receive the reward³⁵ may underlie the reduced performance of DAT-tg animals in the appetitive RAM.

In contrast in the MWM and the discrimination reversal water comprises a strongly aversive component providing the means to motivate movement (swimming) as a necessity to approach the hidden platform. Nevertheless DAT-tg rats were severely compromised also in performance in these tasks. In the MWM, thigmotaxis, which is swimming along the walls of the pool, was the most prominent behaviour seen in DAT-tg rats. Initial thigmotaxis is commonly observed in rats but is usually rapidly replaced by efficient cognitive strategies that depend on the association between environmental cues and the spatial location of the platform. Also in the present study, control rats showed an immediate shift to approach the platform limiting thigmotactic behaviour to the first trials and exhibiting a steep learning curve. DAT-tg animals however showed continuous thigmotaxis over all trials and thus were severely impaired in locating the hidden platform. There are several explanations for excessive thigmotaxis found in the literature: motor impairments, lack of orientation, increased anxiety or an inability to deploy spatial search strategies. With respect to motor impairments analysis of open field behaviour showed no apparent defects in coordination. Additionally, when placed in water DAT-tg rats were capable of swimming with normal swim speed. DAT-tg rats further displayed normal sensorimotor function indicated by visual performance using optomotor tracking (Supplement) and adequate performance using the visible platform as an intra-maze cue thus demonstrating a general awareness of surroundings and orientation. Additionally, DAT-tg rats in a previous study scored normal in an anxiety paradigm²⁹.

Evidence from our search strategy analysis rather suggests that DAT-tg rats were unable to deploy spatial search strategies. Mura and Feldon³⁶, who performed 6-OHDA lesions of the nigrostriatal system, abolishing DA signalling, were the first to suggest that excessive thigmotaxis results from an impairment to choose the correct strategy to solve the task. More recently a similar conclusion was derived following lesion experiments to the dorsomedial striatum³⁷. Consequently, an aberrant striatal DA state may at least partially explain the observed learning deficits.

An alternative explanation is given by the observation of DA changes in the DAT-tg rat translating into a stress and amphetamine induced repetitive behaviour phenotype²⁹. Pathological repetitive behaviour can be exacerbated by specific environmental and psychological triggers, including sensory stimulation frustration, anxiety or stress³⁸. As the DAT-tg model has been discussed to represent a model of repetitive phenotypes and the aversive environment in the MWM represents a well-known stress inducing factor, the observed thigmotactic swimming may alternatively represent a repetitive behaviour. Within the present behavioural scheme we did not observe excessive grooming or other types of repetitive behaviour however as it was not systematically assessed its occurrence cannot be fully excluded. Such hypothesis thus remains to be further investigated.

Behavioural analysis additionally suggests an inability to acquire spatial reference memory (probe trial defects) thus evidence for a hippocampal dependent learning deficit. In line with the literature DA plays an important role in the spatial components of learning^{13,39–41}. Such hippocampus-dependent learning is sustained by continuous cell rearrangement via adult neurogenesis and the several steps of adult generation of neurons, i.e. proliferation, differentiation and functional integration, which have been shown to be modulated by DA signalling. The observed behavioural defect suggests that changes in dopamine homeostasis in the DAT-tg model may affect hippocampal adult neurogenesis contributing to the spatial learning deficits. We do not see a reduction in proliferation in our model, though we do find a reduced proportion of newly born functional integrated (BrdU+/NeuN+) neurons, indicative of reduced incorporation of newly generated neurons into hippocampal circuitry in DAT-tg rats. An alternative explanation may be a general reduction of mature hippocampal neuronal circuitry in DAT-tg rats as a result of continuous DAT overexpression, which yet seems unlikely as prior analysis has not found differences in NeuN expressing cells in several brain regions including the hippocampus between DAT-tg and control rats²⁹. Further experiments however need to evaluate causality between reduced numbers of newly integrated neurons and impaired learning considering that DAT-tg animals displayed lower physical activity in the testing situation, which can reduce integration of newly generated neurons⁴².

Conclusion

Given the important role of DA signalling for the ability to execute proper learning functions, altered DA homeostasis, hippocampal structures and disinhibition of the striatum may in combination underlie impaired performance in the DAT-tg rats. DA homeostasis clearly constitutes a critical component of the cellular network sub serving information processing per se but may be similarly essential for the proper development of such a network during embryogenesis, postnatal or even adult stages.

Materials and Methods

Animals. All animal experiments were carried out in accordance to the European Communities Council Directive of 22th September 2010 (2010/63/EU) under protocols approved by the animal ethics committees of the Technische Universität Dresden and the Landesdirektion Sachsen. Animals were generated in our lab as described elsewhere²⁹. Briefly a construct containing the NSE promoter, murine DAT coding sequence, and bovine growth hormone polyadenylation sequence was used for microinjection into the pronucleus of zygotes from Sprague-Dawley (SD) Hanover rats (Janvier labs). Transgenics are maintained on SD-background in a continuous hemizygous x wildtype offspring breeding scheme (>20 generations). Genotypes were verified using PCR. Animals were housed in mixed genotype groups of two–four in a 12-h light dark cycle (light on at 06:00 am) with food and water ad libitum. All efforts were made to reduce animal suffering and number of animals used.

Experimental design. Animals were BrdU injected to quantify adult neurogenesis (Fig. 1). Animals were habituated to the experimenter during 5-min handling sessions over 3 consecutive days prior to injections. Rats were injected with BrdU (50 mg/kg) every 6 hours over a period of eighteen hours (three injections total). The majority of adult born neurons die before they mature, the surviving neurons are functionally integrated into existing neural circuits within one month^{43–45}. The rate of survival of newborn neurons is regulated by experiences, including hippocampus-dependent learning^{46,47}. As we aimed to assess learning in relation to baseline neurogenesis rather than performance-dependent hippocampal neurogenesis we chose to start behavioural experiments when labelled neurons are functionally integrated. Thus, testing took place between 4–10 weeks post injection, which also represents a time window with a stable number of BrdU-labelled cells⁴⁵. Animals were sacrificed immediately following the last behavioural experiment and brains processed for post mortem analysis.

Behavioural testing. Testing took place in three parallel batches with distinct test orders. Animals never performed more than one test a day and between each behavioural test animals were allowed to rest for 3–5 days to reduce stress and support recovery e.g. following weight loss from food deprivation. All behavioural testing took place between 10:00 and 16:00 h. Experimenters were blind to the genotype of the rats during all experimental sessions. If not otherwise stated all behavioural data were collected using EthoVisionXT video tracking equipment and software (Noldus Information Technology) at a rate of 5 frames per second. Learning was assessed using the Morris water maze, radial arm maze and discrimination reversal. Open field analysis, novel object recognition and sucrose consumption tests were included to assess factors that may interfere with learning performance such as locomotion, anxiety, novelty response and taste perception.

The Morris water maze. Hidden platform test was used to investigate spatial learning and memory. A pool (diameter 1.6 m) was positioned in a room with distal cues visible to the swimming animal. Water in the pool was maintained at 24 °C (± 1 °C), filled to a depth of 33 cm and made opaque by non-toxic white paint. A small platform (14 × 14 cm) was hidden 1 cm beneath the water surface. For analysis, the pool was divided into four quadrants (northwest (NW), southwest (SW), northeast (NE) and southeast (SE)) with the platform being located in NW over all acquisition trials (Fig. 2a). Rats accomplished four trials per day with a 60 s trial limit, in which they had to find the platform followed by a 5 s resting period (on platform) before being removed (inter-trial interval (ITI) of 15 min). Acquisition trials lasted for 4 days, i.e. leading to 16 trials in total. Each day rats were released at four different starting positions randomized over days. If a rat failed to find the platform within the time limit on the first trial on the first day, it was led to the platform. On the fifth day, a 60 s probe trial was performed from a novel start position with the platform removed. Latency (time required to find the hidden platform), mean velocity (swimming speed) and path length (length of path swum by the animal in one trial) were recorded. Acquisition trials were further analysed to identify differential search strategies according to previously described methods³¹. Seven main search strategies were identified ranging from thigmotactic behaviour (rats swimming predominantly close to the wall) to non-spatial strategies (i.e. scanning) to proper spatial strategies (i.e. swimming directly to the platform). During the probe trial, time spent in the former target quadrant and former platform crossings were recorded.

As a control condition, frequently used in the MWM, cued platform trials were performed with a set of animal's naïve to the spatial version of the MWM. Cued trials require identical basic prerequisites such as vision, motor performance (swimming, climbing onto the platform) and motivation to escape as spatial trials. Each animal performed one trial with a 60 s trial limit where the platform was placed 1 cm above the water within the SE quadrant and marked with a balloon hanging 10 cm above the platform.

Discrimination Reversal. was assessed in a T-maze filled with water maintained at 25 °C (± 1 °C), with a hidden platform (15.5 × 15.5 cm) in one of the arms. On the first day (*position discrimination*) rats were trained to acquire left-right position discrimination with the platform consistently positioned in one of the arms. Rats were allowed to choose between arms. Once entered an arm, a door was lowered. If the correct arm was chosen, the rat was allowed to remain on the platform for 5 s, if the wrong one was chosen, the rat was confined to the arm for 5 s. Training continued with a 10 s inter-trial interval until a criterion of five consecutive correct trials was reached within a maximum of 25 trials. On the next day (*reversal*), rats were first retrained until criterion on the position discrimination of the first day was reached, and then trained until reaching the criterion on the reversal of this discrimination, i.e. with the platform located in the opposite arm. The number of trials to reach the criterion was recorded for both sessions.

Radial arm maze. Starting two days before RAM the animals were restricted to approximately 20 g of rat chow per day. The rat's weight was monitored daily to ensure that their health was maintained. An endpoint of 20% weight loss was established; which was not reached thus no animals had to be removed from the study. The RAM apparatus was elevated 65 cm above the floor, consisted of a central platform (47 cm diameter) with eight arms (40 × 15 cm) radiating from it. The apparatus was positioned in a room with distal cues on the walls visible to the animal. One day prior to testing, the baits used (Choco Krispies, KELLOG) were presented to the animals in their home cage. On day 1 to day 3, animals were allowed to explore the maze freely for 10 min or until consuming the baits hidden in the wells at the end of each arm. On day 4 to day 8, three of the arms were baited, randomly assigned but consistent for each animal over all trials. Again, animals were removed after 10 min or after finding all hidden baits. Training took place twice a day. The time spent in the maze, entered arms and the order of entry were recorded, including reference memory errors, i.e. entry into a non-baited arm, and working memory error, i.e. entry into a previously visited arm.

Open-field. An adjusted version was conducted to measure general locomotor activity and anxiety. The arena consisted of a square open-field box (70 × 70 × 40 cm) constructed of grey PVC plastic and evenly illuminated. On the first day the box was used as a platform (standing on its walls) placed elevated 1 m above the floor. The platform was covered with tissue to prevent slipping. Animals were released in the middle of the platform to explore freely for 10 mins. On the second day, the same box was used now placed on a table with the surrounding walls up. The animals were released in the middle and again, allowed to explore for 10 min. The arena was cleaned with 70% EtOH between each rat. A camera was positioned over the arena and behaviour was recorded. For both sessions, open-field (OF) and open-platform (OP), a square of 20 × 20 cm in the middle of the arena was designated as the centre and time spent in border and centre zone was analysed. Additionally, distance travelled and velocity were recorded.

The novel object recognition. test was used to evaluate the rat's ability to recognize a novel object in the environment without positive or negative reinforcers thereby assessing the natural preference for novelty displayed by the animals⁴⁸. The task procedure consisted of three phases: habituation, familiarization, and test phase. Open-field analysis were conducted the day before NOR, and thereby considered as habituation to the test environment⁴⁹. During familiarization, two objects (A + A') different in colour and size were placed in the OF arena on opposite corners with a distance of 20 cm from the walls. Animals were released in the middle of the box facing the opposite wall and could familiarize with the objects for 5 min. After a 24 h retention interval, the animals returned to the arena, were now one object was familiar (A) and the other object was replaced with a novel object, again different in form and colour (B). During the test phase animals were allowed to explore for 5 min. All stimuli consisted of objects made of glass, porcelain, or glazed ceramic and were cleaned with 70% EtOH between each rat. A video camera was positioned over the arena and familiarization and test phases were videotaped for analysis. Time spent exploring each object was measured by two blinded experimenters (within-session inter-rater reliability was moderate $r = 0.752$, $p < 0.001$, range: 0.703–0.840). Exploration was defined as sniffing or touching the object in a radius of 0 to 4 cm with its nose. Climbing and sitting on the object and touching it with the body was not considered exploration. Animals lacking exploration activity i.e. did not spend a minimum of 7 s exploring either object during familiarization phase (9 animals all DAT-tg), were excluded from analysis⁵⁰. The main dependent measure the Discrimination Index was calculated from the exploration time T as $DI = (T_B - T_A)/(T_B + T_A)$ based on the 5 min of the test phase, averaged over two independent assessors. Further distance travelled and velocity was analysed.

Sucrose consumption test (SCT). assesses an animals' response to a stimulus that should be perceived as rewarding. Rats were habituated to single cages and bottles containing sweetened condensed milk (Milchmädchencreme, Nestle; 1:3 mix with water) for 30 min each, 48 h and 24 h before testing, respectively. Following food restriction (15 g food/rat/24 h) rats were exposed to the sweetened bottles in single cages for 10 min. Bottles were weighed before and after the test session and the amount of liquid consumed was normalized to each animal's mean body weight, measured over the three consecutive days.

Post mortem neurobiological assessment. Tissue collection. Rats were transcardially perfused, brains removed and post-fixed overnight in 4% paraformaldehyde. 40 μm coronal sections were cut on a freezing microtome and a series of every sixth section was used for respective analysis.

Immunohistochemistry. Staining were carried out using standard protocols on free-floating sections. Sections for BrdU staining were pre-treatment with 2 N HCl for 30 min at 37 °C. Multiple washes in phosphate-buffered saline were performed between all further steps. After blocking with 10% donkey serum containing 0.2% Triton X-100, sections were incubated overnight with primary antibodies (for BrdU: rat anti-BrdU, AbD Serotec OBT0030, Cambridge, United Kingdom, 1:500; for NeuN: mouse anti-NeuN, Millipore, MAB377, 1:500; for Ki-67+: NCL-Ki67p, Novocastra Laboratories, Newcastle upon Tyne, UK, 1:500) in blocking solution containing 3% donkey serum and 0.2% Triton X-100. Ki67 and BrdU samples were detected with anti-rat or anti-rabbit-biotin coupled secondary antibodies (both 1:500; Dianova) together with the horseradish peroxidase-coupled ABC Elite system (Vector Laboratories, USA) and visualized with 3,3'-diaminobenzidine (Sigma) and 0.04% NiCl as the chromogen before counting under a light microscope. BrdU/NeuN double-labelled samples were detected with fluorescent secondary antibodies (donkey anti-rat Alexa Fluor 488, donkey anti-mouse Cy3 and donkey anti-rabbit Alexa Fluor 647; Jackson ImmunoResearch, UK), the nuclei counterstained with 4',6-diamidino-2-phenylindole, and then visualized for counting using an ApoTome fluorescence microscope (Zeiss, Germany) with Optical Sectioning mode (Structured Illumination Microscopy). Sampling of labelled cells was done exhaustively throughout the GCL in its rostro-caudal extension. A simplified version of the optical fractionator principle was used where labelled cells were categorized according to their localization in the dentate gyrus and counted except for cells in the uppermost focal plane to avoid oversampling at the cutting surfaces⁵¹. The resulting number was then multiplied by 6 (because every sixth section had been used) to give an estimate of the total number of positive cells. All counts were carried out with the experimenter blind to the experimental group.

Statistical analysis. Group differences were tested using two-tailed t-tests or nonparametric Mann-Whitney-U test when applicable. Repeated measures ANOVA models were used for variables taken repetitively on the same animal, such as trial or day, as within-subject factors. Main effects were Bonferroni adjusted, if applicable the Greenhouse-Geisser adjustment was used to correct for violations of sphericity, post-hoc tests applied Bonferroni correction (SPSS; IBM Corp. Released 2013, IBM SPSS Statistics for Windows, and Version 22.0. Armonk, NY: IBM Corp). The probability level of $p < 0.05$ was considered as statistically significant. Data are

presented as mean \pm SEM. For statistical analyses of the effect of genotype on search strategy, we used binomial (logit) mixed-effects models (glmer, package: lme4; R 3.4.3 (<https://www.r-project.org/>)) predicting strategy probabilities (0 vs. 1) for genotypes (0.5 = het vs. -0.5 = wt). A maximum random effects structure was used⁵². From the model odds ratios were calculated to compare the chance of using divergent strategies between genotypes.

Data Sharing

The datasets generated during and/or analysed during the current study are available from the corresponding author on reasonable request.

References

- Björklund, A. & Dunnett, S. B. Dopamine neuron systems in the brain: an update. *Trends Neurosci.* **30**, 194–202 (2007).
- Schultz, W. Multiple Dopamine Functions at Different Time Courses. *Annu. Rev. Neurosci.* **30**, 259–288 (2007).
- Floresco, S. B., West, A. R., Ash, B., Moore, H. & Grace, A. A. Afferent modulation of dopamine neuron firing differentially regulates tonic and phasic dopamine transmission. *Nat. Neurosci.* **6**, 968–973 (2003).
- Bromberg-Martin, E. S., Matsumoto, M. & Hikosaka, O. Dopamine in motivational control: rewarding, aversive, and alerting. *Neuron* **68**, 815–834 (2010).
- Cohen, J. Y., Haesler, S., Vong, L., Lowell, B. B. & Uchida, N. Neuron-type-specific signals for reward and punishment in the ventral tegmental area. *Nature* **482**, 85–88 (2012).
- Tsai, H.-C. *et al.* Phasic firing in dopaminergic neurons is sufficient for behavioral conditioning. *Science* **324**, 1080–1084 (2009).
- Steinberg, E. E. *et al.* A causal link between prediction errors, dopamine neurons and learning. *Nat. Neurosci.* **16**, 966 (2013).
- Niv, Y., Daw, N. D. & Dayan, P. How fast to work: Response vigor, motivation and tonic dopamine. In *Advances in neural information processing systems* 1019–1026 (2006).
- Zweifel, L. S. *et al.* Disruption of NMDAR-dependent burst firing by dopamine neurons provides selective assessment of phasic dopamine-dependent behavior. *Proc. Natl. Acad. Sci.* **106**, 7281–7288 (2009).
- Ihalainen, J. A., Riekkinen, P. Jr & Feenstra, M. G. P. Comparison of dopamine and noradrenaline release in mouse prefrontal cortex, striatum and hippocampus using microdialysis. *Neurosci. Lett.* **277**, 71–74 (1999).
- Kentros, C. G., Agnihotri, N. T., Streater, S., Hawkins, R. D. & Kandel, E. R. Increased Attention to Spatial Context Increases Both Place Field Stability and Spatial Memory. *Neuron* **42**, 283–295 (2004).
- Lisman, J. E. & Grace, A. A. The Hippocampal-VTA Loop: Controlling the Entry of Information into Long-Term Memory. *Neuron* **46**, 703–713 (2005).
- McNamara, C. G., Tejero-Cantero, Á., Trouche, S., Campo-Urriza, N. & Dupret, D. Dopaminergic neurons promote hippocampal reactivation and spatial memory persistence. *Nat. Neurosci.* **17**, 1658–1660 (2014).
- Rosen, Z. B., Cheung, S. & Siegelbaum, S. A. Midbrain dopamine neurons bidirectionally regulate CA3-CA1 synaptic drive. *Nat. Neurosci.* **18**, 1763 (2015).
- Li, S., Cullen, W. K., Anwyl, R. & Rowan, M. J. Dopamine-dependent facilitation of LTP induction in hippocampal CA1 by exposure to spatial novelty. *Nat. Neurosci.* <https://doi.org/10.1038/nn1049> (2003).
- Pezze, M. & Bast, T. Dopaminergic modulation of hippocampus-dependent learning: Blockade of hippocampal D1-class receptors during learning impairs 1-trial place memory at a 30-min retention delay. *Neuropharmacology* **63**, 710–718 (2012).
- Kentros, C. *et al.* Abolition of Long-Term Stability of New Hippocampal Place Cell Maps by NMDA Receptor Blockade. *Science* **280**, 2121–2126 (1998).
- Ferbinteanu, J. Contributions of Hippocampus and Striatum to Memory-Guided Behavior Depend on Past Experience. *J. Neurosci.* **36**, 6459–6470 (2016).
- DeCoteau, W. E. *et al.* Learning-related coordination of striatal and hippocampal theta rhythms during acquisition of a procedural maze task. *Proc. Natl. Acad. Sci.* **104**, 5644–5649 (2007).
- Berg, D. A., Belnoue, L., Song, H. & Simon, A. Neurotransmitter-mediated control of neurogenesis in the adult vertebrate brain. *Dev. Camb. Engl.* **140**, 2548–2561 (2013).
- Gonçalves, J. T., Schafer, S. T. & Gage, F. H. Adult Neurogenesis in the Hippocampus: From Stem Cells to Behavior. *Cell* **167**, 897–914 (2016).
- Ohtani, N., Goto, T., Waeber, C. & Bhida, P. G. Dopamine Modulates Cell Cycle in the Lateral Ganglionic Eminence. *J. Neurosci. Off. J. Soc. Neurosci.* **23**, 2840–2850 (2003).
- Freundlieb, N. Dopaminergic Substantia Nigra Neurons Project Topographically Organized to the Subventricular Zone and Stimulate Precursor Cell Proliferation in Aged Primates. *J. Neurosci.* **26**, 2321–2325 (2006).
- Höglinger, G. U. *et al.* Dopamine depletion impairs precursor cell proliferation in Parkinson disease. *Nat. Neurosci.* **7**, 726–735 (2004).
- Diaz, J. *et al.* Selective Expression of Dopamine D3 Receptor mRNA in Proliferative Zones during Embryonic Development of the Rat Brain. *J. Neurosci.* **17**, 4282–4292 (1997).
- Winner, B. *et al.* Dopamine receptor activation promotes adult neurogenesis in an acute Parkinson model. *Exp. Neurol.* **219**, 543–552 (2009).
- Baker, S. A., Baker, K. A. & Hagg, T. Dopaminergic nigrostriatal projections regulate neural precursor proliferation in the adult mouse subventricular zone. *Eur. J. Neurosci.* **20**, 575–579 (2004).
- McHugh, P. C. & Buckley, D. A. The structure and function of the dopamine transporter and its role in CNS diseases. *Vitam. Horm.* **98**, 339–369 (2015).
- Hadar, R. *et al.* Rats overexpressing the dopamine transporter display behavioral and neurobiological abnormalities with relevance to repetitive disorders. *Sci. Rep.* **6** (2016).
- Redish, A. *Beyond the Cognitive Map*. (MIT Press, 1999).
- Garthe, A., Behr, J. & Kempermann, G. Adult-Generated Hippocampal Neurons Allow the Flexible Use of Spatially Precise Learning Strategies. *PLOS ONE* **4**, e5464 (2009).
- Cohen, M. X., Krohn-Grimberghe, A., Elger, C. E. & Weber, B. Dopamine gene predicts the brain's response to dopaminergic drug. *Eur. J. Neurosci.* **26**, 3652–3660 (2007).
- Palmiter, R. D. Dopamine Signaling in the Dorsal Striatum Is Essential for Motivated Behaviors: Lessons from Dopamine-deficient Mice. *Ann. N.Y. Acad. Sci.* **1129**, 35–46 (2008).
- Hamid, A. A. *et al.* Mesolimbic dopamine signals the value of work. *Nat. Neurosci.* **19**, 117 (2016).
- Rømer Thomsen, K. Measuring anhedonia: impaired ability to pursue, experience, and learn about reward. *Front. Psychol.* **6** (2015).
- Mura, A. & Feldon, J. Spatial learning in rats is impaired after degeneration of the nigrostriatal dopaminergic system. *Mov. Disord.* **18**, 860–871 (2003).
- Pooters, T., Gantois, I., Vermaercke, B. & D'Hooge, R. Inability to acquire spatial information and deploy spatial search strategies in mice with lesions in dorsomedial striatum. *Behav. Brain Res.* **298**, 134–141 (2016).

38. Godar, S. C. & Bortolato, M. What makes you tic? Translational approaches to study the role of stress and contextual triggers in Tourette syndrome. *Neurosci. Biobehav. Rev.* **76**, 123–133 (2017).
39. Packard, M. G. & McGaugh, J. L. Double dissociation of fornix and caudate nucleus lesions on acquisition of two water maze tasks: Further evidence for multiple memory systems. *Behav. Neurosci.* **106**, 439–446 (1992).
40. Gasbarri, A., Sulli, A., Innocenzi, R., Pacitti, C. & Brioni, J. D. Spatial memory impairment induced by lesion of the mesohippocampal dopaminergic system in the rat. *Neuroscience* **74**, 1037–1044 (1996).
41. Devan, B. D., McDonald, R. J. & White, N. M. Effects of medial and lateral caudate-putamen lesions on place- and cue-guided behaviors in the water maze: relation to thigmotaxis. *Behav. Brain Res.* **100**, 5–14 (1999).
42. van Praag, H., Christie, B. R., Sejnowski, T. J. & Gage, F. H. Running enhances neurogenesis, learning, and long-term potentiation in mice. *Proc. Natl. Acad. Sci.* **96**, 13427–13431 (1999).
43. van Praag, H. *et al.* Functional neurogenesis in the adult hippocampus. *Nature* **415**, 1030–1034 (2002).
44. Jessberger, S. & Kempermann, G. Adult-born hippocampal neurons mature into activity-dependent responsiveness. *Eur. J. Neurosci.* **18**, 2707–2712 (2003).
45. Snyder, J. S. *et al.* Adult-born hippocampal neurons are more numerous, faster-maturing and more involved in behavior in rats than in mice. *J. Neurosci. Off. J. Soc. Neurosci.* **29**, 14484–14495 (2009).
46. Gould, E., Beylin, A., Tanapat, P., Reeves, A. & Shors, T. J. Learning enhances adult neurogenesis in the hippocampal formation. *Nat. Neurosci.* **2**, 260–265 (1999).
47. Olariu, A., Cleaver, K. M., Shore, L. E., Brewer, M. D. & Cameron, H. A. A natural form of learning can increase and decrease the survival of new neurons in the dentate gyrus. *Hippocampus* **15**, 750–762 (2005).
48. Ennaceur, A. & Delacour, J. A new one-trial test for neurobiological studies of memory in rats. 1: Behavioral data. *Behav. Brain Res.* **31**, 47–59 (1988).
49. Boersma, G. J. *et al.* Exposure to activity based anorexia impairs contextual learning in weight-restored rats without affecting spatial learning, taste, anxiety, or dietary-fat preference. *Int. J. Eat. Disord.* **49**, 169–181 (2016).
50. Tagliatalata, G., Hogan, D., Zhang, W.-R. & Dineley, K. T. Intermediate- and Long-Term Recognition Memory Deficits in Tg2576 Mice Are Reversed with Acute Calcineurin Inhibition. *Behav. Brain Res.* **200**, 95–99 (2009).
51. Kempermann, G., Gast, D., Kronenberg, G., Yamaguchi, M. & Gage, F. H. Early determination and long-term persistence of adult-generated new neurons in the hippocampus of mice. *Development* **130**, 391–399 (2003).
52. Barr, D. J., Levy, R., Scheepers, C. & Tily, H. J. Random effects structure for confirmatory hypothesis testing: Keep it maximal. *J. Mem. Lang.* **68** (2013).

Acknowledgements

We thank Doris Zschaber for excellent technical support and Elisabeth Obst for assistance regarding statistical analysis. The study was funded by the Federal Ministry of Education and Research, Germany (Grant 01EW1409 (EraNet Neuron framework) and Grant 01EE1403A (GCBS) and co-financed by the German Research Foundation (WI 2140/3-1).

Author Contributions

N.B. contributed to experimental design, data analysis and interpretation and wrote the manuscript. M.K.L., E.B.H., B.H., F.W., H.E.C. conducted experiments, contributed to data analysis and writing the manuscript. A.G. supervised histological investigations and contributed to experimental design and writing. C.W. conceived the study, designed experiments, conducted data analysis and interpretation and wrote the manuscript.

Additional Information

Supplementary information accompanies this paper at <https://doi.org/10.1038/s41598-018-32608-7>.

Competing Interests: The authors declare no competing interests.

Publisher's note: Springer Nature remains neutral with regard to jurisdictional claims in published maps and institutional affiliations.



Open Access This article is licensed under a Creative Commons Attribution 4.0 International License, which permits use, sharing, adaptation, distribution and reproduction in any medium or format, as long as you give appropriate credit to the original author(s) and the source, provide a link to the Creative Commons license, and indicate if changes were made. The images or other third party material in this article are included in the article's Creative Commons license, unless indicated otherwise in a credit line to the material. If material is not included in the article's Creative Commons license and your intended use is not permitted by statutory regulation or exceeds the permitted use, you will need to obtain permission directly from the copyright holder. To view a copy of this license, visit <http://creativecommons.org/licenses/by/4.0/>.

© The Author(s) 2018

ARTICLE

Open Access

Non-invasive modulation reduces repetitive behavior in a rat model through the sensorimotor cortico-striatal circuit

Henriette Edemann-Callesen^{1,2,3}, Bettina Habelt², Franziska Wieske^{1,2}, Mark Jackson⁴, Niranjana Khadka⁴, Daniele Mattei⁵, Nadine Bernhardt⁶, Andreas Heinz¹, David Liebetanz⁶, Marom Bikson⁴, Frank Padberg⁷, Ravit Hadar^{1,2}, Michael A. Nitsche^{8,9} and Christine Winter^{1,2}

Abstract

Involuntary movements as seen in repetitive disorders such as Tourette Syndrome (TS) results from cortical hyperexcitability that arise due to striato-thalamo-cortical circuit (STC) imbalance. Transcranial direct current stimulation (tDCS) is a stimulation procedure that changes cortical excitability, yet its relevance in repetitive disorders such as TS remains largely unexplored. Here, we employed the dopamine transporter-overexpressing (*DAT-tg*) rat model to investigate behavioral and neurobiological effects of frontal tDCS. The outcome of tDCS was pathology dependent, as anodal tDCS decreased repetitive behavior in the *DAT-tg* rats yet increased it in wild-type (*wt*) rats. Extensive deep brain stimulation (DBS) application and computational modeling assigned the response in *DAT-tg* rats to the sensorimotor pathway. Neurobiological assessment revealed cortical activity changes and increase in striatal inhibitory properties in the *DAT-tg* rats. Our findings show that tDCS reduces repetitive behavior in the *DAT-tg* rat through modulation of the sensorimotor STC circuit. This sets the stage for further investigating the usage of tDCS in repetitive disorders such as TS.

Introduction

Repetitive symptoms as observed in among others Tourette Syndrome (TS) can in severe cases hinder social and professional development^{1, 2}. The pathology underlying the manifestation of repetitive symptomatology remains inconclusive, yet vast evidence points to an imbalanced striato-thalamo-cortical circuit (STC), where a combined action of dopaminergic hyperresponsivity and striatal disinhibition results in cortical hyperexcitability and ultimately impaired movement control³⁻⁷.

Current drug therapies, especially those applied for repetitive symptoms seen in TS, lack precision, which may

account for their inability to provide sufficient and enduring symptom relief. One treatment strategy allowing for focal intervention is deep brain stimulation (DBS) in which electrical stimulation is delivered directly to pathology-relevant brain areas through implanted electrodes⁸. DBS has already been applied to several brain structures within the STC circuit to reduce repetitive behavior as seen in TS⁹⁻¹². However, despite positive results, its invasive nature hinders a general application and is therefore mostly considered for only severely affected adult patients^{13, 14}. To increase the treatment options for repetitive disorders, there is the need for more subtle strategies suitable for a broader patient group.

Transcranial direct current stimulation (tDCS) is a non-invasive, safe and well-tolerated strategy that modulates cortical excitability through application of weak electrical current. The effect on excitability depends on stimulation polarity, with cathodal stimulation decreasing and anodal

Correspondence: Christine Winter (christine.winter@charite.de)

¹Department of Psychiatry and Psychotherapy, Charité Universitätsmedizin Berlin, Berlin, Germany

²Department of Psychiatry and Psychotherapy, Medical Faculty Carl Gustav Carus, Technische Universität Dresden, Dresden, Germany

Full list of author information is available at the end of the article

© The Author(s) 2017



Open Access This article is licensed under a Creative Commons Attribution 4.0 International License, which permits use, sharing, adaptation, distribution and reproduction in any medium or format, as long as you give appropriate credit to the original author(s) and the source, provide a link to the Creative Commons license, and indicate if changes were made. The images or other third party material in this article are included in the article's Creative Commons license, unless indicated otherwise in a credit line to the material. If material is not included in the article's Creative Commons license and your intended use is not permitted by statutory regulation or exceeds the permitted use, you will need to obtain permission directly from the copyright holder. To view a copy of this license, visit <http://creativecommons.org/licenses/by/4.0/>.

stimulation increasing membrane excitability at the macroscopic level^{15–21}. Beyond acute effects, prolonged stimulation results in neuroplastic after effects, which share some similarities with long-term potentiation and depression^{15, 17, 22}. tDCS has already been applied in depression²³, chronic pain²⁴ and schizophrenia^{25, 26} with so far largely positive results. Only one study documents the usage of cathodal tDCS as a mean to reduce cortical hyperexcitability and thus repetitive behavior in TS²⁷. Results seem promising, yet a thorough evaluation of its therapeutic relevance in repetitive disorders is missing. Still outstanding is an investigation on the preferable current intensity and stimulation polarity for repetitive pathology and subsequent symptoms. Obviously, such in-depth assessment is clinically challenging, yet is overcome preclinically by employing validated animal models.

The dopamine transporter-overexpressing (*DAT-tg*) rat model exhibits multiple neurobiological abnormalities considered to underlie repetitive disorders, including TS. Apart from far-reaching dopaminergic alterations, these include decrease in striatal GABAergic PV+ expressing interneurons and increased c-fos levels in cortical areas, demonstrating the existence of an imbalanced STC circuit in this model also seen in TS. On a behavioral level, *DAT-tg* rats display amphetamine sensitivity and subsequent repetitive behavior that specifically responds to TS-drug treatment, i.e. administration of the $\alpha 2$ adrenergic and imidazoline receptor agonist clonidine. The occurrence of repetitive behavior in the *DAT-tg* rat is time locked, which allows for evaluation of therapeutic interventions when behavioral manifestation is proven to be most prominent²⁸.

In this study, we sought to investigate the effects of frontal tDCS on repetitive behavior in the *DAT-tg* rat. Combining extensive DBS application alongside computational modeling of current spread we sought to identify the sub-circuitry involved in the therapeutic response. Finally, neurobiological assessment of the most therapeutically potent tDCS application enabled mechanistic insight into cortical activity patterns, neurotransmitter levels and inhibitory properties of the striatum. Taken together, our study provides a thorough investigation into the effect of tDCS on repetitive symptomatology and its underlying pathophysiology.

Materials and methods

Animals

Experiments were performed in accordance to the European Communities Council Directive of 22 September 2010 (2010/63/EU) after approval by the local ethics committees (Senate of Berlin, Regierungspräsidium Dresden). Experiments were conducted on male Wistar *DAT-tg* rats ($n = 38$) and their respective littermate controls (*wild types* (*wt*) ($n = 37$)) with a Sprague Dawley

background once they reached postnatal day (PND) >90 ²⁸. Following surgery, animals were single housed in a 12 h light/dark cycle (light on at 06:00 am) with food and water ad libitum. All efforts were made to reduce animal suffering and number of animals used.

Experimental design

In this study, the experimental groups consisted of subjects randomly allocated to the tDCS or DBS groups, prior to surgeries. Animals ordained to receive tDCS following surgery were subdivided into the tDCS group (*DAT-tg*, $n = 9$, *wt* $n = 7$) and an overall control group (*DAT-tg*, $n = 8$, *wt* $n = 8$). Common for all animals was the implementation of an epicranial electrode, surgically fixed onto the skull over the frontal cortex, through which tDCS/sham stimulation was applied. Animals ordained to receive DBS were subdivided into three groups (groups 1–3) prior to surgery and subsequently implanted bilaterally with monopolar electrodes into cortical and sub-cortical areas of the STC circuit. These included the orbitofrontal cortex (OFC) and caudate putamen (CPu) (group 1) (*DAT-tg*, $n = 8$, *wt* $n = 8$), the medial prefrontal cortex (mPFC) (group 2) (*DAT-tg*, $n = 8$, *wt* $n = 8$) or the primary motor cortex (M1) and thalamus (Thal) (group 3) (*DAT-tg*, $n = 5$, *wt* $n = 6$). All animals recovered for 1 week after surgery before starting experiments. Animals in the tDCS group received either sham, cathodal (100 or 200 μ A) or anodal (100, 200 or 300 μ A) stimulation. Animals in the DBS group (groups 1–3) received either sham, high (130 Hz) or low (10 Hz) frequency stimulation in the respective brain areas. Animals in the control group only received sham stimulation (see SI, Table S1 for overview of group specifics and number of animals). The repetitive behavioral paradigm described by Hadar *et al.*²⁸ was employed to study the effect of tDCS and DBS on behavior. Stimulation was applied in the beginning of the paradigm and subsequent behavior was assessed during the stereotypy phase. Experiments were conducted in a crossover design and different types of stimulation were applied in a randomized fashion over the course of the experiment. Animals could rest for 1 week in between stimulation. Rats in the control group, receiving sham stimulation, only went through the behavioral paradigm once. These rats served as an overall control group for later neurobiological assessment. For finalization of the experiment, animals were stimulated with the most therapeutic-relevant stimulation settings as assessed by behavioral analysis. As such, animals in the tDCS group received anodal 200 μ A stimulation. Following the finalization of the last experimental round, animals were immediately sacrificed and brains were snap frozen for later post mortem neurobiological assessment. Computational modeling was constructed to investigate the electrical current spread mediated by tDCS. The

investigators who run the analysis were blind to the group allocation as well as when analyzing the data. More details are included in the supplementary information.

Surgery

Animals went through surgery after reaching PND 90 (body weight of >280 g). Animals were handled 3–4 days prior to surgery. Surgery was performed under subcutaneous (s.c.) general anesthesia: fentanyl (0.005 mg/kg), midazolam (2 mg/kg) and medetomidine dihydrochloride (0.135 mg/kg). The skull was fixed in a stereotactic frame and bregma was exposed. For animals in the tDCS and control group, an epicranial electrode (2.1 mm diameter) composed of a tubular plastic jacket was placed over the left frontal cortex (AP +3.2; ML1.5) and fixed using glass ionomer cement (Ketac Cem; ESPE Dental AG, Seefeld, Germany). For DBS application, monopolar electrodes (0.5 mm, MS303-6-AIU, Plastics One Inc., USA) were implanted bilaterally into the OFC (AP +3.7; ML +2.4; DV -3.3), CPu (AP +1.5; ML +1.5; DV -4.0), mPFC (AP +3.5; ML +0.6; DV -3.4), M1 (AP +1.5; ML +2.7; DV -1.5) and Thal (AP -4.1; ML +1.3; DV -6.4). Anchor screws were drilled into the skull for fixation and the individual ground electrode from each DBS electrode was wrapped around the closest screw and fixed with dental cement (Technovit, Heraeus Kulzer GmbH, Wehrheim, Germany). All coordinates were in accordance to Paxinos rat brain atlas²⁹. Upon completion of surgery, anesthesia was antagonized by a cocktail of naloxone (0.12 mg/kg), flumazenil (0.2 mg/kg) and antipamzol (0.75 mg/kg). Analgesia (meloxicam: 0.2 mg/kg, s.c.) was given for 3 days following surgery.

Repetitive behavior paradigm

As identified by Hadar *et al.*,²⁸ *DAT-tg* rats display a time-locked induction of repetitive behavior following the injection of amphetamine. In this experiment, animals were injected with amphetamine (2.0 mg/kg, i.p., dissolved in 0.9% saline at a volume of 1.0 ml/kg, Sigma Aldrich, Germany) and thereafter immediately subjected to stimulation (either tDCS or DBS). Animals in the DBS group received 60 min of stimulation. Cables were removed following DBS application and the animals could move freely for additional 60 min. Animals in the tDCS conditions received 30 min of tDCS or sham stimulation, respectively. Cables and jackets were removed following tDCS application and the animals could move freely for an additional 90 min (See SI, Figure S1). Behavior was recorded via web cameras throughout the paradigm. The occurrence of repetitive behavior (oral stereotypy or head movements) was later analyzed during the stereotypy phase (90–120 min following injection) by a blinded observer using the scoring protocol of Hadar *et al.*²⁸

tDCS application

For delivery of tDCS, the epicranial electrode was filled with saline (0.9%) (contact area of 3.5 cm²) after which a gold pin was inserted for stimulation application. A counter electrode (8 cm²; From Physiomed Elektromedizin AG, Schnaittach, Germany) was placed onto the thorax together with electroencephalography (EEG) conducting crème (GVB-geliMED KG, Germany) and kept in place by a jacket^{30, 31}. Animals were exposed to either 30 min anodal (100, 200 or 300 μ A), cathodal (100 or 200 μ A) or sham stimulation in the beginning of the repetitive behavioral paradigm. Both cathodal and anodal stimulation were applied by a computer-interfaced current generator (STG4008 Multi Channel System GmbH Reutlingen, Germany). The current strength was ramped for 10 s to prevent abrupt interruption and stimulation break effects. For sham stimulation, animals were connected to the system, yet no current was flowing.

DBS application

DBS was applied as biphasic 100 μ s pulses with either a current intensity of 150 μ A and frequency of 130 Hz (high frequency) or with a current intensity of 300 μ A and frequency of 10 Hz (low frequency). Stimulation was controlled by the STG4008 Multi Channel System GmbH Reutlingen, Germany. At 1 day prior to testing, DBS or sham stimulation was performed twice for 1 h (morning and afternoon). On testing day, animals were subjected to 60 min of either high- or low-frequency stimulation in the respective areas during the beginning of the behavioral paradigm. Sham stimulation was applied in an identical fashion yet no current was flowing.

Post mortem neurobiological assessment

Decapitation and snap freeze

Animals were immediately sacrificed following finalization of the experiment. Brains were extracted within less than 20 s, snap frozen for 2 min in methylbutane cooled with liquid nitrogen to a temperature of -40 °C and then stored at -80 °C until required. Next to electrode localization, frozen coronal sections of 1 or 0.5 mm were cut on a cryostat (see Table S2 for coordinates).

High-performance liquid chromatography (HPLC)

Tissue samples were taken via micropunches of 1 mm diameter and were homogenized by ultrasonication in 250 μ l (per punch) 0.1 N perchloric acid at 4 °C. Then, 100 μ l of the homogenate was added to equal volumes of 1N sodium hydroxide for measurement of protein content. The remaining homogenate was centrifuged at 13,000 g and 4 °C for 15 min. The supernatant was added to equal volumes (20 μ l) of 0.5 M borate buffer and stored at -80 °C for subsequent analyses of amino acids. The remaining supernatant was used for immediate

measurement of monoamines. Monoamine levels (3,4-dihydroxyphenylacetic acid (DOPAC) and dopamine (DA)) were measured by HPLC with electrochemical detection as previously described^{32, 33}.

Quantitative polymerase chain reaction (qPCR)

Tissue samples from the left hemisphere were taken via micropunches of 1 mm diameter from the mPFC, M1 and OFC. Further tissue samples were taken in the same way from both hemispheres from the CPU. Tissue was homogenized by ultrasonication in the buffer provided by the NucleoSpin RNA/Protein-Kit (Machery-Nagel, Düren, Germany). The total RNA and protein was extracted as recommended in its user manual. RNA concentrations were determined using a Nanodrop Spectrophotometer (peqlab). cDNA was synthesized using the High Capacity RNA-to-cDNA Kit (Lifetechnologies). TaqMan qPCR was performed with StepOne Real-Time PCR System (Lifetechnologies) using TaqMan fast advanced master mix (Lifetechnologies). The following TaqMan Gene Expression assays (Lifetechnologies) were used: Pvalb Assay (Rn00574541_m1) and c-Fos Assay (Mm00487425_m1). CT values were normalized to the housekeeping gene GFAP (Rn01253033_m1). Fold change was calculated using the $\Delta\Delta CT$ method.

Electrode localization

At the respective coordinates, brains were sliced into 20 mm coronal sections and Nissl-stained for light microscopic inspection of electrode tip placements as previously explained^{34–36}. One animal with a wrong-positioned electrode was excluded from the study.

Computational modeling

To determine the effect of various current densities on the cortex, a state-of-the-art model was constructed from a magnetic resonance imaging (MRI; 7.0 Tesla70/30 Bruker Biospec) and micro computed tomography scan (Siemens Inveon) of a template rat head³⁷.

MRI data collection and segmentation

MRI resolution was 0.282 mm, as previously mentioned³⁷. The scans were segmented into 9 tissues: skin, skull, cerebral spinal fluid (CSF), air, gray matter, white matter, hippocampus, cerebellum and spinal cord. A Rat Brain Atlas³⁸ was used to identify the hippocampal region of the brain. Remaining brain regions were appropriately grouped as either gray or white matter. Manual segmentation was used to generate an initial segmentation of scalp, skin, CSF, air, gray matter, white matter, hippocampus, cerebellum and spinal cord. Tissue continuity was verified after segmentation by extensively reviewing the data. Further manual adjustments were made to guarantee continuity and improve the segmentation

accuracy to closely match the tissue masks to the real anatomy of the rodent using ScapIP 7.0 (Simpleware Ltd, Exeter, UK).

Modeling of tDCS

The tDCS in vivo electrode placement protocol described above was modeled in SolidWorks (Dassault Systemes Corp. Waltham, MA) and imported into ScanIP for meshing. The modeled epicranial electrode had a contact area of 3.5 cm² and was placed in accordance to coordinates used in the behavioral experiment (AP: +3.2; ML:1.5). The 1.0 mm diameter gold pin serving as the anode was placed on the skull inside of the epicranial electrode. An 8 cm² cathode was placed on the thorax with EEG conducting crème as an electrolyte. An adaptive tetrahedral meshing algorithm was used in ScanIP to generate meshes of 8×10^6 quadratic elements. A Finite Element Method (FEM) model was created in COMSOL Multiphysics 4.3 (COMSOL, Inc., Burlington, MA) using the mesh mentioned above. The model was created using electrostatic volume conductor physics with material conductivities defined as follows (in S/m): skin, 0.465; skull, 0.01; CSF, 1.65; air, $1e^{-15}$; spinal cord, 0.126; gray matter, 0.276; white matter, 0.126; hippocampus, 0.126; cerebellum, 0.276; dental cement, $1e^{-15}$; electrode jacket, $1e^{-15}$; saline, 1.4; and electrode, $5.99e^7$. Conductivity values were taken from a combination of in vitro and in vivo measurements^{39, 40}. Current boundaries were applied to simulate direct current stimulation, and internal boundaries between tissues were assigned the continuity condition ($n \cdot (J_1 - J_2) = 0$), and the Laplace equation ($\nabla \cdot (\sigma \nabla V) = 0$) was solved. The surface of the cathode was grounded ($V = 0$) while the surface of the anode had a current density of $3.252e^{-4}$ A/m². All other exterior surfaces were electrically insulated. Brain current density data were collected from the left cortical hemisphere above the corpus callosum and averaged for analysis. High-resolution models predicted the concentration and distribution of brain current density for the in vivo rodent model using the electrode montage.

Statistics

Sample size was chosen based on the convention that for behavioral experiments n of 8–10 ensures adequate power to detect a prespecified effect size and on our previous experience with the chosen methods²⁸. Inclusion criterion was the complete endurance of the neuromodulation period. This criterion is an integral part of the study objectives and design as it was designed to study DBS as a preventive avenue. Exclusion criterion for outliers was ± 2 standard deviations of the means. Behavioral analysis was performed using a one-way analysis of variance (ANOVA) repeated measure with Treatment as variables. Post-hoc tests utilized the Holm–Sidak for

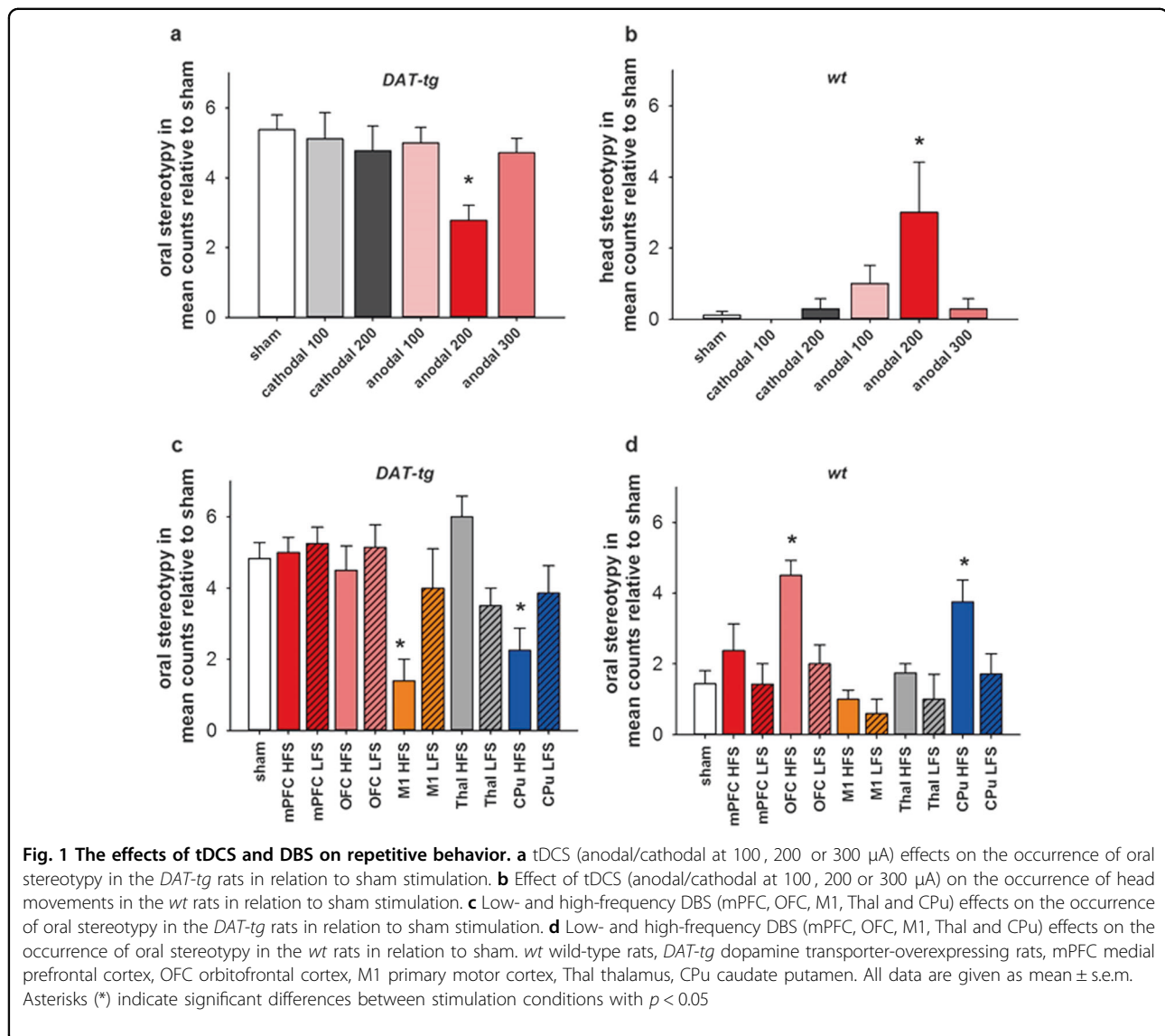
multiple comparisons. Neurobiological analysis for HPLC was performed using a two-Way ANOVA with treatment (sham, tDCS and DBS) and phenotype (*DAT-tg* vs. *wt*) as variables. Analysis of qPCR data was conducted following normalization to sham stimulation, with a one-way ANOVA used for *c-fos* analysis and a non-parametric Mann–Whitney test employed for parvalbumin (PV) analysis. Statistical significance was set at $p < 0.05$. Results are expressed as mean \pm s.e.m. The experiment shown was replicated once in our lab.

Results

Behavioral effects

The after-effect of tDCS (anodal and cathodal) on behavior was assessed during the stereotypy phase of a

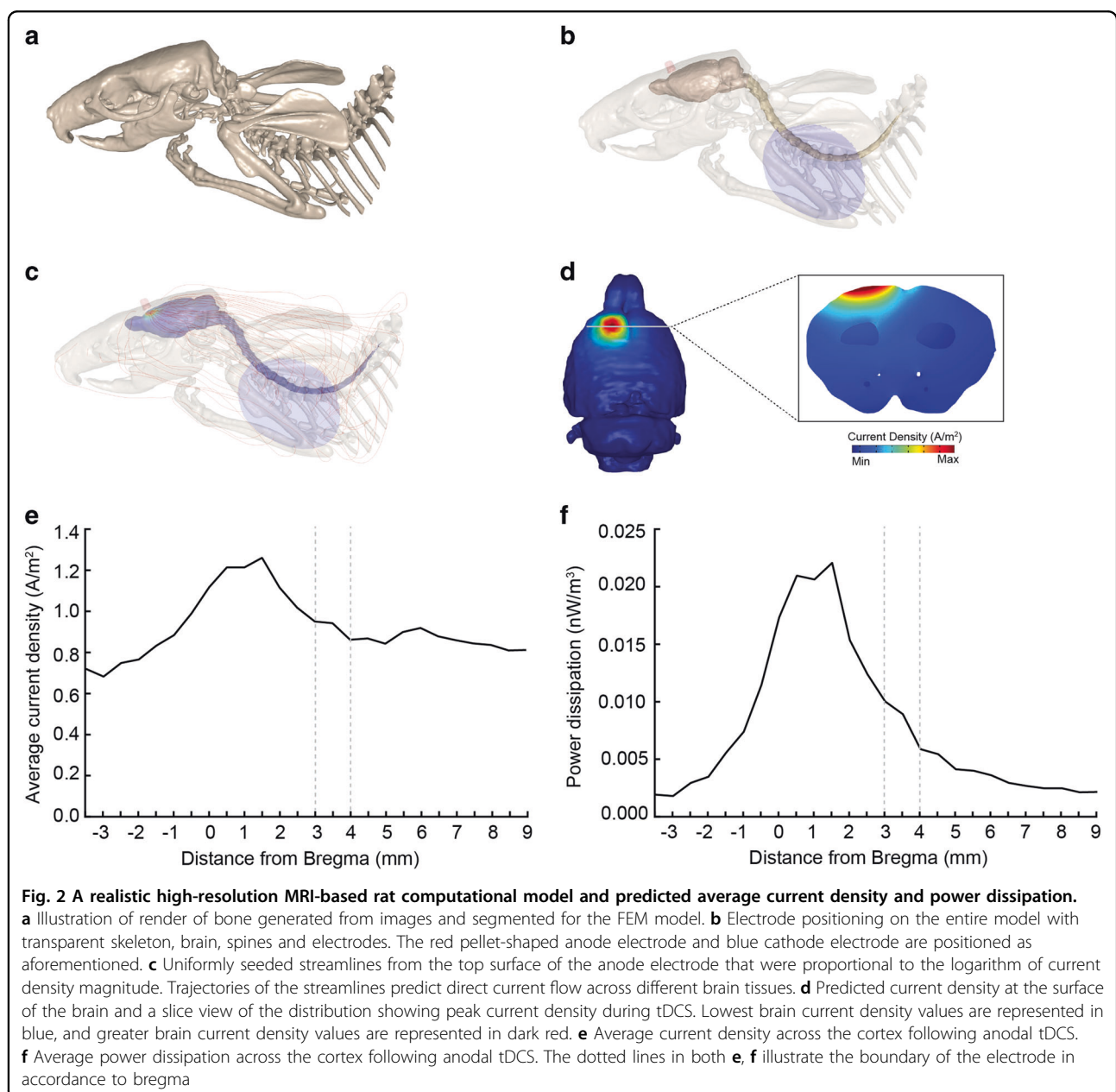
repetitive paradigm²⁸. In *DAT-tg* rats, one-way repeated measure analysis of variance (rmANOVA) tDCS effects on behavior in relation to sham revealed a significant effect for treatment ($F^{5,33} = 2.727$, $p = 0.036$), with a further post-hoc test showing that frontal anodal tDCS at 200 μ A significantly reduced oral stereotypy when compared to sham stimulation ($p = 0.012$) (Fig. 1a). In *wt* rats, one-way rmANOVA showed a significant effect for the factor treatment ($F^{5,28} = 3.388$, $p = 0.016$), with anodal tDCS at 200 μ A significantly increasing head movements in comparison to sham stimulation ($p = 0.015$) (Fig. 1b), whereas no effect of either anodal or cathodal tDCS was seen on oral stereotypy (data not shown). The effect of high- and low-frequency DBS was assessed following the application to several cortical and subcortical structures. In *DAT-tg* rats, one-way rmANOVA showed a significant

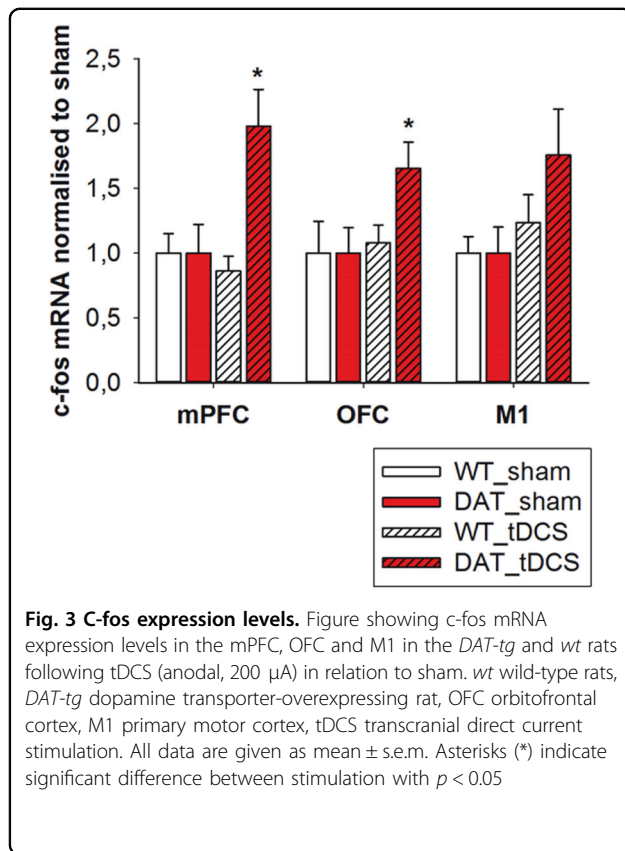


effect for treatment ($F^{10,51} = 4.112$, $p < 0.001$), as oral stereotypy significantly decreased following high-frequency DBS to the CPu ($p = 0.001$) and M1 ($p = 0.019$) in comparison to sham stimulation. In contrast, no effect was found following DBS to the mPFC, OFC or thalamus (thal) at either low- or high-frequency stimulation (Fig. 1c). In *wt* rats, a significant effect was found for the factor treatment ($F^{10,54} = 4.102$, $p < 0.001$), with an increase in oral stereotypy seen after high-frequency DBS to the OFC ($p = 0.001$) and CPu ($p = 0.026$) in comparison to sham stimulation. No effect was seen following DBS to the mPFC, M1 or thal at either low- or high-frequency stimulation (Fig. 1d).

Activity measures

The current density resulting from anodal tDCS at 200 μA was predicted by computational modeling. Current density distribution following anodal tDCS for the in vivo rodent model is shown in Fig. 2c. Results show a prominent peak of both average current density and average power dissipation approximately 1.5 mm anterior to bregma (average current density $1,18825\text{E}-06$; average power dissipation $2,0979\text{E}-11$) (Fig. 2a, b). Analysis of *c-fos* mRNA expression levels was conducted to quantify cortical activity pattern following effective tDCS in relation to sham stimulation. A one-way ANOVA showed a significant difference in the mPFC, ($F^{1,13} = 7.732$,





$p = 0.016$) and OFC ($F^{1,10} = 5.129$, $p = 0.043$) such that within these areas anodal tDCS at 200 μ A significantly increased c-fos mRNA levels in the *DAT-tg* rats. No difference in c-fos levels was detected in the *wt* rats. (Fig. 3).

Neurobiological assessment

Neurobiological investigations were conducted for frontal anodal tDCS at 200 μ A. HPLC post mortem biochemical analysis was made to investigate the persisting effect on neurotransmitter levels. Based on previously proven relevance²⁸, DA levels and DA turnover (DOPAC/DA) were assessed in the OFC, CPu and NAcc. Looking at DA levels, two-way ANOVA revealed a significant main effect for phenotype in the OFC ($F^{1,22} = 5.270$, $p = 0.032$), CPu ($F^{1,23} = 247.623$, $p < 0.001$) and NAcc ($F^{1,23} = 29.285$, $p < 0.001$) with *DAT-tg* rats generally displaying lower DA levels in comparison to *wt* rats (Fig. 4a–c, Table 1). Further investigation into DA turnover revealed in the OFC, CPu and NAcc a significant effect for phenotype (OFC: $F^{1,22} = 37.471$, $p < 0.001$; CPu: $F^{1,23} = 43.789$, $p < 0.001$; NAcc: $F^{1,22} = 45.293$, $p < 0.001$), with *DAT-tg* rats showing a higher degree of DA turnover as compared to the *wt* rats (Fig. 4d–f, Table 1).

To quantify inhibitory properties of the striatum, a qPCR on PV mRNA in the CPu was employed. The

Mann–Whitney test revealed a significant reduction in PV mRNA levels following tDCS in the *DAT-tg* rats as compared to sham stimulation (Mann–Whitney $U = 1.500$, $p = 0.005$). No difference was observed in the *wt* rats. (Fig. 5). See Supplementary Information (SI) for neurobiological assessment and computational modeling of DBS application.

Discussion

Here, we demonstrate that anodal tDCS applied at 200 μ A to the rat frontal cortex significantly reduced repetitive behavior in the *DAT-tg* rat model. By mathematically modeling current density distribution and multisite DBS application, we further show that the tDCS-therapeutic effects involved a modulation of the sensorimotor STC circuit.

The cumulative outcome of tDCS relies on several factors including stimulation intensity, duration and polarity in combination with the initial neuronal baseline activity, neurotransmitter profile and target structure composition^{41–43}. These interacting components all challenge direct comparisons between studies and demonstrate the need for specific assessment of tDCS effects in a given disorder. Well-controlled studies in appropriate animal models provide a platform for investigating interactions between the respective pathology and stimulation parameters that ultimately will determine the tDCS procedure needed for therapeutic relief. We found repetitive behavior to significantly decrease in *DAT-tg* rats following application of frontal anodal tDCS (200 μ A), whereas the same stimulation type increased it in *wt* rats. Higher (300 μ A) and lower (100 μ A) current intensities had no effect in either phenotype. In the context of repetitive behavior, these results demonstrate a polarity-specific and non-linear dose dependency of tDCS. *DAT-tg* rats display heightened cortical activity levels due to an underlying hyperresponsive dopaminergic system in comparison to *wt* rats²⁸. In line with this, it was previously shown that alterations in the underlying dopaminergic state, either pharmacologically induced or due to disease-related alterations, could modify and even invert the facilitating effects of tDCS^{44–48}. As the final tDCS response depends on initial cortical activity and underlying DA levels, the opposing behavioral outcome between the two phenotypes further reflects a state-dependent modulation of tDCS. Of note, repetitive behavior observed in *wt* rats (i.e., head movements) following tDCS differed from that induced in *DAT-tg* rats (oral stereotypy) further corroborating the notion of a differential modulation mediated by tDCS in the two phenotypes.

The STC circuit is composed of several topographically organized pathways that are separately associated with different aspects of repetitive symptomatology. The

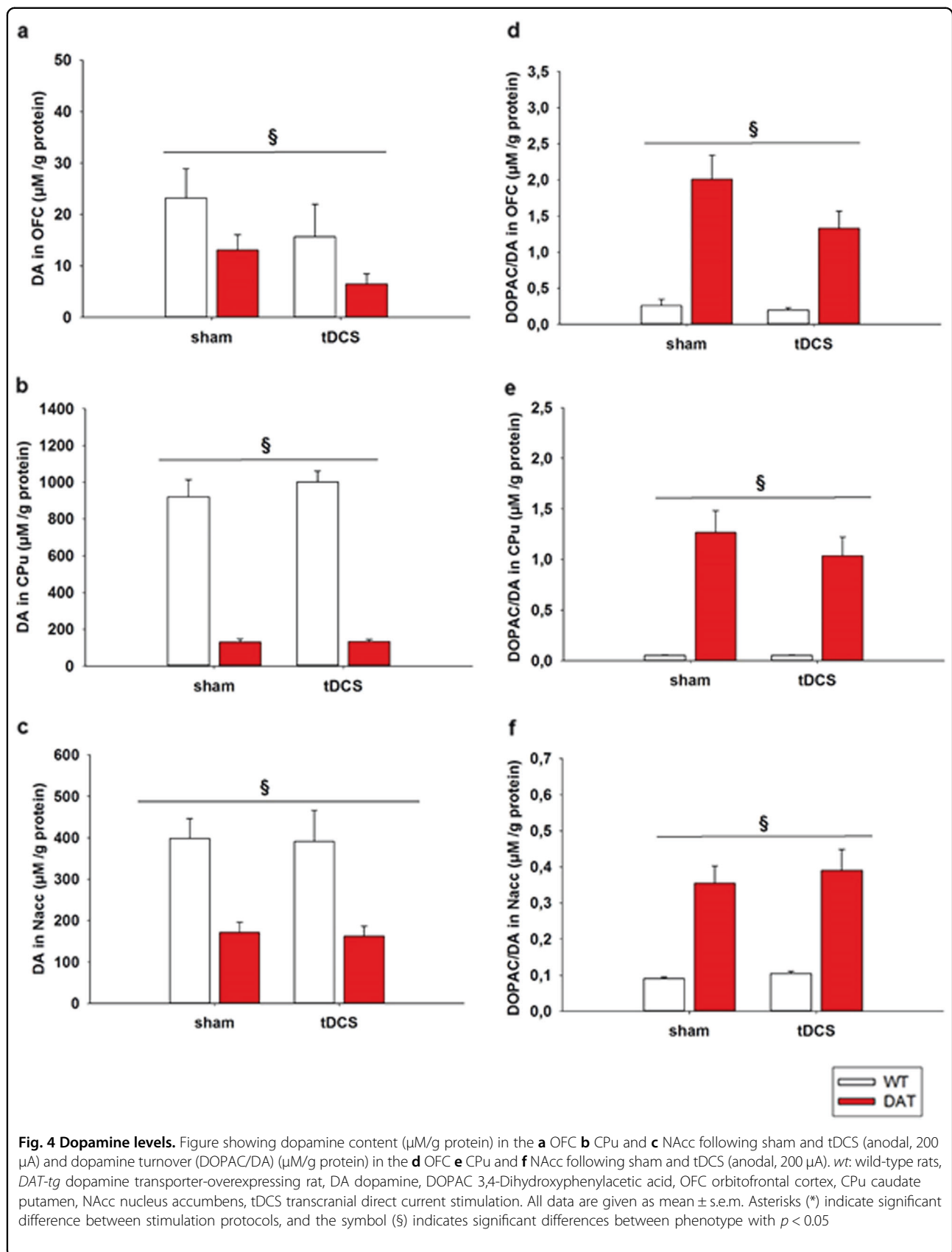


Table 1 Neurotransmitter contents

Region	Transmitter	Pheno	Stim	$\mu\text{M/g protein}$	Two-way ANOVA	DF	F-value	P-value
OFC	DA	wt	sham	23.185 \pm 4.319	Pheno	(1,22)	5.27	0.032 ^a
			tDCS	15.630 \pm 4.731	Stim	(1,22)	2.82	0.107
	DAT-tg	wt	sham	13.034 \pm 3.740	Interaction	(1,22)	0.0129	0.911
			tDCS	6.435 \pm 3.999				
DOPAC	wt	wt	sham	0.257 \pm 0.266	Pheno	(1,21)	37.471	<0.001 ^a
			tDCS	0.194 \pm 0.291	Stim	(1,21)	4.243	0.052
	DAT-tg	wt	sham	2.353 \pm 0.230	Interaction	(1,21)	3.328	0.082
			tDCS	1.328 \pm 0.266				
CPu	DA	wt	sham	963.86 \pm 52.35	Pheno	(1,23)	247.623	<0.001 ^a
			tDCS	1002.0 \pm 61.95	Stim	(1,23)	0.146	0.706
	DAT-tg	wt	sham	129.65 \pm 48.97	Interaction	(1,23)	0.105	0.749
			tDCS	132.78 \pm 52.35				
DOPAC	wt	wt	sham	0.052 \pm 0.160	Pheno	(1,23)	43.789	<0.001 ^a
			tDCS	0.052 \pm 0.190	Stim	(1,23)	0.497	0.497
	DAT-tg	wt	sham	1.264 \pm 0.150	Interaction	(1,23)	0.495	0.495
			tDCS	1.035 \pm 0.160				
NAcc	DA	wt	sham	398.19 \pm 40.73	Pheno	(1,23)	29.285	<0.001 ^a
			tDCS	390.92 \pm 48.19	Stim	(1,23)	0.0359	0.851
	DAT-tg	wt	sham	171.01 \pm 38.11	Interaction	(1,23)	0.00028	0.987
			tDCS	162.32 \pm 40.74				
DOPAC	wt	wt	sham	0.090 \pm 0.038	Pheno	(1,22)	45.293	<0.001 ^a
			tDCS	0.104 \pm 0.045	Stim	(1,22)	0.372	0.548
	DAT-tg	wt	sham	0.354 \pm 0.036	Interaction	(1,22)	0.072	0.791
			tDCS	0.390 \pm 0.041				

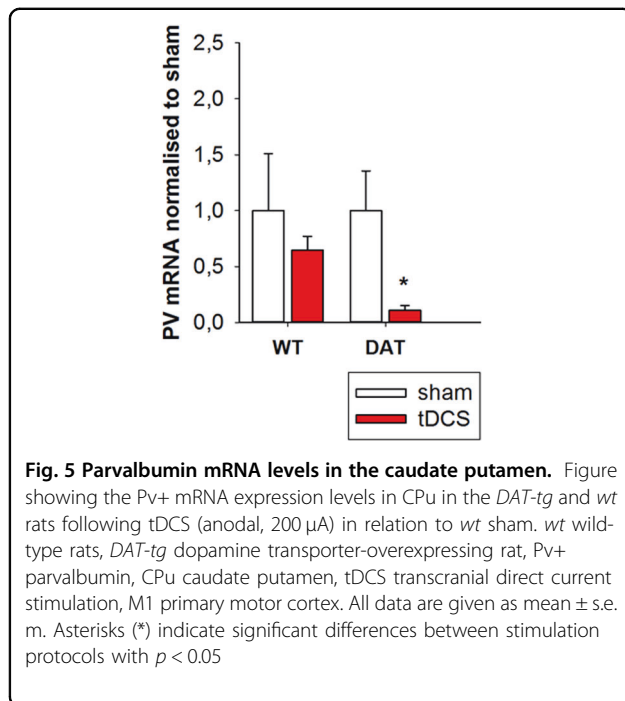
OFCorbitofrontal cortex, NAcc nucleus accumbens

Neurochemical content was examined in the *DAT-tg* and *wt* rats following sham and tDCS. Dopamine levels and dopamine turnover were measured in the medial OFC, NAcc and CPu. Data are presented as mean \pm s.e.m. Asterisks (*) indicate significant differences between phenotype with $p < 0.05$

sensorimotor circuit is considered the site of tic origin, whereas the limbic and associative circuits are linked to comorbidity and cognitive deficiency^{49, 50}. To further identify the sub-circuit involved in modulation of repetitive behavior in *DAT-tg* rats by tDCS, we applied DBS to several cortical and subcortical areas of the STC circuit. On a cortical level, repetitive behavior significantly decreased in *DAT-tg* rats when stimulating the primary motor cortex (M1). Contrary, repetitive behavior in *DAT-tg* rats was not affected when DBS was applied to the mPFC or OFC. This indicates that modulation of sensorimotor pathways is essential for improving movement control in *DAT-tg* rats, a notion that is further corroborated by our findings showing that also DBS of the CPu but not the Thal decreased repetitive behavior in *DAT-tg*

rats. Of note, DBS modeling identified maximum current density to subside especially within the M1 and CPu following high-frequency DBS, indicating elevated susceptibility of these regions to stimulation (see SI, Figure S5). High-frequency DBS has, as opposed to low-frequency DBS and sham stimulation, proven capable of modulating widespread neuronal circuits, which subsequently has been linked to its therapeutic effect⁵¹. In correlation, repetitive behavior only decreased in *DAT-tg* rats following high-frequency DBS, whereas the effect of low-frequency DBS was equivalent to sham stimulation.

Indeed, tic generation has been often linked to abnormal motor cortex excitability, with a subsequent modulation of the M1 needed for therapeutic relief^{27, 52–58}. Frontal anodal tDCS applied in this study ultimately targets



multiple cortical areas, which hinders the ability to specify the precise cortical region underlying the therapeutic response. To further dissect cortical impact of anodal tDCS, an individualized model of current distribution was constructed. Despite uniform application, tDCS has shown to produce a complex spatial pattern of current density across cortical regions⁴². Indeed, variation in current density was found across the cortex, with results revealing a specific peak of average current density and power dissipation over the coordinates matching the M1 target, of which DBS exerted beneficial effects. Together, these findings identify the motor cortex as a potential key region for the therapeutic action of anodal tDCS.

Nevertheless, our data also show that M1 is not the only cortical structure of relevance to repetitive behavior in general and tics in particular but that both the OFC and the mPFC also play a crucial role. Same as frontal anodal tDCS, DBS applied to the OFC led to repetitive behavior in *wt* rats, which underlines the involvement of the OFC in the occurrence of repetitive behavior^{59–61}. The mechanism of action leading to this stimulation-induced behavior in *wt* rats still remains to be elucidated. Further, our data on *c-Fos* mRNA showed persistent activity in the OFC and mPFC in *DAT-tg* rats after tDCS, whereas no change was observed in the *wt* rats. A major proportion of TS patients ultimately gain control over symptoms when approaching adulthood⁶². The ability to voluntarily suppress tics has been linked to adaptive cortical changes, by which a persistent, increased activity between frontal and sensorimotor areas ultimately minimizes unwanted movement execution. As opposed to healthy subjects, this

adaptive cortical interaction is continuously heightened in TS and persists even during voluntary movement suppression^{3, 54}. In correlation, anodal tDCS has been shown to induce compensatory cortical activity changes in Parkinson's disease, which has been linked to the symptom relief mediated by tDCS^{63, 64}. The persistent cortical activity observed after the end of anodal tDCS in the *DAT-tg* rat leaves thought for further investigation into how cortico-cortical interaction between the frontal and sensorimotor cortices are modified by tDCS and thus ultimately influences behavior in the *DAT-tg* rats.

Cortical hyperexcitability is considered a consequence of underlying striatal disinhibition. In this regard, we observed that CPu-DBS reduces repetitive behavior in *DAT-tg* rats and increases it in *wt* rats. DBS is regarded as being capable to induce functional inhibition of the stimulated target, however preclinical studies show that DBS effects are phenotype dependent and thus rely on the underlying pathology^{34, 65–67}. Hence, the induction of repetitive behavior in *wt* rats following CPu-DBS may reflect striatal silencing shown to drive repetitive behavior, whereas the reduction in the *DAT-tg* rats indicates the need for modifying the dysfunctional striatum to improve symptoms.

Striatal disinhibition in TS is largely believed to originate from a loss of GABAergic PV+ expression interneurons^{68, 69}. This notion is further corroborated by animal studies showing that repetitive behavior occurs in both rodents and primates following striatal lesion but also selective GABAergic pharmacological inactivation of the striatum^{70–72}. Identical to TS patients, *DAT-tg* rats display a specific reduction of striatal PV+ expressing interneurons²⁸. In accordance to the translational importance of striatal disinhibition in both TS patients and *DAT-tg* rats, we observed a general decrease in PV+ mRNA levels in the striatum following anodal tDCS. Interestingly, PV+ mRNA expression levels and loss of PV+ interneurons promote opposing effects on activity balance, as decrease in mRNA levels enhances whereas interneuron loss reduces inhibition, respectively⁷³. In accordance, studies investigating the role of PV+ in synaptic transmission show that decrease in PV+ expression levels increase short-term facilitation of GABA release, thus leading to increased inhibition^{73, 74}. This suggests that modulation of striatal activity properties is involved in the reduction of repetitive behavior in the *DAT-tg* rats. However, more studies are needed on this matter including the investigation into how tDCS affects mRNA turnover levels and how this translates into expression of PV+ striatal interneurons. Of note, a significant decrease in striatal PV mRNA levels was also observed following application of therapeutic M1-DBS in the *DAT-tg* rats, indicating a general proficiency of M1 stimulation to affect the CPu (see SI, Figure S4).

Moreover, it has been shown that only anodal tDCS but not cathodal stimulation of the M1 can modulate subcortical structures of the STC circuit⁷⁴. Given that we did not observe improvement in behavior following cathodal stimulation at any intensity tested, we may speculate that the therapeutic effect of anodal tDCS at least in part depends on its ability to affect striatal inhibition reflected in abnormal PV+ control.

The majority of literature supports the hypothesis of a deregulated DA system in TS pathology. This notion is supported by clinical findings as DA antagonists ameliorate and DA stimulants exacerbate tics, respectively.^{75, 76} In line, *DAT-tg* rats display a general decrease in DA levels and increase in DA turnover due to DAT overexpression. Our results show no effect of tDCS on either DA levels or turnover, indicating that the therapeutic effect of tDCS goes beyond the dopaminergic system. Of note, therapeutic DBS led to modulation of the dopaminergic system in the *DAT-tg* rats, which correlates with the mechanism of DBS in TS patients (see SI, Figs. S2–S3 and Table S3)⁷⁷.

Taken together, we find that tDCS reduces repetitive behavior in the *DAT-tg* rats presumably through a restoration of the previously imbalanced sensorimotor STC circuit. Given the importance of the STC circuit in repetitive pathology, this indicates that tDCS may be employed as stimulation approach to provide symptom relief for repetitive disorders. From a clinical perspective, the primary motor cortex is the best-studied brain area with respect to tDCS application. Based on the initial contradicting line of reasoning, anodal tDCS to the motor cortex has so far not been assessed as a mean to *reduce* cortical excitability for treatment of, for example, TS. Yet, given the underlying pathology found in repetitive disorders and in TS, application of anodal tDCS might just have a positive effect on repetitive behavior as indicated by our findings. Our results thus set the stage for further investigation into the therapeutic application of tDCS in repetitive disorders. If successful, tDCS would provide a non-invasive and safe treatment strategy suitable for patients at all age groups.

Acknowledgements

We thank Susanne Müller for profound support on MRI studies and Renate Winter and Doris Zschaber for excellent technical assistance.

Funding

This research was supported by the BMBF, Germany (01EW1409 (EraNet Neuron RD_aDBS) and 01EE1403A (GCBS)) and co-financed by the DFG, Germany (WI2140/1-1/2; WI2140/2-1).

Author details

¹Department of Psychiatry and Psychotherapy, Charité Universitätsmedizin Berlin, Berlin, Germany. ²Department of Psychiatry and Psychotherapy, Medical Faculty Carl Gustav Carus, Technische Universität Dresden, Dresden, Germany. ³International Graduate Program Medical Neurosciences, Charité Universitätsmedizin Berlin, Berlin, Germany. ⁴Department of Biomedical Engineering, The City College of The City University of New York, New York, NY,

USA. ⁵Cellular Neuroscience, Max-Delbrueck-Center for Molecular Medicine in the Helmholtz Association, Berlin, Germany. ⁶Department of Clinical Neurophysiology, University Medical Center, Georg-August-University, Goettingen, Germany. ⁷Department of Psychiatry and Psychotherapy, Ludwig Maximilian University, Munich, Germany. ⁸Department of Psychology and Neurosciences, Leibniz Research Centre for Working Environment and Human Factors, Dortmund, Germany. ⁹Department of Neurology, University Medical Hospital Bergmannsheil, Bochum, Germany

Competing interests

Frank Padberg has received speaker's honorarium from Mag&More GmbH and neuroCare Group GmbH as well as support with equipment from neuroCare Group GmbH, Munich, Germany, Mag&More GmbH, Munich, Germany and Brainsway Inc., Jerusalem, Israel.

Publisher's note

Springer Nature remains neutral with regard to jurisdictional claims in published maps and institutional affiliations.

Supplementary information

The online version of this article (doi:10.1038/s41398-017-0059-5) contains supplementary material.

Received: 24 June 2017 Revised: 26 September 2017 Accepted: 1 October 2017

Published online: 10 January 2018

References

1. Leckman, J. F. Tourette's syndrome. *Lancet* **360**, 1577–1586 (2002).
2. Cavanna, A. E. & Rickards, H. The psychopathological spectrum of Gilles de la Tourette syndrome. *Neurosci. Biobehav. Rev.* **37**, 1008–1015 (2013).
3. Jackson, G. M., Draper, A., Dyke, K., Pépés, S. E. & Jackson, S. R. Inhibition, disinhibition, and the control of action in Tourette syndrome. *Trends Cogn. Sci.* **19**, 655–665 (2015).
4. Singer, H. S. & Minzer, K. Neurobiology of Tourette's syndrome: concepts of neuroanatomic localization and neurochemical abnormalities. *Brain Dev.* **25**, 70–84 (2003).
5. Mink, J. W. Basal ganglia dysfunction in Tourette's syndrome: a new hypothesis. *Pediatr. Neurol.* **25**, 190–198 (2001).
6. Leckman, J. F., Vaccarino, F. M., Kalanithi, P. S. A. & Rothenberger, A. Annotation: Tourette syndrome: a relentless drumbeat - driven by misguided brain oscillations. *J. Child. Psychol. Psychiatry Allied Discip.* **47**, 537–550 (2006).
7. Leckman, J. F., Bloch, M. H., Smith, M. E., Larabi, D. & Hampson, M. Neurobiological substrates of Tourette's disorder. *J. Child. Adolesc. Psychopharmacol.* **20**, 237–247 (2010).
8. Tye, S. J., Frye, M. A. & Lee, K. H. Disrupting disordered neurocircuitry: treating refractory psychiatric illness with neuromodulation. *Mayo Clin. Proc.* **84**, 522–532 (2009).
9. Andrade, P. & Visser-Vandewalle, V. DBS in Tourette syndrome: where are we standing now? *J. Neural. Transm.* **123**, 791–796 (2016).
10. Frait, A. & Pal, G. Deep brain stimulation in Tourette's syndrome. *Front. Neurol.* **6**, 1–7 (2015).
11. Bour, L. J. *et al.* Tic related local field potentials in the thalamus and the effect of deep brain stimulation in Tourette syndrome: report of three cases. *Clin Neurophysiol.* **126**, 1578–1588 (2014).
12. Priori, A. *et al.* Deep brain electrophysiological recordings provide clues to the pathophysiology of Tourette syndrome. *Neurosci. Biobehav. Rev.* **37**, 1063–1068 (2013).
13. Müller-Vahl, K. R. Surgical treatment of Tourette syndrome. *Neurosci. Biobehav. Rev.* **37**, 1178–1185 (2013).
14. Akbarian-Tefaghi, L., Zrinzo, L. & Foltynic, T. The use of deep brain stimulation in Tourette Syndrome. *Brain Sci.* **6**, 35 (2016).
15. Nitsche, M. A. *et al.* Pharmacological modulation of cortical excitability shifts induced by transcranial direct current stimulation in humans. *J. Physiol.* **553**, 293–301 (2003).

16. Nitsche, M. A., Paulus, W. Sustained excitability elevations induced by transcranial DC motor cortex stimulation in humans. *Neurology* **57**, 39–40 (2001)
17. Nitsche, M. A. *et al.* Transcranial direct current stimulation: state of the art 2008. *Brain Stimul.* **1**, 206–223 (2008).
18. Wachter, D. *et al.* Transcranial direct current stimulation induces polarity-specific changes of cortical blood perfusion in the rat. *Exp. Neurol.* **227**, 322–327 (2011).
19. Bikson, M., Datta, A. & Elwassif, M. Establishing safety limits for transcranial direct current stimulation. *Clin. Neurophysiol.* **120**, 1033–1034 (2009).
20. Aparício, L. V. M. *et al.* A systematic review on the acceptability and tolerability of transcranial direct current stimulation treatment in neuropsychiatry trials. *Brain Stimul.* **9**, 671–681 (2016). no. 5.
21. Russowsky Brunoni, A. *et al.* A systematic review on reporting and assessment of adverse effects associated with transcranial direct current stimulation. *Int. J. Neuropsychopharmacol.* **14**, 1133–1145 (2011).
22. Nitsche, M. A. *et al.* Consolidation of human motor cortical neuroplasticity by D-cycloserine. *Neuropsychopharmacology* **29**, 1573–1578 (2004).
23. Brunoni, A. R. *et al.* Transcranial direct current stimulation for acute major depressive episodes: meta-analysis of individual patient data. *Br. J. Psychiatry* **110**, 1–10 (2016).
24. Lefaucheur, J.-P. *et al.* Evidence-based guidelines on the therapeutic use of transcranial direct current stimulation (tDCS). *Clin. Neurophysiol.* **128**, 56–92 (2016).
25. Palm, U. *et al.* Prefrontal transcranial direct current stimulation for treatment of schizophrenia with predominant negative symptoms: a double-blind, sham-controlled proof-of-concept study. *Schizophr. Bull.* **42**, 1253–1261 (2016).
26. Mondino, M. *et al.* Effects of fronto-temporal transcranial direct current stimulation on auditory verbal hallucinations and resting-state functional connectivity of the left temporo-parietal junction in patients with schizophrenia. *Schizophr. Bull.* **4**, 318–326 (2016). Mar.
27. Mrakic-Sposta, S. *et al.* Transcranial direct current stimulation in two patients with Tourette syndrome. *Mov. Disord.* **23**, 2256–2257 (2008).
28. Hadar, R. *et al.* Rats overexpressing the dopamine transporter display behavioral and neurobiological abnormalities with relevance to repetitive disorders. *Sci. Rep.* **6**, 39145 (2016).
29. Paxinos, G. & Watson, C. *The Rat Brain in Stereotaxic Coordinates*. 3rd edn (Acad Press, San Diego, 1997).
30. Dockery, C. A., Liebetanz, D., Birbaumer, N., Malinowska, M. & Wesienska, M. J. Cumulative benefits of frontal transcranial direct current stimulation on visuospatial working memory training and skill learning in rats. *Neurobiol. Learn. Mem.* **96**, 452–460 (2011).
31. Liebetanz, D. *et al.* Anticonvulsant effects of transcranial direct-current stimulation (tDCS) in the rat cortical ramp model of focal epilepsy. *Epilepsia* **47**, 1216–1224 (2006).
32. Felice, L. J., Felice, J. D. & Kissinger, P. T. Determination of catecholamines in rat brain parts by reverse-phase ion-pair liquid chromatography. *J. Neurochem.* **31**, 1461–1465 (1978).
33. Sperk, G. Simultaneous determination of serotonin, 5-hydroxyindoleacetic acid, 3,4-dihydroxyphenylacetic acid and homovanillic acid by high performance liquid chromatography with electrochemical detection. *J. Neurochem.* **38**, 840–843 (1982).
34. Edemann-Calleesen, H. *et al.* Medial forebrain bundle deep brain stimulation has symptom-specific anti-depressant effects in rats and as opposed to ventromedial prefrontal cortex stimulation interacts with the reward system. *Brain Stimul.* **8**, 714–723 (2015).
35. Rea, E. *et al.* Anti-anhedonic effect of deep brain stimulation of the prefrontal cortex and the dopaminergic reward system in a genetic rat model of depression: an intracranial self-stimulation paradigm study. *Brain Stimul.* **7**, 21–28 (2014). Jan.
36. Rummel, J. *et al.* Testing different paradigms to optimize antidepressant deep brain stimulation in different rat models of depression. *J. Psychiatr. Res.* **81**, 36–45 (2016).
37. Song, W., Truong, D. Q., Bikson, M. & Martin, J. H. Transspinal direct current stimulation immediately modifies motor cortex sensorimotor maps. *J. Neurophysiol.* **113**, 2801–2811 (2015).
38. Paxinos, G., Watson, C. *The Rat Brain in Stereotaxic Coordinates*, 6th edn, Elsevier Acad Press. **170**, 547–612 (2007)
39. Datta, A. *et al.* Gyri-precise head model of transcranial direct current stimulation: improved spatial focality using a ring electrode versus conventional rectangular pad. *Brain Stimul.* **2**, 201–207 (2009).
40. Minhas, P. *et al.* Electrodes for high-definition transcutaneous DC stimulation for applications in drug delivery and electrotherapy, including tDCS. *J. Neurosci. Methods* **190**, 188–197 (2010).
41. Ridding, M. C. & Ziemann, U. Determinants of the induction of cortical plasticity by non-invasive brain stimulation in healthy subjects. *J. Physiol.* **588**, 2291–2304 (2010).
42. Jackson, M. P. *et al.* Animal models of transcranial direct current stimulation: methods and mechanisms. *Clin. Neurophysiol.* **127**, 3425–3454 (2016).
43. Stagg, C. J. & Nitsche, M. A. Physiological basis of transcranial direct current stimulation. *Neuroscience* **17**, 37–53 (2011).
44. Kuo, M. F., Paulus, W. & Nitsche, M. A. Boosting focally-induced brain plasticity by dopamine. *Cereb. Cortex* **18**, 648–651 (2008).
45. Monte-Silva, K., Liebetanz, D., Grundey, J., Paulus, W. & Nitsche, M. A. Dose-dependent non-linear effect of L-dopa on human motor cortex plasticity. *J. Physiol.* **588**, 3415–3424 (2010). Pt 18.
46. Hasan, A. *et al.* Dysfunctional long-term potentiation-like plasticity in schizophrenia revealed by transcranial direct current stimulation. *Behav. Brain Res.* **224**, 15–22 (2011).
47. Baeken, C., Brunelin, J., Duprat, R. & Vanderhasselt, M. A. The application of tDCS in psychiatric disorders: a brain imaging view. *Socioaffect. Neurosci. Psychol.* **6**, 29588 (2016).
48. Nitsche, M. A. *et al.* Dopaminergic modulation of long-lasting direct current-induced cortical excitability changes in the human motor cortex. *Eur. J. Neurosci.* **23**, 1651–1657 (2006).
49. Tremblay, L., Worbe, Y., Thobois, S., Scambato-Faure, V. & Féger, J. Selective dysfunction of basal ganglia subterritories: from movement to behavioral disorders. *Mov. Disord.* **30**, 1155–1170 (2015).
50. Groenewegen, H. J., Van Den Heuvel, O. A., Cath, D. C., Voorn, P., Veltman, D. J. Does an imbalance between the dorsal and ventral striatopallidal systems play a role in Tourette's syndrome? A neuronal circuit approach. *Brain Dev.* **25**, S3–S14 (2003)
51. McCracken, C. B. & Grace, A. A. High-frequency deep brain stimulation of the nucleus accumbens region suppresses neuronal activity and selectively modulates afferent drive in rat orbitofrontal cortex in vivo. *J. Neurosci.* **27**, 12601–12610 (2007).
52. Ziemann, U., Paulus, W. & Rothenberger, A. Decreased motor inhibition in Tourette's disorder: Evidence from transcranial magnetic stimulation. *Am. J. Psychiatry* **154**, 1277–1284 (1997).
53. Orth, M., Münchau, A. & Rothwell, J. C. Corticospinal system excitability at rest is associated with Tic severity in Tourette Syndrome. *Biol. Psychiatry* **64**, 248–251 (2008).
54. Serrien, D. J., Orth, M., Evans, A. H., Lees, A. J. & Brown, P. Motor inhibition in patients with Gilles de la Tourette syndrome: Functional activation patterns as revealed by EEG coherence. *Brain* **128**, 116–125 (2005).
55. Mantovani, A. *et al.* Repetitive transcranial magnetic stimulation (rTMS) in the treatment of obsessive-compulsive disorder (OCD) and Tourette's syndrome (TS). *Int. J. Neuropsychopharmacol.* **9**, 95 (2005).
56. Stern, E. *et al.* A functional neuroanatomy of tics in Tourette syndrome. *Arch. Gen. Psychiatry* **57**, 741–748 (2000).
57. Berardelli, A., Currà, A., Fabbrini, G., Gilio, F. & Manfredi, M. Pathophysiology of tics and Tourette syndrome. *J. Neurol.* **250**, 781–787 (2003).
58. Wang, Z. *et al.* The neural circuits that generate tics in Tourette's syndrome. *Am. J. Psychiatry* **168**, 1326–1337 (2011).
59. Millad, M. R. & Rauch, S. L. Obsessive-compulsive disorder: Beyond segregated cortico-striatal pathways. *Trends Cogn. Sci.* **16**, 43–51 (2012).
60. Saxena, S. *et al.* Cerebral glucose metabolism in obsessive-compulsive hoarding. *Am. J. Psychiatry* **161**, 1038–1048 (2004).
61. Ahmari, S. E. *et al.* Repeated cortico-striatal stimulation generates persistent OCD-like behavior. *Science* **340**, 1234–1239 (2013).
62. Jackson, S. R. *et al.* Compensatory neural reorganization in Tourette syndrome. *Curr. Biol.* **21**, 580–585 (2011).
63. Fregni, F. *et al.* Noninvasive cortical stimulation with transcranial direct current stimulation in Parkinson's disease. *Mov. Disord.* **21**, 1693–1702 (2006).
64. Orban de Xivry, J. J. & Shadmehr, R. Electrifying the motor engram: effects of tDCS on motor learning and control. *Exp. Brain Res.* **232**, 3379–3395 (2014).
65. Benazzouz, A. & Hallett, M. Mechanisms of action of deep brain stimulation (DBS). *Neurology* **55**, S13–S16 (2000).

66. McIntyre, C. C., Savasta, M., Kerkerian-Le Goff, L. & Vitek, J. L. Uncovering the mechanism(s) of action of deep brain stimulation: activation, inhibition, or both. *Clin. Neurophysiol.* **115**, 1239–1248 (2004).
67. Friedman, A. *et al.* Programmed acute electrical stimulation of ventral tegmental area alleviates depressive-like behavior. *Neuropsychopharmacology* **34**, 1057–1066 (2009).
68. Kataoka, Y. *et al.* Decreased number of parvalbumin and cholinergic interneurons in the striatum of individuals with tourette syndrome. *J. Comp. Neurol.* **518**, 277–291 (2010).
69. Kalanithi, P. S. A. *et al.* Altered parvalbumin-positive neuron distribution in basal ganglia of individuals with Tourette syndrome. *Proc. Natl. Acad. Sci. USA* **102**, 13307–13312 (2005).
70. Pogorelov, V., Xu, M., Smith, H. R., Buchanan, G. F. & Pittenger, C. Corticostriatal interactions in the generation of tic-like behaviors after local striatal disinhibition. *Exp. Neurol.* **265**, 122–128 (2015).
71. Bronfeld, M., Yael, D., Belevovsky, K. & Bar-Gad, I. Motor tics evoked by striatal disinhibition in the rat. *Front Syst. Neurosci.* **7**, 50 (2013).
72. McCairn, K. W., Iriki, A. & Isoda, M. High-frequency pallidal stimulation eliminates tic-related neuronal activity in a nonhuman primate model of Tourette syndrome. *Neuroreport* **23**, 206–210 (2012).
73. Schwaller, B. The use of transgenic mouse models to reveal the functions of Ca²⁺ buffer proteins in excitable cells. *Biochim. Biophys. Acta Gen. Subj.* **1820**, 1294–1303 (2012).
74. Polanía, R., Paulus, W. & Nitsche, M. A. Modulating cortico-striatal and thalamo-cortical functional connectivity with transcranial direct current stimulation. *Hum. Brain Mapp.* **33**, 2499–2508 (2012).
75. Singer, H. S. Treatment of tics and Tourette syndrome. *Curr. Treat. Options Neurol.* **12**, 539–561 (2010).
76. Felling, R. J. & Singer, H. S. Neurobiology of Tourette syndrome: current status and need for further investigation. *J. Neurosci.* **31**, 12387–12395 (2011).
77. Kuhn, J. *et al.* In vivo evidence of deep brain stimulation-induced dopaminergic modulation in Tourette's Syndrome. *Biol. Psychiatry* **71**, e11–e13 (2012). Mar.

Supplementary information

Non-invasive modulation reduces repetitive behavior in a rat model through the sensorimotor cortico-striatal circuit

Henriette Edemann-Callesen, Bettina Habelt, Franziska Wieske, Mark Jackson, Niranjan Khadka, Daniele Mattei, Nadine Bernhardt, Andreas Heinz, David Liebetanz, Marom Bikson, Frank Padberg Ravit Hadar, Michael A. Nitsche, Christine Winter*

1. Experimental setup



Figure S1: Repetitive behavioral paradigm. A timeline of the repetitive behavioral paradigm starting from injection of amphetamine (0 min) (2.0mg/kg) to the occurrence of repetitive behavior (90-120min, stereotypy phase). Stimulation (sham, tDCS and DBS) was applied in the beginning of the paradigm. Behavioral effects were assessed in the stereotypy phase. tDCS: transcranial direct current stimulation; DBS; deep brain stimulation, HF: high frequency stimulation, LF: low frequency stimulation

Groups	Animal no.	Implementation	All stimulation type tested	Final stimulation
Control	WT n= 8, DAT n= 8	Frontal cortex	Sham	Sham
tDCS	WT n= 9, DAT n= 7	Frontal cortex	Sham Anodal (100µA, 200µA, 300µA) Cathodal (100µA, 200µA)	Anodal, 200µA
DBS				
<i>Group 1</i>	WT n= 8, DAT n= 8	OFC, CPu	Sham High frequency DBS Low frequency DBS	CPu, High frequency
<i>Group 2</i>	WT n= 8, DAT n= 8	mPFC	Sham High frequency DBS Low frequency DBS	-
<i>Group 3</i>	WT n= 5, DAT n= 6	M1, Thal	Sham High frequency DBS Low frequency DBS	M1, High frequency

Table S1: Group specifics. Table showing the number of animals in the control, tDCS and DBS groups. For tDCS, stimulation was applied over the frontal cortex. Stimulation tested included sham, anodal (100µA, 200µA, 300µA) and cathodal (100µA, 200µA) stimulation. Either high or low frequency DBS was applied to the OFC and CPu (*group 1*), the mPFC (*group 2*) or the M1 and CmPf (*group 3*). For the final testing round, animals were stimulated with the most therapeutic-relevant setting as identified by the behavioral assessment. *wt*: wildtypes, *DAT-tg*: dopamine transporter overexpressing rats, tDCS: transcranial direct current stimulation, DBS: Deep brain stimulation, OFC: orbitofrontal cortex, CPu: caudate putamen, mPFC: medial prefrontal cortex, M1: primary motor cortex, Thal: thalamus.

2. Neurobiological assessment

HPLC						
	Sham and tDCS group		Group 1		Group 2	
OFC	3,2 - 2,2	2 from right	3,2 - 2,2	2 from right	3,2 - 2,2	2 from right
Nacc	1,7 - 0,7	right+left	1,2 - 0,7	right+left	1,2 - 0,7	right+left
CPu	1,7 - 0,7	right+left	1,2 - 0,7	right+left	1,2 - 0,7	right+left
qPCR						
	c-Fos			Parv		
mPFC	3,2 - 2,2		3 from left			
OFC	3,2 - 2,2		3 from left			
M1	3,2 - 2,2		3 from left			
CPu				0,7 - -0,3	3 from right and 3 from left	

Table S2: Neurobiological assessment. Deep brain stimulation (DBS) animals that previously underwent behavioral scoring were subjected to DBS settings that elicited the most therapeutic behavioral results, i.e. high frequency DBS in either the caudate putamen (CPu) (group 1) or primary motor cortex (M1) (group 3) and sacrificed immediately thereafter. Brains were extracted and snap frozen for same post mortem assessment as animals in the transcranial direct current stimulation (tDCS) and sham groups. Table shows coordinates for coronal sections in accordance to bregma in mm anterior-posterior. For HPLC and qPCR quantification, animals from the following groups were used: sham, tDCS, group 1 (CPu) and group 3 (M1). Coordinates are in accordance to Paxinos & Watson brain atlas (1997). OFC: orbitofrontal cortex; NAcc: nucleus accumbens; mPFC: medial prefrontal cortex; Parv: parvalbumin

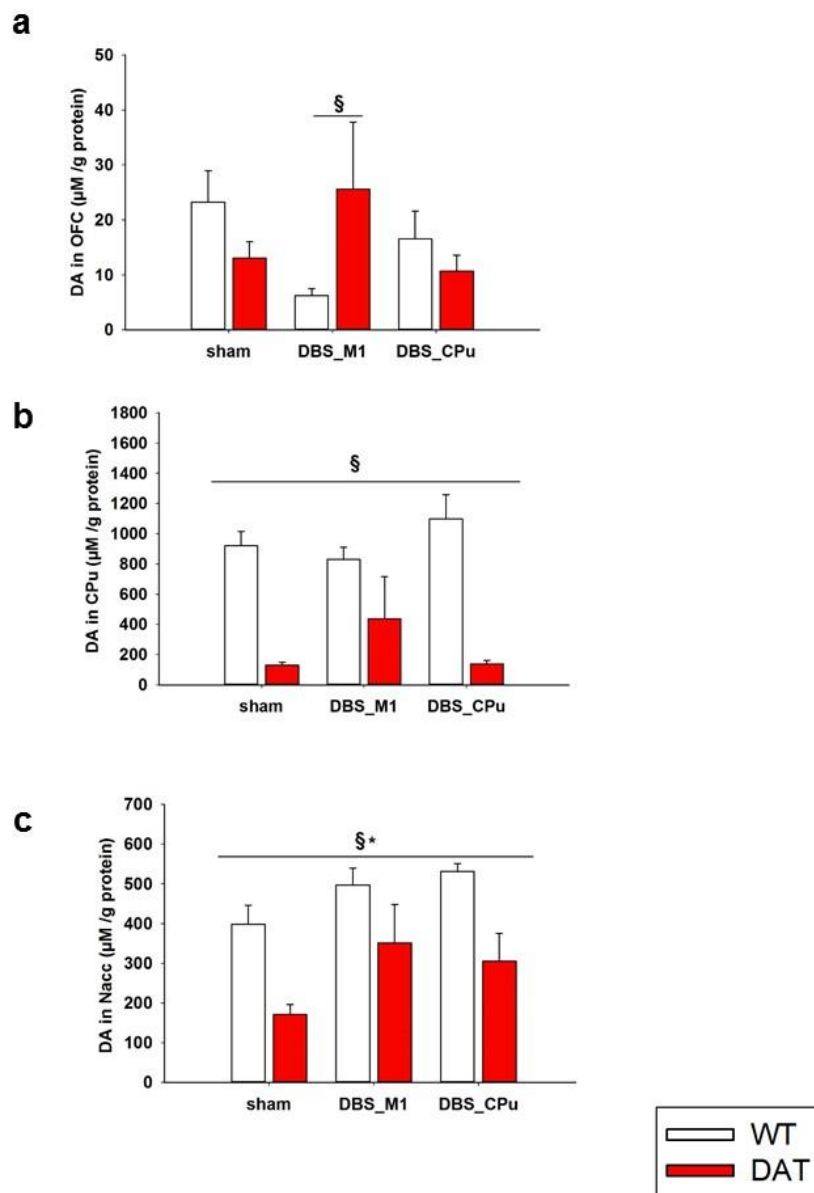


Figure S2: Dopamine levels. Figure showing dopamine content ($\mu\text{M/g}$ protein) in the a) orbitofrontal cortex (OFC) b) caudate putamen (CPu) and c) nucleus accumbens (Nacc) following sham and high frequency deep brain stimulation (HF-DBS) to the primary motor cortex (M1) and CPu. In the OFC, a two-way ANOVA revealed a significant interaction ($F(2,28)=4.807$, $p=0.016$) with a further post-hoc showing significant difference in dopamine (DA) levels between sham and M1-DBS (a). In the CPu, a main effect was found for phenotype ($F(1,29)=69,995$ $p<0.001$) with dopamine transporter overexpressing rat (*DAT-tg*) rats displaying decreased DA levels in comparison to wildtype rats (*wt*) rats (b). In the Nacc, a significant main effect for phenotype ($F(1,28)=19.329$ $p<0.001$) and treatment ($F(2,28)=4,825$ $p=0.016$) with the lowest level of DA levels seen in the *DAT-tg* rats (c). All data are given as mean \pm s.e.m. Asterisks (*) indicates significant difference between stimulation protocols, paragraph (§) indicates significant difference between phenotype with $p < 0.05$.

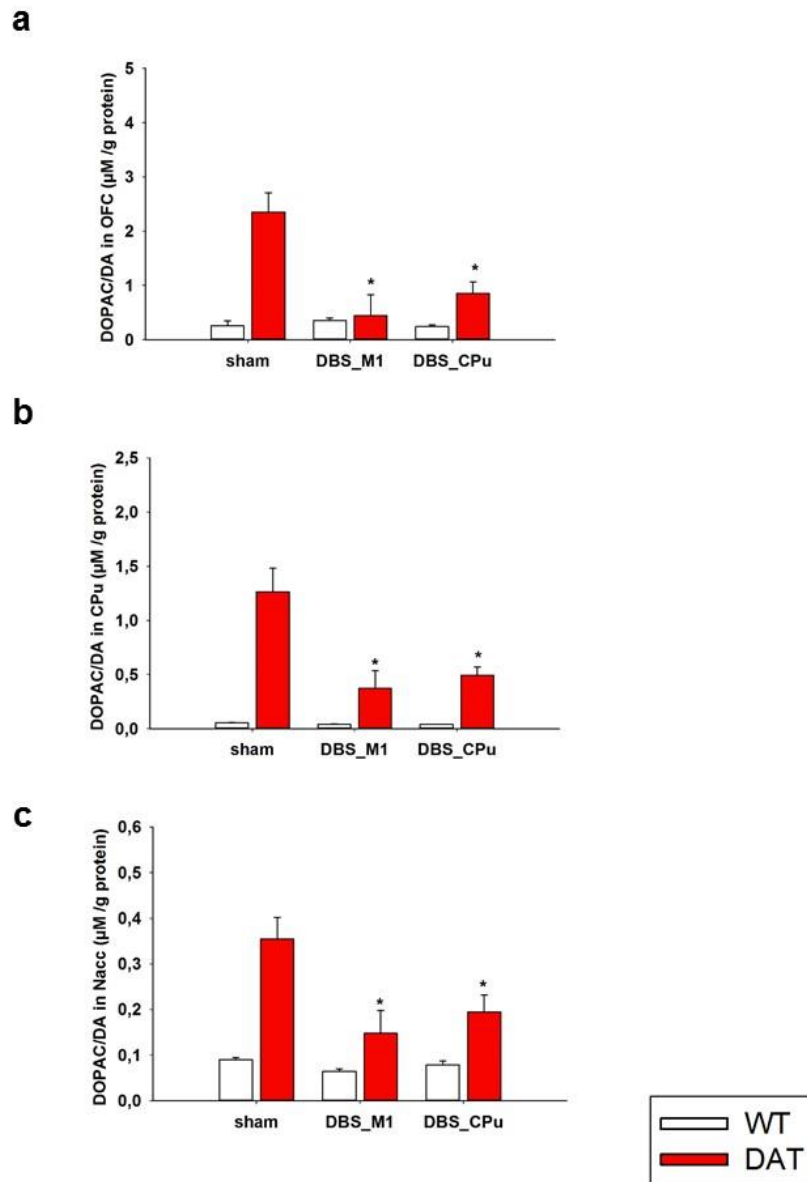


Figure S3: Dopamine turnover. Figure showing dopamine turnover (DOPAC/DA) ($\mu\text{M/g}$ protein) in the a) orbitofrontal cortex (OFC) b) caudate putamen (CPu) and c) nucleus accumbens (Nacc) following sham and high frequency deep brain stimulation (HF-DBS) to the primary motor cortex (M1) and caudate putamen (CPu). In both the OFC, CPu and Nacc a significant main effect was found for phenotype (OFC, $F(1,26)=16.837$, $p < 0.001$); CPu, $F(1,29)=34.158$ $p < 0.001$; Nacc, $F(1,27)=25.419$ $p < 0.001$), treatment (OFC, $F(2,26)=7.302$, $p=0.003$; CPu, $F(2,29)=7.138$ $p=0.003$; Nacc, $F(2,27)=5.921$ $p=0.007$) and interaction (OFC, $F(2,26)=8.004$, $p=0.002$; CPu, $F(2,29)=6.708$ $p=0.004$; Nacc, $F(2,27)=3.841$ $p=0.034$) with further post-hoc tests revealing significant differences in dopamine turnover following M1-DBS and CPu-DBS in the dopamine transporter overexpressing rat (DAT-tg) rats as compared to sham stimulation. All data are given as mean \pm s.e.m. Asterisks (*) indicates significant difference between stimulation protocols, paragraph (§) indicates significant difference between phenotype with $p < 0.05$.

Region	Transmitter	Pheno	Stim	$\mu\text{M/g}$ protein	2wayANOVA	DF	F-value	P-Value
OFC	DA	wt	sham	23,185 \pm 4,426	Pheno stim Interaction	(1,28) (2,28) (2,28)	0.0831 0.551 4.807	0.775 0.583 0.016*
			DBS_M1	6,200 \pm 4,849				
	DBS_Cpu	16,515 \pm 4,849						
	DAT-tg	sham	13,034 \pm 3,833					
DBS_M1		25,60 \pm 6,259						
DOPAC	wt	wt	sham	0,257 \pm 0,239	Pheno stim Interaction	(1,26) (2,26) (2,26)	16.837 7.302 8.004	<0.001* 0.003* 0.002*
			DBS_M1	0,354 \pm 0,261				
	DBS_Cpu	0,244 \pm 0,261						
	DAT-tg	sham	2,353 \pm 0,207					
DBS_M1		0,444 \pm 0,413						
CPU	DA	wt	sham	963,86 \pm 92,71	Pheno stim Interaction	(1,29) (2,29) (2,29)	69.995 0.430 3.230	<0.001* 0.655 0.054
			DBS_M1	829,96 \pm 109,7				
	DBS_Cpu	1097,81 \pm 100						
	DAT-tg	sham	129,65 \pm 86,73					
DBS_M1		437,38 \pm 141,6						
DOPAC	wt	wt	sham	0,0523 \pm 0,121	Pheno stim Interaction	(1,29) (2,29) (2,29)	34.158 7.138 6.708	<0.001* 0.003* 0.004*
			DBS_M1	0,0405 \pm 0,144				
	DBS_Cpu	0,0385 \pm 0,131						
	DAT-tg	sham	1,264 \pm 0,114					
DBS_M1		0,372 \pm 0,185						
Nacc	DA	wt	sham	398,19 \pm 47,14	Pheno stim Interaction	(1,28) (2,28) (2,28)	19.329 4.825 0.308	<0.001* 0.016* 0.737
			DBS_M1	496,78 \pm 55,78				
	DBS_Cpu	531,55 \pm 62,36						
	DAT-tg	sham	171,01 \pm 44,09					
DBS_M1		351,30 \pm 72,01						
DOPAC	wt	wt	sham	0,0903 \pm 0,031	Pheno stim Interaction	(1,27) (2,27) (2,27)	25.419 5.921 3.841	<0.001* 0.007* 0.034*
			DBS_M1	0,0641 \pm 0,037				
	DBS_Cpu	0,0783 \pm 0,041						
	DAT-tg	sham	0,354 \pm 0,029					
DBS_M1		0,148 \pm 0,048						
DBS_Cpu	sham	0,195 \pm 0,034						

Table S3: Neurotransmitter content. Table summarizes neurochemical results. Neurochemical content was examined in the dopamine transporter overexpressing rat (*DAT-tg*) and wildtype (*wt*) rats following sham and deep brain stimulation (DBS) when applied to the caudate putamen (CPu) and primary motor cortex (M1). Dopamine levels and dopamine turnover were measured in the medial orbitofrontal cortex (OFC), nucleus accumbens (Nacc) and CPu. Data are presented as mean \pm s.e.m.

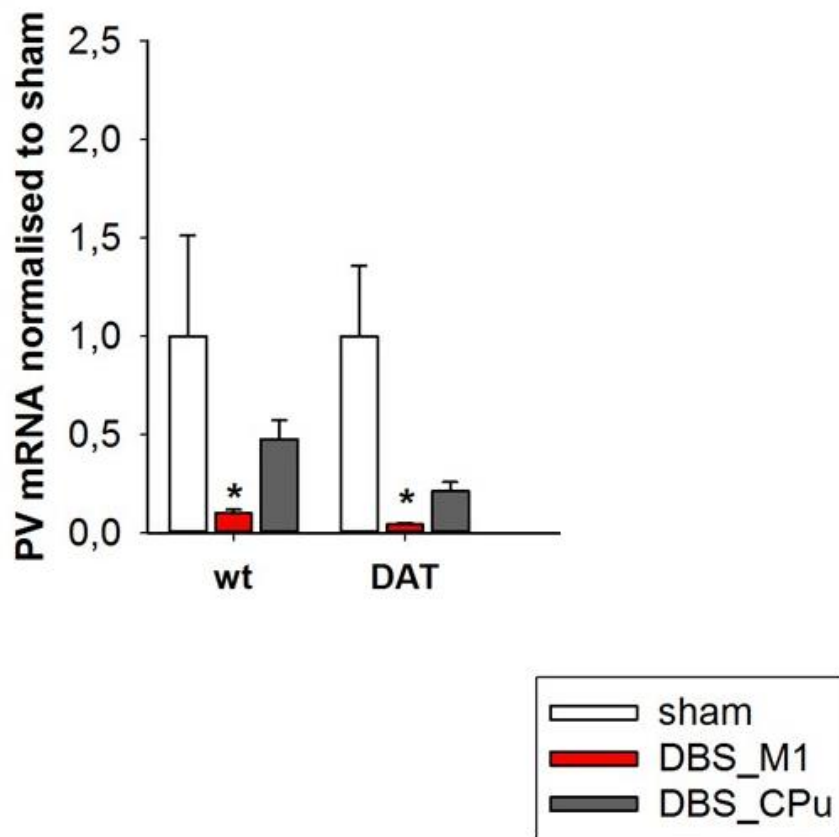


Figure S4: Pv+ levels in the caudate putamen. Figure showing the parvalbumin (Pv+) mRNA expression levels in caudate putamen (CPu) in the dopamine transporter overexpressing rat (*DAT-tg*) and wildtype (*wt*) rats following sham and deep brain stimulation (DBS) when applied to the CPu and primary motor cortex (M1). Following quantification of mRNA levels in the CPu, a Kruskal-Wallis One-Way analysis revealed a significant difference in PV+ expression levels between DBS-M1 relative to sham in both *DAT-tg* ($H(2)= 9.692, p=0.008$) and *wt* rats ($H(2)= 9.038, p= 0.011$). No significant difference was found following CPu-DBS relative to sham in either of the two phenotypes. All data are given as mean \pm s.e.m. Asterisks (*) indicates significant difference between stimulation protocols, paragraph (§) indicates significant difference between phenotype with $p < 0.05$.

2. DBS modeling

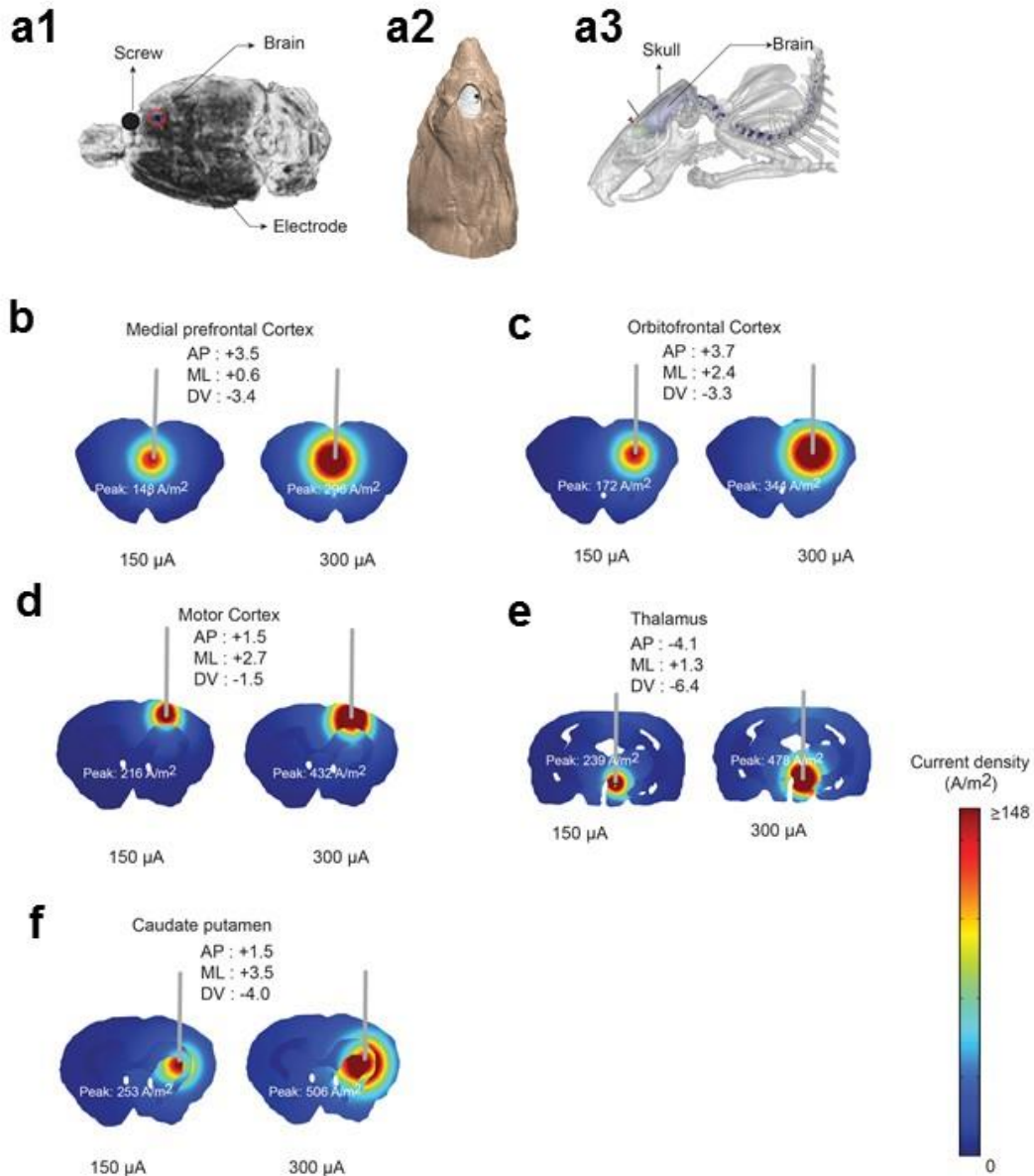


Figure S5: DBS modeling. Conductivity values were assigned as, scalp: 0.465 S/m; skull: 0.01 S/m; csf: 1.65 S/m; air: 1×10^{-15} ; gray matter: 0.276 S/m; cerebellum: 0.276 S/m; hippocampus: 0.126 S/m; white matter: 0.126 S/m; thalamus: 0.276 S/m, screw: 1.28×10^8 ; and electrode: 5.99×10^7 S/m. (Bikson *et al.*, 2015; Song *et al.*, 2015) Computer aided model (CAD) geometry of the electrode and the screw were first imported into the head model and positioned for each montage (orbitofrontal cortex, medial prefrontal cortex, motor cortex, caudate putamen and thalamus) based on the coordinates values as used in the main manuscript. Volumetric meshes were later imported into COMSOL Multiphysics 4.3 (COMSOL Inc., MA, USA) to solve the model. The final finite element head assembly was solved for greater than 10,000,000 degrees of freedom and had greater than

8,500,000 tetrahedral elements. For electrical stimulation, a quasistatic approximation was implemented and boundary conditions were applied as normal current density (inward current flow) at the exposed surface of the electrode and ground at the surface of the screw. Remaining external surfaces of the model were electrically insulated. Simulation was carried out for both 150 μA and 300 μA current intensities. Current density slice plots for each intensities and montages were generated and the peak values were reported. The predicted current density plots for high- and low frequency DBS application and corresponding was assessed through computational modeling. Electrode and a screw configuration in one of the montage is shown as an exemplary configuration of electrode positioning at the incision area (a). Current density for each electrode configuration was doubled when intensity was increased by two-fold. On a cortical level, maximum current density was observed in the M1 following HF-DBS (300 μA = 432 A/m^2). On a subcortical level, maximum current density was found in the CPu following HF-DBS (300 μA = 506 A/m^2) (b-f).

Mein Lebenslauf wird aus datenschutzrechtlichen Gründen in der elektronischen Version meiner Arbeit nicht veröffentlicht.

(For reason of data protection the CV is not published in the electronic version of my thesis).

List of publications

Published:

Bernhardt N, Lieser MK, Hlusicka EB, Habelt B, Wieske F, **Edemann-Callesen H**, Garthe A, Winter C. Learning deficits in rats overexpressing the dopamine transporter. *Scientific reports*. 2018 Sep 21;8(1):14173. Impact Factor: **4.1**

Ryrsø CK, Godtfredsen NS, Kofod LM, Lavesen M, Mogensen L, Tobberup R, Farver-Vestergaard I, **Callesen HE**, Tendal B, Lange P, Iepsen UW. Lower mortality after early supervised pulmonary rehabilitation following COPD-exacerbations: a systematic review and meta-analysis. *BMC pulmonary medicine*. 2018;18(1):154. Impact Factor: **2.7**

Edemann-Callesen H, Habelt B, Wieske F, Jackson M, Khadka N, Mattei D, Bernhardt N, Heinz A, Liebetanz D, Bikson M, Padberg F. Non-invasive modulation reduces repetitive behavior in a rat model through the sensorimotor cortico-striatal circuit. *Translational psychiatry*. 2018 Jan 10;8(1):11. Impact Factor: **5.6**

Hadar R, **Edemann-Callesen H**, Reinel C, Wieske F, Voget M, Popova E, Sohr R, Avchalumov Y, Priller J, Van Riesen C, Puls I. Rats overexpressing the dopamine transporter display behavioral and neurobiological abnormalities with relevance to repetitive disorders. *Scientific reports*. 2016 Dec 15;6:39145. Impact Factor: **4.1**

Hadar R, Dong L, del-Valle-Anton L, Guneykaya D, Voget M, **Edemann-Callesen H**, Schweibold R, Djodari-Irani A, Goetz T, Ewing S, Kettenmann H. Deep brain stimulation during early adolescence prevents microglial alterations in a model of maternal immune activation. *Brain, behavior, and immunity*. 2017 Jul 1;63:71-80. Impact Factor: **6.3**

Shen C, Stasch J, Velenosi L, Madipakkam AR, **Edemann-Callesen H**, Neuhaus AH. Face identity is encoded in the duration of N170 adaptation. *Cortex*. 2017 Jan 1;86:55-63. Impact Factor: **4.3**,

Szechtman H, Ahmari SE, Beninger RJ, Eilam D, Harvey BH, **Edemann-Callesen H**, Winter C. Obsessive-compulsive disorder: Insights from animal models. *Neuroscience & Biobehavioral Reviews*. 2017 May 1;76:254-79. Impact Factor: **9.4**

Edemann-Callesen H, Voget M, Empl L, Vogel M, Wieske F, Rummel J, Heinz A, Mathé AA, Hadar R, Winter C. Medial forebrain bundle deep brain stimulation has symptom-specific anti-depressant effects in rats and as opposed to ventromedial prefrontal cortex stimulation interacts with the reward system. *Brain stimulation*. 2015 Jul 1;8(4):714-23. Impact Factor: **6.0**

Submitted:

Hadar, R, Winter, R, **Edemann-Callesen, H**, Wieske, F, Habelt, B, Khadka, N, Felgel, V, Barroeta Hlusicka, E, Reis, J, Funke, K, Fritsch, B, Bernhardt, N, Bikson, M, Nitsche, M.A, Winter, C. Prevention of schizophrenia deficits via non-invasive adolescent frontal cortex stimulation in rats.

Ravit Hadar, **Henriette Edemann-Calleen**, Elizabeth Barroeta Hlusicka, Fransiska Wieske, Martin Vogel, Lydia Guenther, Barbara Vollmayr, Rainer Hellweg, Andreas Heinz, Alexander Garthe, Christine Winter. Stress-induced depressive episodes across life – an inducer of cognitive impairment or resilience?

Contributions to conferences:

Mediterranean Neuroscience society (MSN) 6th conference, Malta 2017. Brain stimulation techniques in the context of repetitive disorders (**Talk**)

International DBS Symposium, Clinical Research Group KFO 247. Berlin, Germany 2016. Using an animal model of repetitive behavior for investigating DBS targets (**Poster**)

II International Conference on Deep Brain Stimulation. Düsseldorf, Germany 2016. Identification of electrophysiological biomarkers in a novel animal model of Tourette Syndrome and Deep Brain Stimulation improves behavior and modulates neural circuits in a rodent model of schizophrenia (**2x Poster**)

10th FENS Forum of Neuroscience. Copenhagen, Denmark 2016. Identification of electrophysiological biomarkers in a novel animal model of Tourette Syndrome (**Poster**)

ENCODS PhD Conference. Helsingør, Denmark 2016. Identification of electrophysiological biomarkers in a novel animal model of Tourette Syndrome (**Poster**)

ERANET Neuron II Consortium. Helsinki, Finland 2015 RD_aDBS and Identification of electrophysiological biomarkers in a novel animal model of Tourette Syndrome (**Talk and Poster**)

DGPPN Congress. Berlin, Germany 2015 A new animal model of Tourette syndrome and Identification of electrophysiological biomarkers to treat repetitive disorders (**2x Poster**)

2nd International of the Clinical Research Group 219. Cologne, Germany 2015. Characterisation of the DAT over-expressing rat line – a new animal model for studying repetitive behavior? (**Poster**)

DGPPN Congress. Berlin, Germany 2014. Anti-depressant effects of medial forebrain bundle deep brain stimulation in rats are symptom-specific and as opposed to ventromedial prefrontal cortex mediated via the reward system (**Poster**)

Acknowledgements

Thank you to my supervisors Prof. Dr. Dr. Andreas Heinz and Prof. Dr. med Christine Winter for giving me the opportunity to conduct this PhD thesis.

Thank you, Christine, for assigning me with much responsibility from the beginning, yet with all the support that was needed. I am happy that I landed under your roof and became a part of your team. Thank you so much.

Thank you, Berlin-team: Dr. Ravit Hadar, Dr. Mareike Voget, Dr. Franziska Wieske, Christian Tatarau and Renate Winter. You made lab fun and you were always there to help when I needed it, no matter the problem.

Thank you, Dresden-team: Dr. Nadine Bernhardt, Elisabeth Barroeta Hlusicka, Bettina Habelt, Rebecca Winter, Sabine Einert and Doris Zschaber. Despite the distance between Berlin and Dresden, you made me feel at home right away and made it worth all the long-distance rides. Especially a big thank you, to you Nadine, for all your help and encouragement.

Last but not least, thanks to my dear family; Helle, John, Camilla and Jacob. Despite me being far from home, you were there on the side with nothing but support and excitement concerning this project.